ADDIS ABABA UNIVERSITY

COLLEGE OF TECHNOLOGY AND BUILT ENVIRONMENT

SCHOOL OF CIVIL AND ENVIRONMENTAL ENGINEERING

GEOTECHNICAL ENGINEERING CHAIR

Dynamic Soil Characteristics of Selected Sites in Bole Sub-City of Addis Ababa

By

Yeabsira Bekele

A Thesis Submitted to the School of Graduate Studies of Addis Ababa University College of Technology and Built Environment in Partial Fulfillment of the Requirements for the Degree of Master of Science in Civil Engineering (Geotechnical Engineering)

Advisor

Dr. Tensay Gebremedhin

Addis Ababa, Ethiopia

May, 2025

Declaration

This is to certify that the thesis presented by Yeabsira Bekele Ejigu, entitled "Dynamic Soil Characteristics of Selected Sites in Bole Sub-City of Addis Ababa" and submitted to the School of Civil and Environmental Engineering in partial fulfillment of the requirements for the award of the Master of Science in Geotechnical Engineering with the university regulations, and meeting accepted standards concerning originality and quality.

Yeabsira Bekele Ejigu	_____	_____
Name	Signature	Date

This thesis has been submitted for examination with approval as a university advisor.

Dr Tensay Gebremedhin	_____	_____
Advisor	Signature	Date

Addis Ababa University

Addis Ababa Institute of Technology

School of Graduate Students

Dynamic Soil Characteristics of Selected Sites in Bole Sub-City of Addis Ababa

By

Yeabsira Bekele Ejigu

Addis Ababa Institute of Technology

Approved by Board of Examiners

Tensay Gebremedhin (Ph.D.)	_____	_____
Advisor	Signature	Date
_____	_____	_____
Internal Examiner	Signature	Date
_____	_____	_____
External Examiner	Signature	Date
_____	_____	_____
School Chair-Man	Signature	Date

ABSTRACT

Addis Ababa which is situated on the margins of ethiopian rift valley system is positioned in seismic zone 3 according to ES EN 2015. The city has a moderate seismicity. This study investigates the dynamic properties of soils taken from selected test pits in bole Subcity of Addis Ababa city at 2.5m sampling depth. To assess the area's capacity to resist dynamic loads from potential earthquakes, both index and dynamic properties of the soils were evaluated. Index property tests including atterberg limits, particle size analysis, free swell, and specific gravity revealed a wide range of test results. Based on USCS soil classification system the soils samples were identified primarily as plastic clay and clayey sand . Dynamic behavior was further examined using cyclic simple shear tests at varying strain amplitudes (0.01% to 5%) and axial stresses (100 kPa to 400 kPa). The stress strain responses were recorded, and the shear modulus and damping ratio were obtained for each soil sample. The findings were compared with local and international studies, contributing valuable data for seismic hazard assessment and earthquake-resilient design in the region.

Key words: Shear modulus, Damping ratio, Unified soil classification system, Dynamic property

ACKNOWLEDGMENT

First and foremost, I would like to thank the Almighty God for providing me with the strength and guidance to overcome the challenges throughout this journey. I am deeply grateful to my adviser, Dr. Tensay Gebremedhin, for his invaluable encouragement, supervision, and insightful guidance from the beginning to the completion of this research. His critical feedback and constant support were instrumental in the success of this work. I also owe a special thanks to my mother, Mestawot, my husband, Ermiyas, my sisters, and all of my family members for their unwavering encouragement and positive words, without which I would not have made it this far. Finally, I would like to express my sincere gratitude to the lecturers of Addis Ababa University's Geotechnical Engineering Department and the Geotechnical Engineering Laboratory staff for their cooperation and support in successfully completing this research.

Yeabsira Bekele

Table of Content

LIST OF TABLES

LIST OF FIGURES

NOMENCLATURE

A loop	Area of a loop
ASTM	American society for testing materials
e	Void ratio
D	Damping ratio
G	Shear modulus
Gs	Specific gravity
Gmax	Initial (maximum) shear modulus
LL	Liquid limit
LI	Liquidity index
PI	Plasticity index
PL	Plastic limit
OCR	Over consolidation ratio
USCS	Unified Soil Classification system
ρ_d	Density of soil
ρ_w	Density of water
τ	Shear stress
γ	Shear strain
τ_c	Shear stress at the tip of hysteresis loop
MER	Main Ethiopian rift
PGA	Peak ground acceleration

CHAPTER 1

INTRODUCTION

1.1 Overview

This chapter provides a comprehensive overview of the study by outlining its background, identifying the motivation behind the research, clearly defining the problem statement, and stating the specific objectives the study aims to achieve. It also delineates the scope and limitations of the research, describe the methodology employed to carry out the investigation, and presents the overall structure and organization of the entire study.

1.2 Background of the Study

Earthquake is one of the most destructive natural phenomena, often resulting in loss of life, severe property damage, and long-term economic disruptions. Although written records of earthquakes date back around 3,000 years in countries like China, this represents only a brief moment in the Earth's geological history. Despite advancements in technology and engineering, hundreds of millions of people worldwide still live in earthquake-prone regions. The threat is global affecting not only countries like the United States and Japan but also many developing nations. With billions of dollars' worth of infrastructure at constant risk, there is an urgent need for strategies to mitigate earthquake impacts.

One of the key factors influencing earthquake damage is the behavior of local soils under dynamic loading. Civil engineering projects, especially those involving foundations, embankments, and critical infrastructures, must account for how soil responds during seismic events. Dynamic loading can cause a range of geotechnical problems, including loss of bearing capacity, excessive settlement, tilting of footings, flow failures, landslides, and ground failures such as lateral spreading and liquefaction. These types of failures can greatly amplify the destructive effects of an earthquake and are largely influenced by the mechanical properties of the soil.

For dynamic analysis, two fundamental properties are particularly important: shear modulus (stiffness) and damping ratio. These properties determine how soil absorbs and dissipates energy under cyclic or repeated loading. Engineers use them to predict how the ground will

behave during an earthquake. Understanding these properties is essential for designing safe and resilient structures, especially in seismically active areas.

In Ethiopia, several studies have already investigated dynamic soil properties in towns such as Dessie, Ziway, Adama, Arba Minch, and areas of Addis Ababa like Gullele and Yeka sub-cities. However, there has been limited research focused on Bole Sub-City, despite its rapid urbanization and growing infrastructure demands. This study aims to fill that gap by determining the dynamic soil properties in Bole using the cyclic simple shear testing method, a reliable laboratory technique for simulating earthquake-like loading. The findings will serve as a valuable resource for future structural designs and earthquake risk assessments in the area.

1.3 Motivation

Addis Ababa, the capital city of Ethiopia, is situated in seismic zone 3 according to the ES EN 2015 standard, indicating a moderate risk of seismic activity. This is especially concerning for rapidly urbanizing areas such as the Bole district, where high-rise buildings and dense infrastructure development are expanding quickly. The behavior of soil during an earthquake plays a critical role in determining the extent of damage to structures, as certain soil types can amplify ground shaking or undergo significant deformation. The extent of structural damage during seismic events is not determined by building design alone but is also heavily influenced by the dynamic properties of the underlying soil. Understanding how the local soil will respond to dynamic loading is therefore essential for ensuring the safety and resilience of buildings in this area. This study aims to address a critical research question: what are the dynamic properties of soils in bole sub city specifically shear modulus and damping ratio that influence its resistance and energy dissipation capacity under earthquake-induced forces?

To address this, it is necessary to conduct a detailed geotechnical investigation focused on identifying the dominant soil types and measuring key dynamic properties namely the shear modulus and damping ratio. These parameters provide insight into the soil’s stiffness and its ability to dissipate seismic energy, directly influencing foundation design and seismic performance of structures. Through this study, we can assess the potential for ground amplification, settlement, or liquefaction, and recommend appropriate engineering solutions to mitigate seismic risk. This investigation is critical not only for protecting current

infrastructure but also for guiding safe urban development in Bole and other growing parts of Addis Ababa.

1.4 Problem Statement

Addis Ababa, the capital of Ethiopia, is located approximately 75–100 km from the western edge of the East African Rift Valley, a region known for its active tectonics and seismicity. However, despite its proximity to an active rift system and the recent occurrence of perceptible seismic events, there has been limited investigation into the dynamic behavior of soils within the city, particularly in rapidly urbanizing areas. One of the most rapidly developing sub-cities, Bole, is experiencing extensive infrastructure growth and increasing population density. In the absence of site-specific data on critical dynamic soil properties such as shear modulus and damping ratio there is a risk that current and future structural designs may not adequately account for local site effects during seismic events. This knowledge gap poses a serious threat to structural safety, public welfare, and long-term urban resilience.

Given the increasing urban density and potential for seismic activity, there is an urgent need to evaluate the dynamic properties of the soils in Bole. This research aims to address this gap and provide essential geotechnical data to inform safer, earthquake-resistant design practices and planning in one of Addis Ababa's most vulnerable and rapidly evolving districts.

1.5 Objectives

1.5.1 General Objective

The general objective of this study is to investigate the dynamic properties of soils in bole sub city, with a specific focus on determining the shear modulus and damping ratio, at selected sites within the Bole sub-city of Addis Ababa. These dynamic soil parameters are critical for understanding how the soil sample behaves under seismic loading conditions. The investigation aims to characterize the stiffness and energy dissipation capacity of the subsoil layers, which directly influence the seismic response of the ground during an earthquake.

1.5.2 Specific Objective

The following specific objectives are comprised:

- ✓ Characterized selected sites in bole sub city conducted through geotechnical field investigations and laboratory testing on both disturbed and undisturbed soil samples collected from selected locations within Bole sub-city.
- ✓ The factors influencing the dynamic properties of soils in the study area were identified and analyzed, including soil type, density, moisture content, and stress conditions.
- ✓ The shear modulus and damping ratio of the soil samples were determined using the cyclic simple shear test, simulating cyclic loading conditions similar to those induced by seismic events.
- ✓ The experimental results were compared with previously published data to evaluate consistency, validate the findings, and assess the variability of soil behavior within comparable geological settings.

1.6 Scope of the Research

- ✓ This thesis was conducted at 2.5 m depth only on five selected sites of bole area.
- ✓ The dynamic property of the soil was determined only by cyclic simple shear testing method.
- ✓ Site characterization was made merely based on geotechnical investigation data.

1.7 Methodology

In conducting this research previous studies and papers related to the determination of dynamic property of soils has been reviewed. In order to have more information about the area, the geology and environmental condition have been studied from available data. For this study site characterization is done by conducting field and laboratory tests namely Grain size distribution, Atterberg limit, Specific gravity, consolidation, in situ density and Natural moisture content test. The Shear modulus and damping ratio of soils in bole area is determined using cyclic simple shear test. Undisturbed sample was used to conduct the dynamic tests.

1.8 Layout of the thesis

This research paper titled "Dynamic Soil Characteristics of Selected Sites in Bole Sub-City is organized into five chapters and appendices. Chapter one covers the introduction, background, problem statement, research motivation, objectives, scope, and methodology. Chapter Two reviews the existing literature on dynamic properties of soils, while Chapter Three details the study area, data collection strategy, resources, and experimental methods.

Chapter Four presents the fundamental soil index test results, the findings from the cyclic shear tests, and a discussion that compares the results with previous research. Finally, Chapter Five concludes the study with key findings and recommendations for future research. The appendices include raw data, supplementary figures, and additional materials referenced throughout the report.

1.9 Chapter Summary

This chapter is a brief entry in to the research paper. It started by introducing the historical aspects of earthquake damage on the world and then proceeded to presenting the driving motivation to conduct the research with the objectives and scope. Then the methodology followed to conduct this thesis is also stated. Finally the layout of the research paper is presented. In the next chapter the review related literatures to the interest topic will be covered in detail.

CHAPTER 2

LITERATURE REVIEW

2.1 Overview

This chapter focused on the theoretical background of dynamic soil properties by identifying and summarizing relevant empirical literature. It began by conceptualizing and defining dynamic soil properties, followed by a review of methods used to determine these properties. The discussion then addressed factors influencing shear modulus and damping ratio, presented typical values for sands and clays, and covered the estimation of maximum shear modulus. The chapter concluded with a summary of key findings from previous research studies.

2.2 Conceptualizing and Defining Dynamic Soil Properties

2.2.1 Dynamic Soil Properties

The behavior of soils under dynamic loads is controlled by the dynamic soil properties [1]. The spread of stress waves through soil layers is referred to as "dynamic loading of soil" [2]. A typical soil subjected to cyclic loading demonstrates hysteresis response. Two parameters can be used to define the general shape of the hysteresis loop created by the cyclic loading of a typical soil, or the loop's course itself. These parameters are damping ratio and shear modulus[3].

2.2.2 Shear Modulus and Damping Ratio

One measure that shows how resistant a material is to the applied dynamic loading is its shear modulus. Put differently, it serves to symbolize the soil stiffness [3]. The secant modulus, G, which is obtained from the extreme points on the hysteresis loop, is commonly employed to represent shear modulus because the majority of soils have curvilinear stress-strain relationships, as illustrated in Figure 1. It must be calculated in connection with the induced strain in a specimen or soil deposit. The amplitude of strain for which the hysteresis loop is calculated determines its value [4], [5]. The slope of the line connecting two extreme points at a particular shear strain on the hysteresis loop, as illustrated in Figure 1 G, is usually considered to be the ratio of the corresponding cyclic shear stress (τ) to the cyclic shear strain (γ) [6].

$$G = \frac{\tau}{\gamma} \quad \text{---------- Equation 2.1}$$

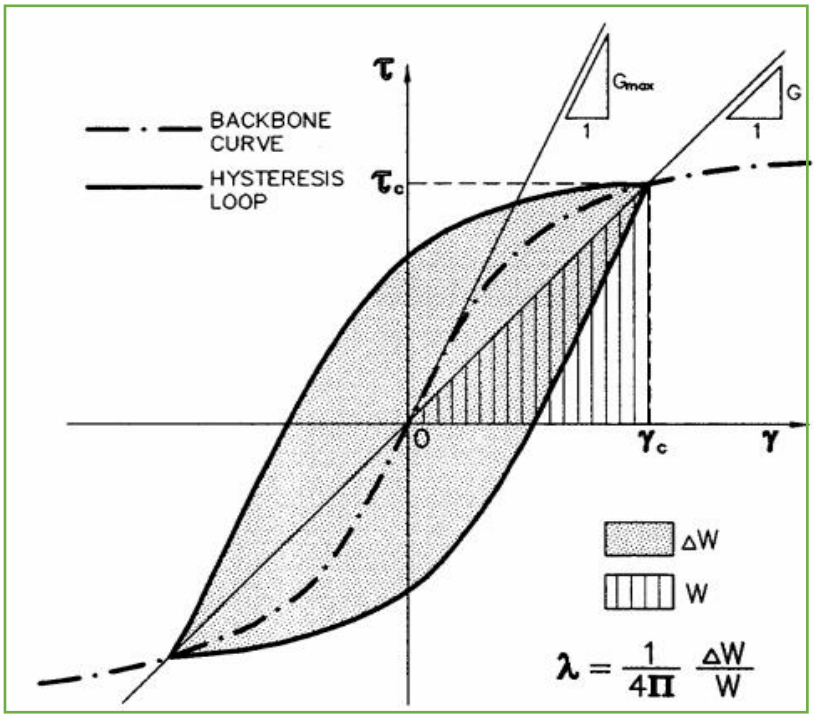

Figure 1 : Hysteretic Stress Strain Response of Soil Subjected to Cyclic loading [9]

The damping ratio, which is a gauge of energy dissipation, rises as cyclic shear strain becomes more intense. As seen in the accompanying image, it is also proportional to the area inside the hysteresis loop. The dissipation of energy in the soil is represented by this hysteresis phenomenon. Heat, friction between the solid components of the skeleton and relative motion between the soil skeleton and the pore fluid are some of the mechanisms that release energy. [1], [3], [4]. The Damping ratio can be determined from the following Equation 2.2 [7].

$$D = \frac{\Delta W}{4\pi W} \text{----------Equation 2.2}$$

Where W – The maximum stored energy

ΔW- The energy lost per cycle inside the hysteresis loop

Radiation damping and material damping are two essentially different damping processes that are related to soils. Any vibration wave in soil can cause material damping, also known as internal damping. It can be thought of as a measurement of the energy lost in vibrations,

mostly due to soil material yielding and hysteretic activity. The energy dissipated from the structure by wave radiation is measured by radiation damping, a purely geometric effect [8].

Excitation progressively decreases until it is undetectable due to soil damping [2]. In the linear elastic range, the hysteretic damping model should theoretically have no energy loss. In contrast, even at very modest strain levels, laboratory specimens consistently exhibit significant energy dissipation. At extremely low strain levels, the damping ratio remains constant and is known as the small-strain damping ratio (D_{min}). At higher strains, nonlinearity in the stress–strain relationship leads to an increase in material damping ratio with increasing strain amplitude [8].

The measurement of dynamic soil properties is essential for understanding soil response to dynamic loads, analyzing earthquake effects on structures, addressing soil-structure interaction problems, predicting ground motion, and conducting seismic zonation [7].

2.2.3 Maximum Shear Modulus (G_{max})

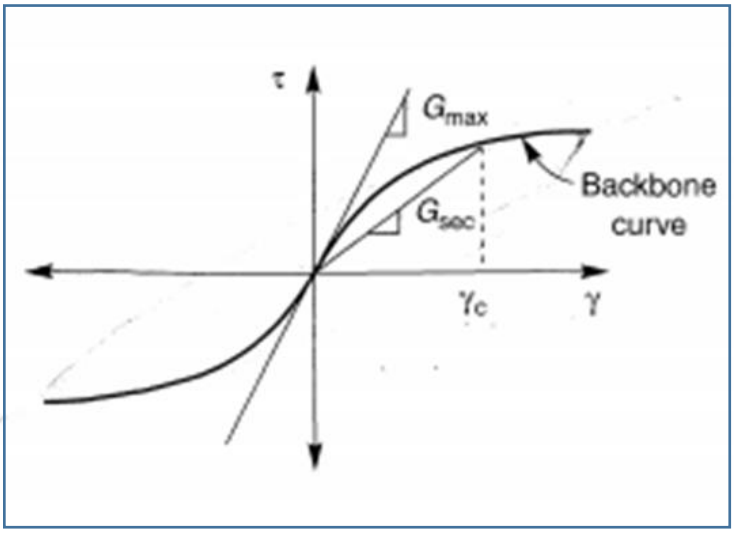

Figure 2: Backbone curve showing variation of $\mathbf{G}_{max}$ with shear strain [1]

The set of points that represent the tips of the hysteresis loops for various cyclic strain amplitudes is called a backbone (skeleton) curve .The greatest value of the shear modulus, G max, is represented by the slope of the backbone (skeleton) curve at the origin (zero cyclic strain amplitude). Small-strain shear wave velocity (V_s) is directly related to small-strain shear modulus (G max) by [1].

$$G_{max} = \rho V_s^2 \quad \text{---------- Equation 2.3}$$

Where G_{max} – is the maximum (initial) shear modulus

ρ – is the density of a soil deposit V_s^2 -is the shear wave velocity

When shear wave velocity measurements are not available, G_{max} can be estimated in different ways. Also Hardin have shown that for many undisturbed cohesive soils as well as sands G_{max} can be calculated from [9].

$$G_{max} = 3.23 \times \frac{(2.97-e)^2}{1+e} \times (OCR)^a \times (\sigma_0)^N \text{ ---------- Equation 2.4}$$

Where e is the void ratio of the soil,

OCR the over consolidation ratio

a - an over consolidation ratio exponent,

σ_0 the mean principal effective stress [$\sigma_0 = (\sigma_1 + \sigma_2 + \sigma_3)/3$],

N a stress exponent, often taken as N=0.5

Table 1: Over consolidation ratio exponent [9]

Plasticity index	0	20	40	60	80	>100
A	0.00	0.18	0.3	0.41	0.48	0.5

2.3 Methods of Determining Dynamic Soil Properties

For field and laboratory tests, various test procedures have been used to determine shear moduli and damping characteristics. The main procedures can be summarized as seen in Figure 3.

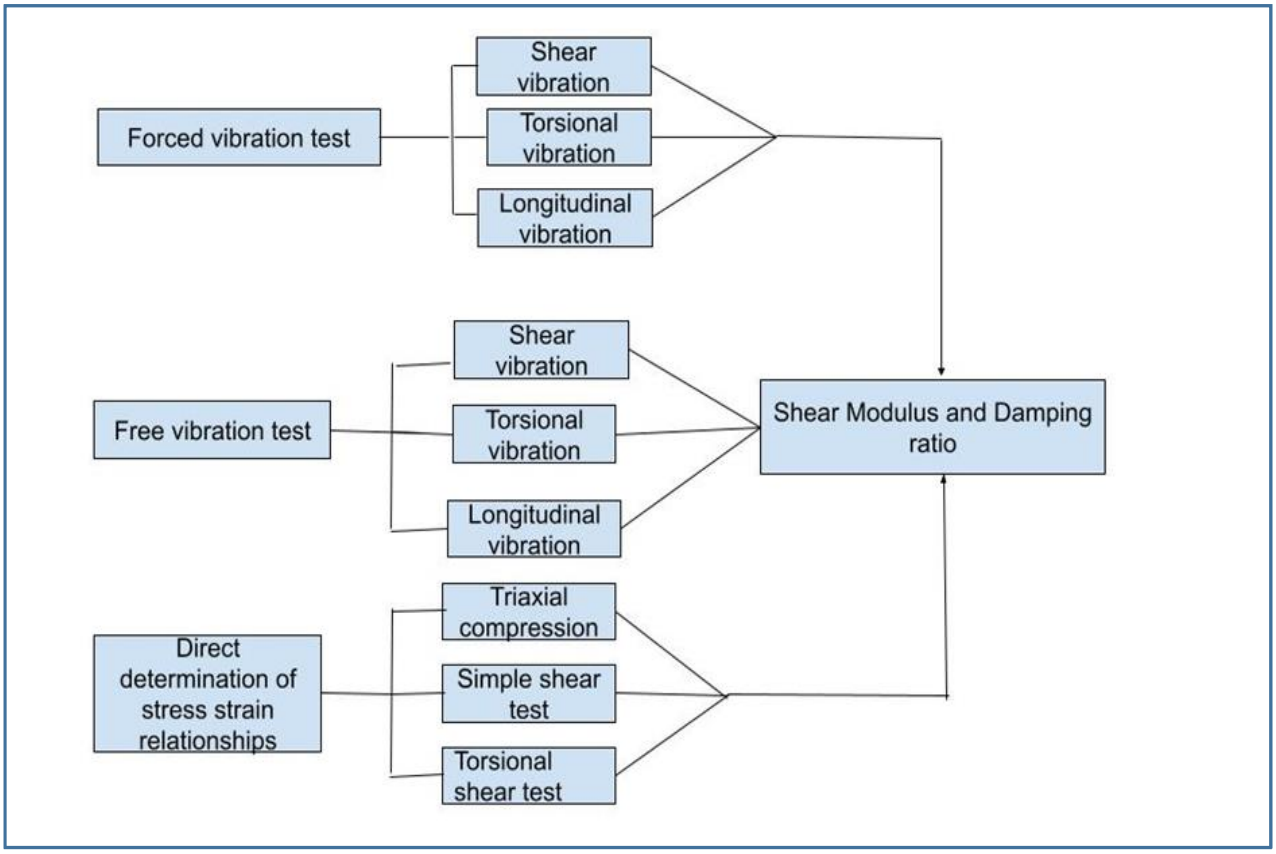

Figure 3: Procedures for determining dynamic soil properties

a. Forced vibration tests

This method finds the damping factor and shear moduli by evaluating the responsiveness at different frequencies and identifying the resonant frequencies. Laboratory tests have made use of shear vibrations applied to soil layers on a shaking table as well as longitudinal and torsional vibrations applied to cylindrical samples [10].

b. Free vibration test

The free vibration test is used to determine a soil's shear modulus and damping ratio by analyzing how vibrations decay after a brief excitation. The soil sample is set into motion and allowed to vibrate freely. The decay response of the soil sample is used to quantify shear moduli and damping factors. This method is effective for assessing soil behavior at low to moderately high strain levels, useful in seismic and dynamic site analysis [10].

c. Direct determination of stress- strain relationship

This approach evaluates the hysteretic stress-strain relationships to estimate the shear moduli and damping factors. The hysteretic stress strain relationships can be assessed in a lab setting

using tri axial compressional testing, simple shear testing, or torsional shear testing under cyclic loading conditions [10].

Table 2: Test procedures [11]

General Procedure	Test condition	Approximate Strain range (γ)	Properties that can be determined
Direct Determination of Hysteresis stress strain relationship (Moderate to high strain)	Tri axial compression	10^{-2} to 5%	Modulus Damping
	Simple shear	10^{-2} to 5%	Modulus Damping
	Torsional shear	10^{-2} to 5%	Modulus Damping
Forced vibration (Low to moderate strain levels)	Longitudinal vibration	10^{-4} to 10^{-2}%	Modulus Damping
	Torsional vibrations	10^{-4} to 10^{-2}%	Modulus Damping
	Shear vibration-lab	10^{-4} to 10^{-2}%	Modulus Damping
	Shear vibration-field	10^{-4} to 10^{-2}%	Modulus Damping
Free vibration tests (Low to moderate high strain levels)	Longitudinal vibration	10^{-3} to 1%	Modulus Damping
	Torsional vibration	10^{-3} to 1%	Modulus Damping
	Shear vibration-lab	10^{-3} to 1%	Modulus Damping
	Shear vibration-field	10^{-3} to 1%	Modulus Damping
Field wave velocity measurements	Compression waves	$5*10^{-4}$%	Modulus
	Shear waves	$5*10^{-4}$%	Modulus

2.4 Deformation Characteristics Based on Strain Ranges

The quantity of shear strains that a soil is subjected to determines how much its deformation characteristic fluctuates. Elastic, Elasto - plastic, and failure states of stress are produced within the approximate range of shear strains caused [2][12].

In the small strain region (less than 10^{-5}), soil behavior is generally linear, as the stress-strain curve closely follows the initial tangent at zero strain. In this range, the deformation exhibited by the soil is purely elastic and fully recoverable, with almost no hysteresis effects observed.

This means energy dissipation is minimal, and the response is dominated by reversible elastic behavior. Phenomena typically associated with this strain range include vibration and wave propagation through soil layers, which are critical in dynamic analyses such as seismic wave transmission and machine-induced ground vibrations.

At strain levels around 10^{-5}, soils typically exhibit a softening nonlinearity, characterized by a decrease in modulus as strain increases. This range also shows larger hysteresis in the stress-strain relationship and strain-dependent material damping. In the middle strain range (10^{-4} to 10^{-2}), soil behavior becomes elasto -plastic, with irrecoverable permanent deformations such as cracks and differential settlements occurring. In the large strain range (greater than 10^{-2}), strains increase significantly without a corresponding rise in shear stress, leading to soil failure. This stage is associated with phenomena like slope slides, compaction, and liquefaction of cohesion less soils, which all induce large strains and can result in catastrophic failure.

2.5 Antecedents of shear modulus and damping ratio

With the dependent variable shear modulus and damping ratio clearly defined this section identifies potential antecedents (independent variables) of such shear modulus and damping ratio.

2.5.1 Shear Strain Amplitude on Shear Modulus and Damping Ratio

Soils exhibit a distinct nonlinear stress-strain behavior as cyclic shear strain increases primarily reflected by the variation of shear modulus and damping ratio. The shear modulus decreases with increasing shear strain. At the same time, the damping ratio, increases with increasing shear strain. These relationships are commonly illustrated in previous researches [2], [4], [6], [8], [13].

2.5.2 Number of Cycles on Shear Modulus and Damping Ratio

Due to strength degradation occurring from cycle to cycle as the number of cycle rises, up to the first 10 cycles the shear modulus marginally increases and the damping ratio falls for a given value of mean effective stress and shear strain. Furthermore, when stress application is repeated for more than 10 times, the effect of the number of cycles essentially vanishes [3], [4], [7], [8] .

2.5.3 Plasticity Index

Soils become more resilient to cyclic loading as Plasticity index increases, and modulus decrease occurs more gradually [14],[2],[6],[13].

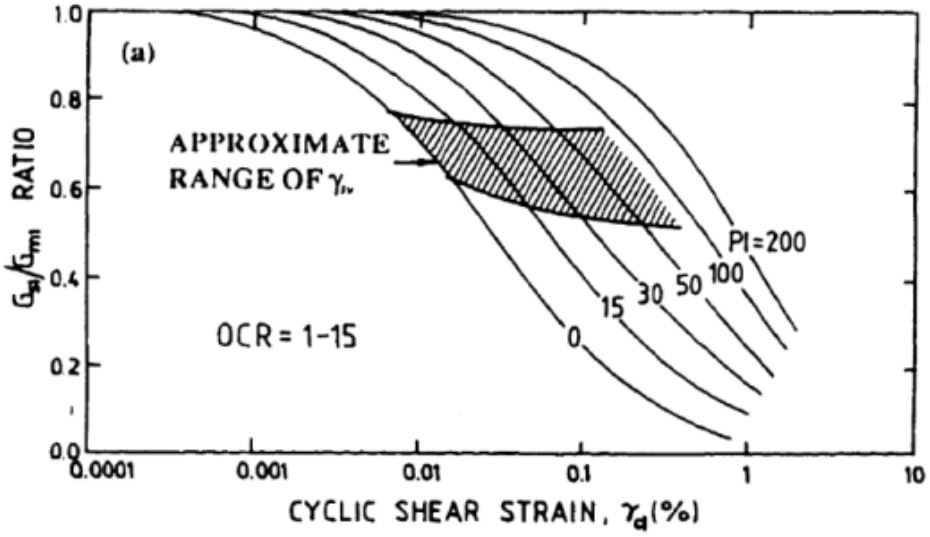

Figure 4: Effect of plasticity index on shear modulus degradation [14]

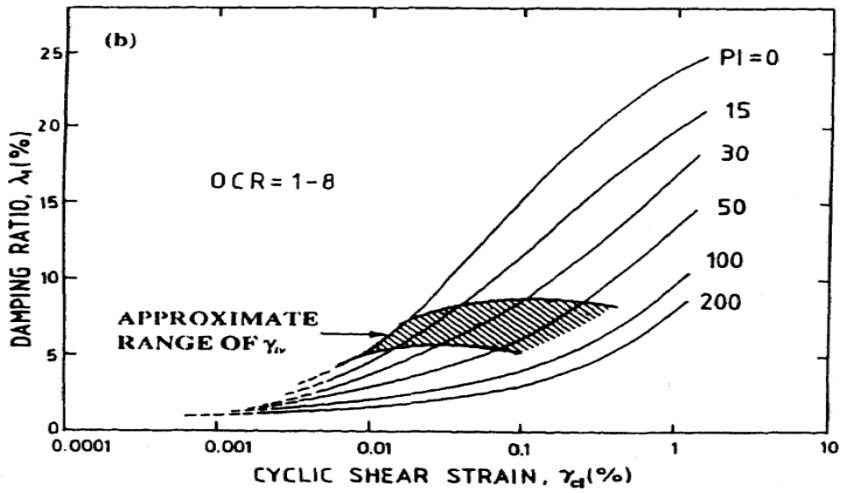

Figure 5 : Effect of plasticity index on damping ratio[14]

2.5.4 Confining Pressure on Shear Modulus and Damping Ratio

The soil's shear modulus rises and the damping ratio falls as confinement increases. This impact is primarily noticeable in soils with low cohesiveness. Nevertheless, the normalized shear modulus values of cohesive soils are not significantly affected by confining pressure [2], [4], [5], [6], [7], [8], [13] .

There is a clear relationship between axial stress and both the shear modulus and the damping ratio. Specifically, as the axial stress increases, the shear modulus also increases, indicating that the soil becomes stiffer and more resistant to deformation under higher axial loading. This is because, at higher axial stresses, soil particles are more tightly compressed, which enhances the soil's ability to resist shear forces. On the other hand, the damping ratio decreases as axial stress increases. This suggests that the soil's ability to dissipate energy, or its tendency to resist vibrations and oscillations, diminishes under higher axial stresses.

Table 3**:** Effect of increase of various factors on G_{max}, G/G_{max} and damping ratio, D of normally consolidated and moderately over consolidated clays[2], [14]

Increasing factor	Maximum shear modulus (G max)	Shear modulus Degradation (G/ G max)	Damping ratio (D)
Confining pressure(σ)	Increase with σ	Stays constant or Increases with σ	Stays constant or decreases with σ
Cementation (c)	Increases with c	May increase with c	May decrease With c
Cyclic strain(γ_c)	—	Decreases with γ_c	Increase with γ_c
Geological age (t)	Increases with t	May increase with t	Decreases With t
Plasticity index (PI)	Increases with PI if OCR >1; stays about Constant if OCR =1	Increase with PI	Decrease With PI
Number of loading Cycles (N)	Decreases after N cycles of Large γc but recover later with time	Decreases after N cycles of Large γ_c (G_{max} measures before N cycles)	Not Significantly for Moderate γ_c And N
Over consolidation (OCR)	Increase with OC	Not affected	Not affected
Void ratio (e)	Decreases with e	Increases with e	Decreases with e

2.6 Shear Modulus and Damping of Sands

The shear modulus and damping ratio of sands are influenced by confining pressure, strain amplitude, void ratio and loading cycles. Higher confining pressure increases shear modulus and decreases damping ratio due to denser particle packing, while increasing strain amplitude reduces shear modulus and raises damping ratio as particle rearrangement and energy dissipation intensify. Lower void ratios (denser sands) result in higher shear modulus and lower damping ratio, whereas higher void ratios (looser sands) show the opposite trend. Repeated loading cycles may weaken the sand structure, reducing shear modulus and

potentially increasing damping ratio over time. Understanding these factors is essential for predicting the dynamic behavior of sandy soils [10], [9] .

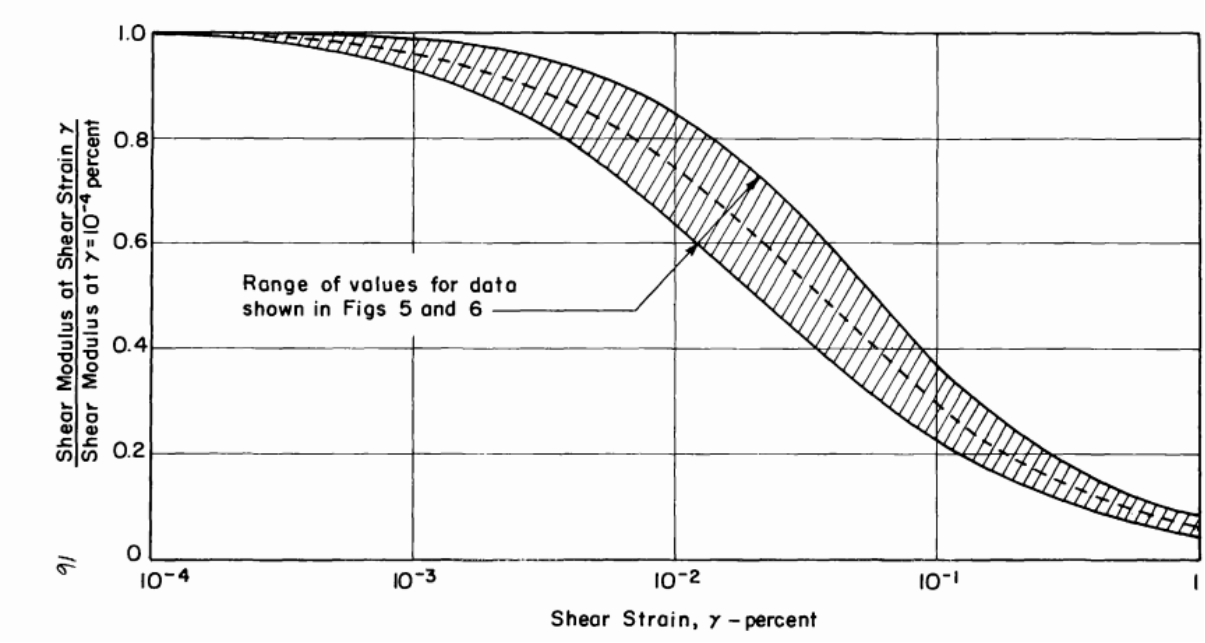

Figure 6: Variation of shear modulus with shear strain for sands [10]

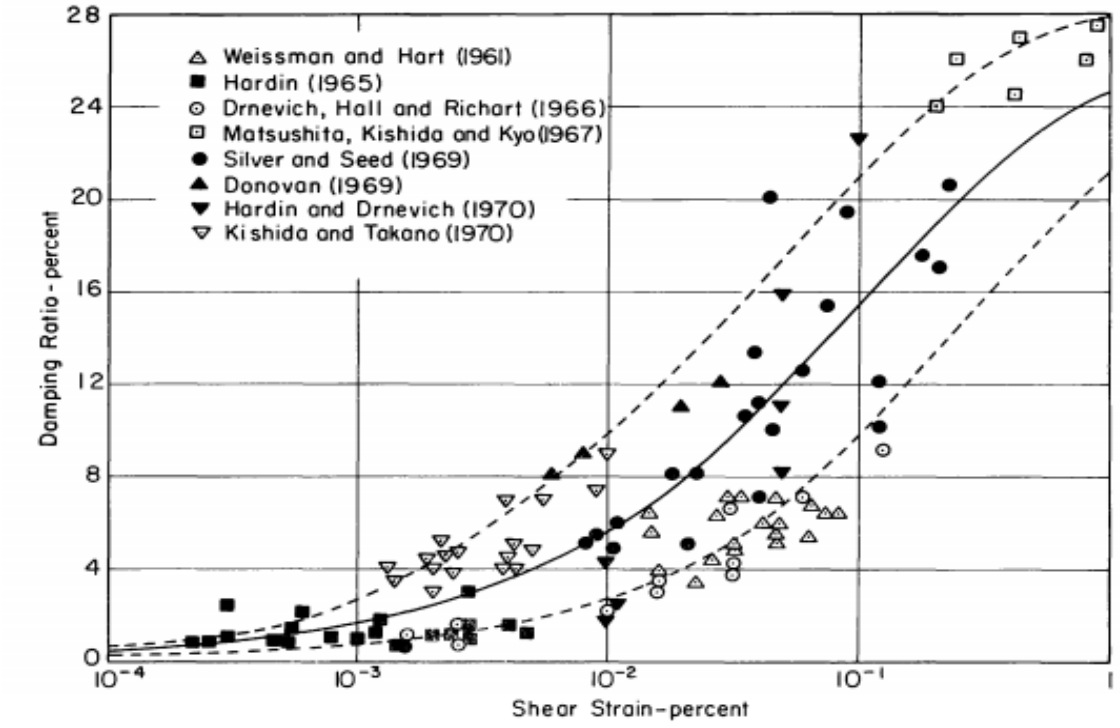

Figure 7 : Variation of damping ratio with shear strain for sand [10]

2.7 Shear Modulus and Damping of Clays

The shear modulus and damping ratio of clays are primarily influenced by shear strain amplitude and sample disturbance, with the clay's relative strength and stiffness also playing a key role. As shear strain amplitude increases, the shear modulus decreases and the damping ratio rises due to structural softening and energy dissipation. Sample disturbance typically reduces the shear modulus and increases the damping ratio by compromising the clay's natural structure. Additionally, stronger and stiffer clays generally exhibit higher shear moduli and lower damping ratios compared to weaker, softer clays [2].

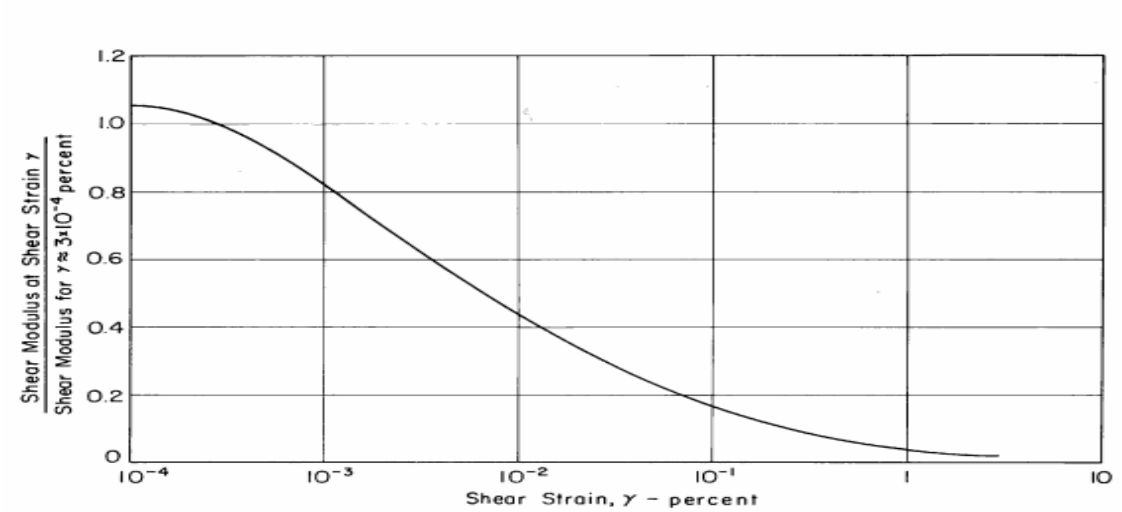

Figure 8: Typical reduction of modulus with shear strain for saturated clay[10]

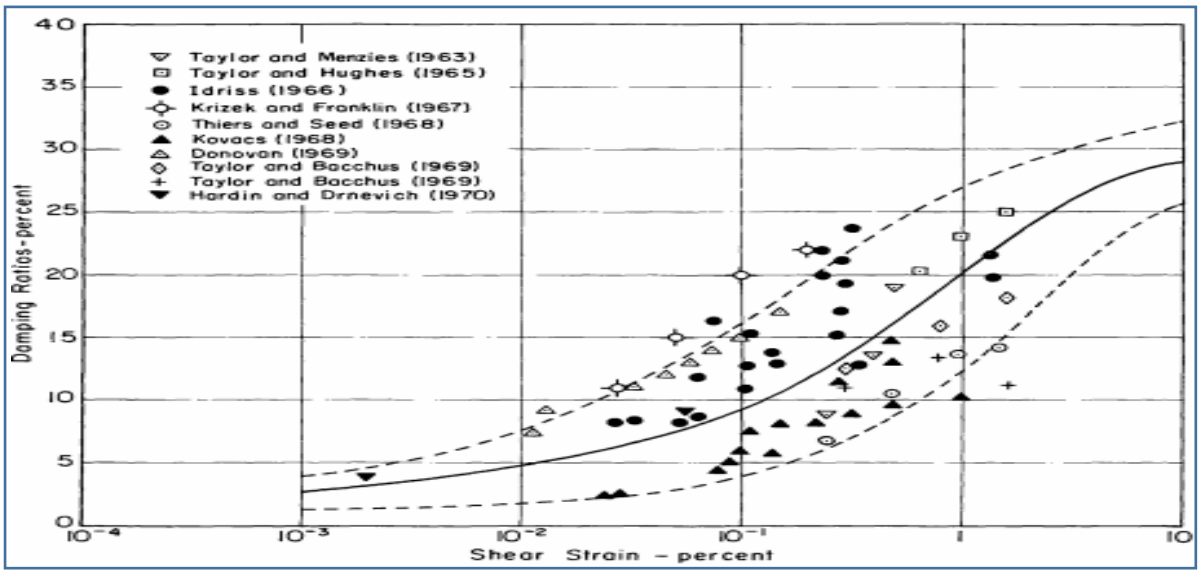

Figure 9: Damping ratio for saturated clay summarized [10]

2.8 Detailed Review of a Previous Works on Dynamic Property Determination

Various investigations have been conducted both outside Ethiopia and in different regions within Ethiopia to study the dynamic properties of soils. Among these studies, Abreham Mengistu (2013) investigated the dynamic properties of soils in Ziway Town. His findings, based on cyclic simple shear test results, revealed that the shear modulus ranged from 1 to 8 MPa for medium strain levels ($0.01\% < \gamma < 0.1\%$) and from 8 to 25 MPa for higher strain levels ($\gamma > 0.1\%$). The damping ratio values varied between 2.85% and 10% for medium strain levels and between 10% and 27% for higher strain levels. Similarly, Abu Gemechu (2011) determined the dynamic properties of soils in Adama Town, finding shear modulus values ranging from 0.17 to 17.3 MPa and damping ratio values between 0.29% and 39.52%. Ayalew (2012) studied the soils in Hawassa Town, with shear modulus values ranging from 0.411 to 12.85 MPa and damping ratios from 0.0219% to 39.3304%. Mengesha (2013) investigated the soils in Arbaminch Town, where the shear modulus values ranged from 1.198 to 17.96 MPa, and the damping ratio varied from 1.9069% to 38.309%.

In addition to these studies, Natnael (2020) focused on the dynamic properties of soils in Yeka Sub city of Addis Ababa, reporting shear modulus values from 0.11 to 27.79 MPa and damping ratios ranging from 1.11% to 34.95%. Teshome (2019) conducted similar research in Jimma Town, finding shear modulus values between 0.33 and 7.01 MPa and damping ratios between 2.03% and 22.98%. Yohannes (2017) studied the soils in Modjo Town, with shear modulus values ranging from 0.11 to 22.98 MPa and damping ratios between 0.25% and 25.63%. These studies contribute valuable data on the dynamic properties of soils across different regions of Ethiopia, helping to enhance the understanding of soil behavior under dynamic loading conditions in the country.

Table 4: Summary of Previous researches on dynamic soil property determination of Ethiopian context

Researcher	Soil type	Dynamic soil property determination technique	Axial stresses and shear strain amplitude	Research findings for the values of shear modulus and damping ratio

Abreham mengistu[15]	Silt and Silty sand	Cyclic simple shear test (Remolded sample)	- 100,200,300 and 400 kPa -0.01%,0.1%, 1%,2.5%,5%	Shear modulus is 1-8MPa for medium strain level (0.01 %< γ <0.1 %) and - 8 to 25MPa for higher strain level (γ >0.1 %) Damping ratio is -2.85 to 10 % for medium strain level -10.0 to 27.0 % for higher strain level
Natnael (2020)[2]	Elastic silt and plastic clay	Cyclic simple shear test (Undisturbed sample)	-100,200 and 400 kPa -0.01%,0.1%, 1%,2.5%,5%	Shear modulus is in the range of 0.11-27.79 MPa Damping ratio is in the range 1.11 % to 34.95 %
Abu gemechu (2011)[4]	Silty sand and silt	Cyclic simple shear test	-100,250,400 kPa -0.01%,0.1%, 1%,2.5%,5%	-Shear modulus is in the range 0.17 -17.3 MPa -Damping ratio is in the range 0.29% to 39.52%
Ayalew (2012)[7]	Sandy silt and Silt	Cyclic simple shear test (remolded)	-100, 250 and 400 kPa -0.01%,0.1%, 1%,2.5%,5%	- Shear modulus values ranges from 0.411 -12.85 MPa - The damping ratio values ranges between 0.0219% to 39.3304%
Mengesha (2013)[8]	Silt and clay	Cyclic simple shear test (remolded)	-100, 200 and 400 kPa -0.01%,0.1%, 1%,2.5%,5%	- Shear modulus values ranges from 1.198 -17.96 MPa - The damping ratio values ranges between 1.9069 % to 38.309%
Teshome (2019)[6]	Silt and clay	Cyclic simple shear test	-0.01%,1%, 2.5%, 5%, -100, 250 and 400kPa	- The shear modulus values ranges from 0.33-7.01 MPa - The damping ratio values ranges between 2.03 % to 22.98 %.
Yohannes (2017)[13]	Highly plastic silt soils and Silty sand	Cyclic simple shear test (remolded)	-0.01%,0.1%, 1%,3%,5% -100, 200, 400 kPa	- Shear modulus values ranges from 0.11-22.98 MPa . The damping ratio values ranges between 0.25 % to 25.63 %

2.9 Literature Context Gaps and Weaknesses

From a contextual standpoint, it is important to note that all previous studies concerning the dynamic properties of soils were conducted in locations outside of Bole Sub-City. In fact, with the exception of a single investigation carried out in Yeka Sub-City, none of these studies were performed within the administrative boundaries of Addis Ababa. This indicates a significant gap in localized geotechnical research, particularly for Bole Sub-City, where understanding the dynamic behavior of soils is crucial for safe and effective urban planning, infrastructure development, and seismic risk assessment. Consequently, there is a pressing need for site-specific investigations to provide accurate and reliable data for engineering design and hazard mitigation in this area.

CHAPTER 3

OVERVIEW OF STUDY AREA AND EXPERIMENTAL METHODS

3.1 Overview

This chapter provides a comprehensive overview of the study areas, focusing on their geographical location, underlying geology, and seismic activity. The section delves into the specific characteristics of the study sites, highlighting the geological formations and structural features that are relevant to understanding the dynamic behavior of the soils in these regions. Additionally, the chapter outlines the seismicity of the areas, offering insights into the historical and potential seismic events that could impact soil stability and infrastructure. In the latter part of the chapter, a detailed description of the research methods employed in this study is presented. This includes the experimental techniques, data collection processes, and analytical approaches used to assess the dynamic properties of soils in the study areas. By combining this background information with a clear explanation of the research methodology, the chapter sets the foundation for the results and discussions that follow, providing readers with a thorough understanding of the study's context and approach.

3.2 Location of Bole

Bole Sub-City is one of the most rapidly developing areas in Addis Ababa, located in the southeastern part of the city. It is composed of 11 woredas (districts), each contributing to the diverse demographic and economic dynamics of the region. The total area of Bole Sub-City spans approximately 6,371 hectares, making it one of the larger sub-cities in Addis Ababa. The region exhibits varying topography, with a minimum elevation of 2,225 meters above sea level and a maximum elevation of 2,344 meters. This relatively mild elevation variation contributes to the region's unique landscape and urban development challenges.

With a current population estimated to be 308,995, Bole Sub-City is experiencing rapid urbanization, with significant increases in both residential and commercial construction. Alongside this population growth, economic activities in the area have been booming, particularly in sectors like retail, hospitality, and transportation. However, such rapid expansion also brings with it considerable risks, particularly in terms of environmental hazards. Given the increasing density of buildings and infrastructure, combined with the region's proximity to seismic fault lines, the threat of earthquakes poses a serious risk to the

safety and stability of the sub-city. In particular, the vulnerability of poorly constructed or unreinforced buildings to seismic forces can result in widespread damage, posing significant challenges for urban planning, disaster preparedness, and risk mitigation strategies in the future.

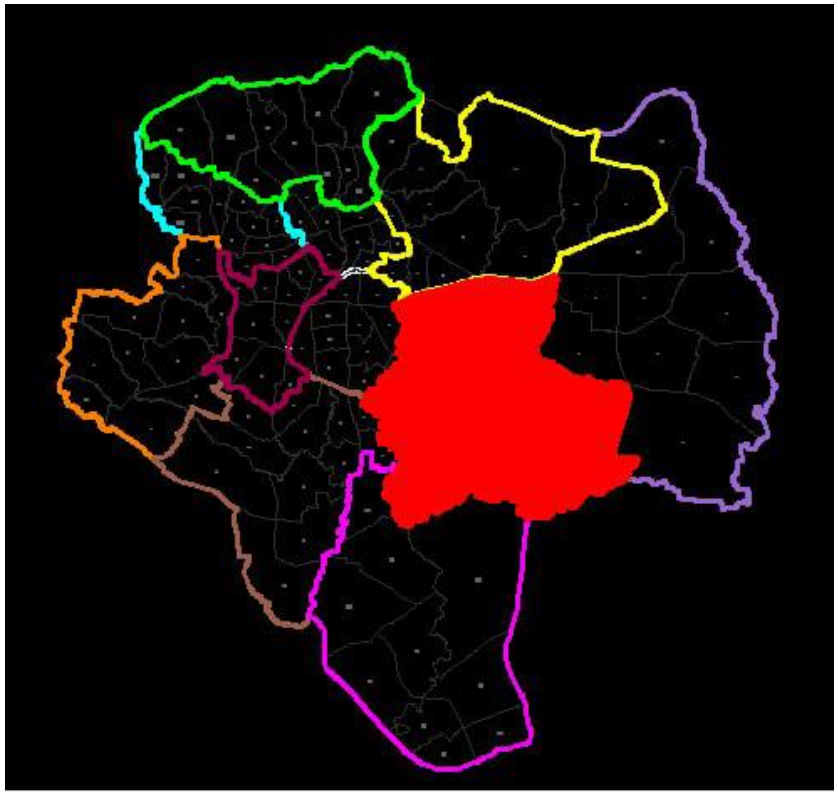

Figure 10 : Sub city boundaries of Addis Ababa city (Addis Ababa City Plan and Development Commission)

3.3 Geology of Addis Ababa

Addis Ababa's geology is predominantly composed of volcanic rocks with both basic and acidic compositions, primarily from the Pliocene to Pleistocene epochs, making them the youngest volcanic formations in the region. The acidic rocks include silicic lavas and pyroclastics, such as the Balchi rhyolites, which consist of tuffs, ignimbrites, rhyolites, and trachytes. These rocks are exposed in the southern and eastern parts of the city and extend beyond its boundaries.

The geology of Bole Sub-City is dominated by Miocene to Pliocene olivine-rich basalts, part of the Bishoftu basalt flows that extend toward Akaki and Debrezeit. These basalts, often columnar jointed, are overlain by pyroclastic deposits like welded tuffs and ignimbrites from

explosive volcanic activity. Surface weathering has produced expansive black cotton soils , which pose construction challenges due to their high shrink-swell potential[16].

3.4 Seismicity of Addis Ababa

The East African Rift system's Main Ethiopian Rift (MER) is a sector that tends toward the northeast and consists of a number of rift segments that run from the Afar Triple Junction at the Red Sea-Gulf of Aden intersection to the Kenya Rift. As seen in the following **Error! eference source not found.**, the MER is defined by vigorous extensional tectonics that can accommodate the relative movement between the African and Somalia plates of about 6–7 mm/yr. [17].

Figure 11 : Geodynamic setting of the Main Ethiopian Rift[17]

3.4.1 Ethiopian building code standard (ES, EN 1998:2015)

According to this code Ethiopia was divided in to five distinct seismic zones based on the local hazard with zone 3 being designated for Addis Ababa with a PGA of 0.1 g. The hazard is described by design ground acceleration. The design ground acceleration was chosen for a seismic zone that corresponds to a reference return period of 475 years.

Table 5 Bedrock acceleration ratio (ES EN 1998:2015**)**

Zone	5	4	3	2	1
α_0	0.2	0.15	0.1	0.07	0.04

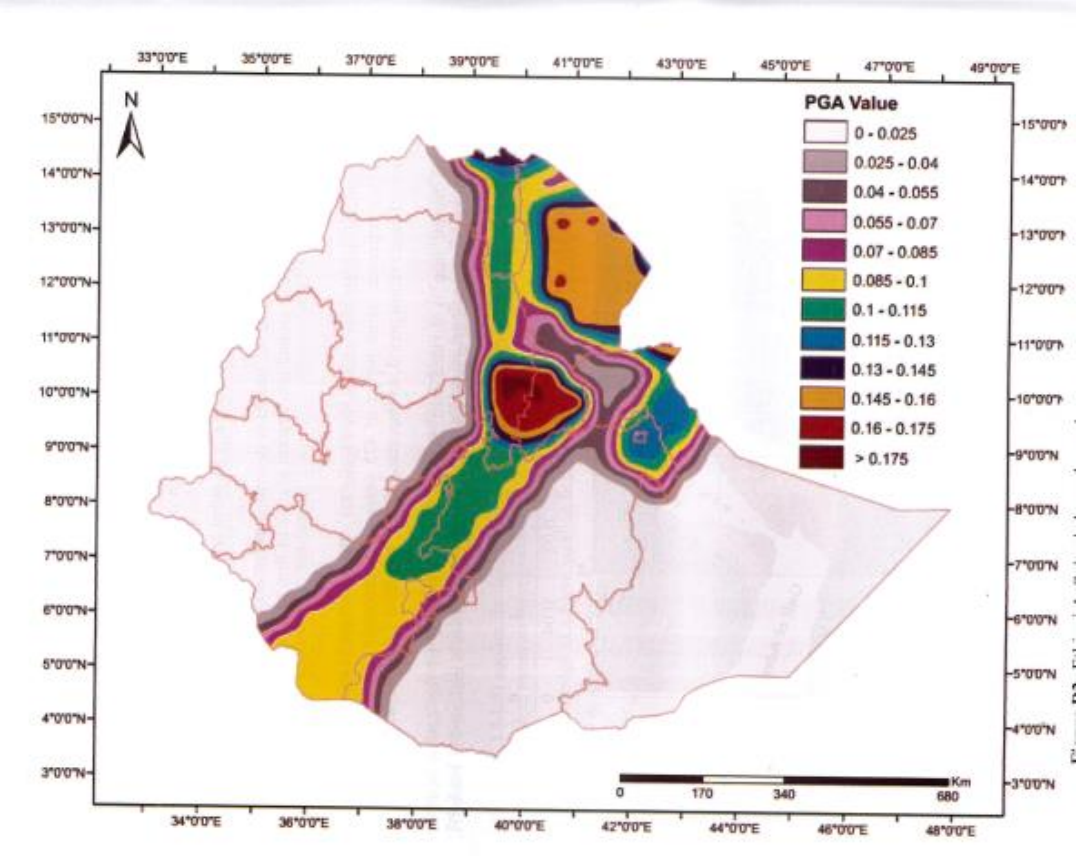

Figure 12 Ethiopia's seismic hazard map in terms of peak ground acceleration [18]

3.5 Experimental Design

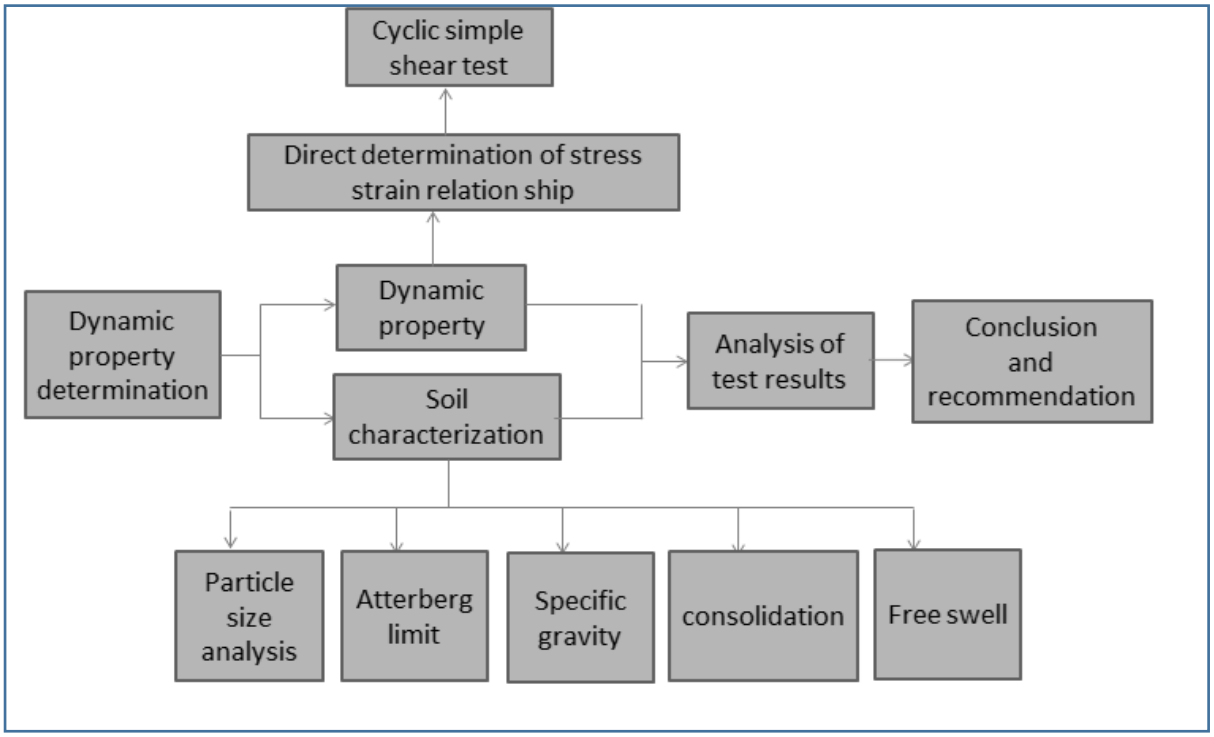

Figure 13: Flow chart showing the general work flow of the study

The chart shows the detail procedure followed for dynamic property determination and soil characterization tests employed in conducting this research , which involves several key steps. Initially, the dynamic properties of the soil are assessed, leading to a direct determination of the stress-strain relationship through a cyclic simple shear test. Simultaneously, soil characterization is performed, including particle size analysis, Atterberg limit determination, specific gravity assessment, consolidation testing, and free swell measurement. The data obtained from dynamic property determination and soil characterization are subsequently analyzed to generate comprehensive test results. Finally, conclusions and recommendations are formulated based on the analysis.

3.5.1 Sample Collection Methods

Soil samples were taken from 5 selected test pits on bole area. The five test pits were excavated using local labor and samples were collected from each test pit at 2.50 m depth. Disturbed and undisturbed soil samples were collected from test pits .The dynamic tests were performed on the undisturbed soil sample. The field density of the soil was determined using core cutter method. Index properties of the soils are also determined using disturbed but representative sample. Tube sampling techniques are used to extract undisturbed soil as per

ASTM D1587-94 specification. Polythene bag is used for sampling and transporting representative disturbed soil samples according to ASTM D 4220-95.

Table 6**:** Location of the selected test pits

Label	N	E
Test pit 1	8°59’39”	38° 47’24”
Test pit 2	9°1’6”	38° 48’8”
Test pit 3	8°59’0.99”	38° 47’0.79”
Test pit 4	9°0’19”	38° 47’43”
Test pit 5	9°1’30”	38° 48’27.24”

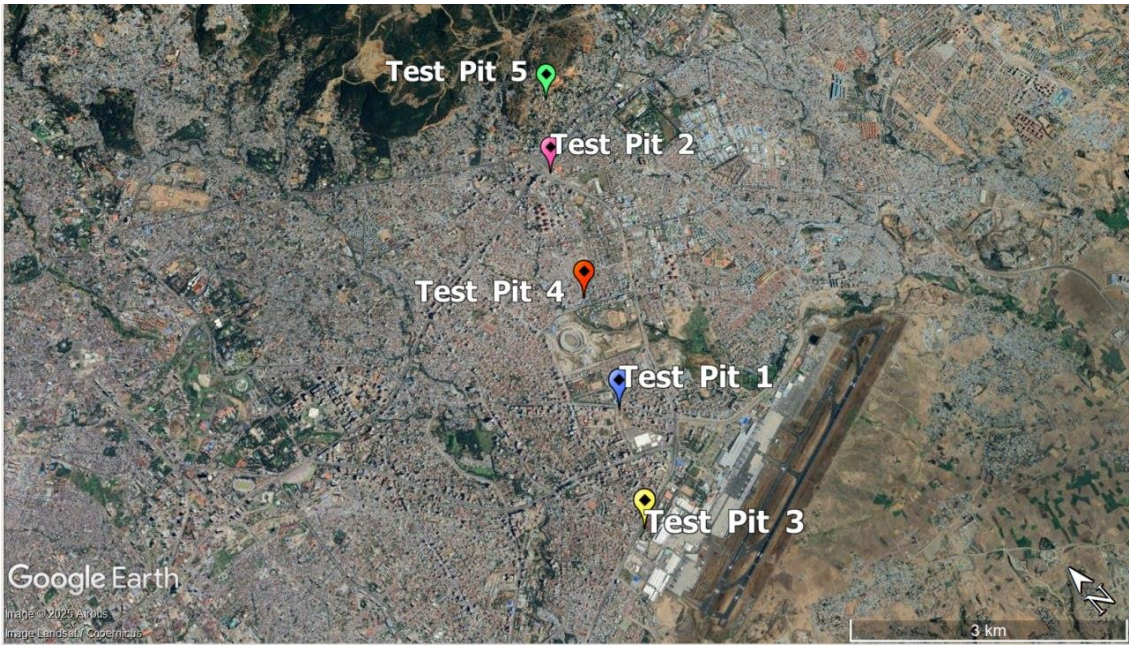

Figure 14 : Location of test pits

3.5.2 Laboratory Tests for Soil Characterization

Soil samples were collected to determine various geotechnical properties essential for the study. Disturbed soil samples were obtained and tested in accordance with the relevant ASTM standards to perform particle size analysis; Atterberg limits determination, specific gravity measurement and free swell .In addition, undisturbed soil samples were collected to carry out tests such as natural moisture content test and in situ density determination, the consolidation test, and the cyclic simple shear test. These tests provide a comprehensive

understanding of the soil's physical and mechanical behavior under different loading conditions.

3.5.3 Dynamic Soil Tests

Soil properties that influence the wave propagation and other low strain phenomena include stiffness, damping, poisson's ratio and density. Of these stiffness and damping are critical to the evaluation of many geotechnical earthquake engineering problems not only for low strain but as soils are nonlinear materials also for intermediate and high strains. A wide variety of low strain and high strain element tests are available to determine both shear moduli and damping characteristics [1].

Low-strain element tests, including the resonant column test, ultrasonic pulse test, and piezoelectric bender element test, evaluate soil properties at low strain levels. In contrast, high-strain element tests assess soil behavior at high shear strain amplitudes, where soils exhibit volume change under drained conditions or changes in pore pressure (and effective stress) under un drained conditions. Since soil behavior is governed by effective stresses, high-strain tests must accurately control pore water drainage and measure volume changes.

The cyclic simple shear test is a convenient method for determining the shear modulus and damping ratio of soils, as well as studying the liquefaction parameters of saturated cohesion less soils to assess their resistance to liquefaction. It is advantageous because it closely represents field conditions by allowing specimens to be consolidated in the K_0 state, and it covers a wide range of strain amplitudes (from 10^{-2}% to about 5%), which is typical of seismic ground motion. The test apparatus, which may consist of a hinged plate rectangle box or a wire-reinforced cylindrical membrane, utilizes an electronic reading system to record lateral and axial forces and displacements, controlled by the UTS004 software application that facilitates consolidation and cyclic simple shear tests. The device is equipped with a mechanism to apply a horizontal cyclic shear force and a continuous vertical load while allowing horizontal deformation of the sample during cyclic loading.[19]

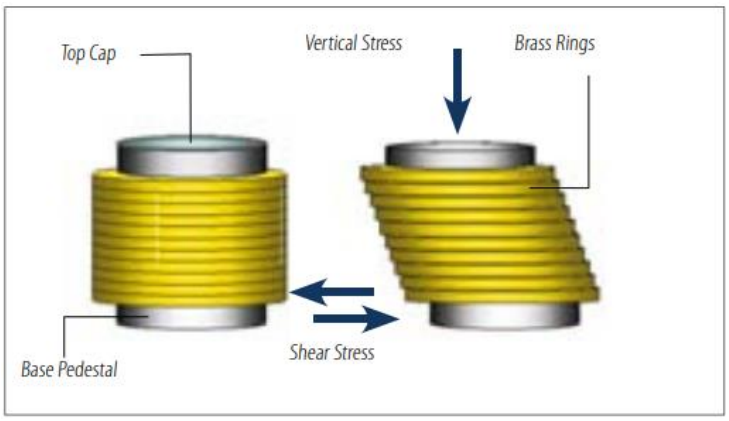

Figure 15 : The movement of rings in shearing stage

The cyclic simple shear machine has a fixed top half with a vertical ram allowing only a vertical movement and a moving bottom half mounted on roller bearings. An undisturbed cylindrical specimen (20 mm height, 70 mm diameter) is supported by a rubber membrane and slip rings to maintain diameter during testing. During the consolidation stage, a static axial stress is applied while the lateral axis is stationary, with effective pressures of 100 kPa, 200 kPa, and 400 kPa selected for comparison with previous studies and axial stress and displacements are recorded as charts and tables. In the cyclic shear stage, a lateral cyclic shear force or displacement is applied while maintaining axial stress or specimen height, measuring axial and lateral load, displacement, and shear-induced pore pressure at 50 points per cycle, with data presented as wave shapes, graphs, and tables. For this study the selected shear strain and corresponding amplitude is shown in Table 7.

Table 7: Selected shear strain and corresponding amplitude for the cyclic simple shear test

Shear strain (%)	0.01	0.1	1	2.5	5
Amplitude(mm)	0.002	0.02	0.2	0.5	1

CHAPTER FOUR

RESULTS AND DISCUSSION

4.1 Overview

This chapter presents the experimental findings and their interpretations based on laboratory tests conducted on soil samples from selected locations within Bole Sub-City. Emphasis is placed on the evaluation of shear modulus and damping ratio, as well as the physical and index properties of the soils. The results are compared with established empirical models and prior research to understand the dynamic behavior of the soils in the study area.

4.2 General

Five representative test pits were excavated to a depth of 2.5 meters across different locations in Bole Sub-City. From these pits, both disturbed and undisturbed soil samples were collected for laboratory analysis. The tests were conducted in accordance with ASTM standards, encompassing particle size analysis, Atterberg limits, specific gravity, moisture content, and cyclic simple shear tests. Table 8 presents the types of laboratory tests conducted to assess soil properties, along with their corresponding ASTM standards.

Table 8: Laboratory tests

No	Type of test	ASTM Standard
1	Particle size analysis	ASTM D 422-63
2	Atterberg limits	ASTM D 4318
3	In-situ density and Natural moisture content	ASTM D2937
4	Specific gravity	ASTM D854
5	Consolidation	ASTM D2435
6	Cyclic Simple Shear test	ASTM D3999

4.3 Laboratory Tests for Soil Characterization

4.3.1 Particle Size Analysis

This test was carried out in compliance with ASTM D 422-63 to separate fine-grained cohesive soils from coarse-grained non-cohesive soils. Wet sieve analysis was used to determine the distribution of coarser and larger particles, while hydrometer analysis was conducted to assess the distribution of finer-grained soils. The grain size analysis revealed a significant variation in soil composition across the sites. Gravel content ranged from 0% to

46.81%, sand content from 1.57% to 43.4%, and fines (silt and clay) ranged from 30.94% to 98.43%. This indicates a predominance of fine-grained soils in some test pits, with coarser materials present in others. A combined analysis was performed for each site, and the results are presented in Appendix C.

4.3.2 Atterberg Limit

The water content at which the soils change from one state to the other is known as Atterberg's limit. The soils displayed high to very high plasticity. Liquid limit values ranged from approximately 49% to 112%, while plasticity index values ranged between 24% and 70%. This suggests a dominance of plastic clays with varying consistency and water retention capacities.

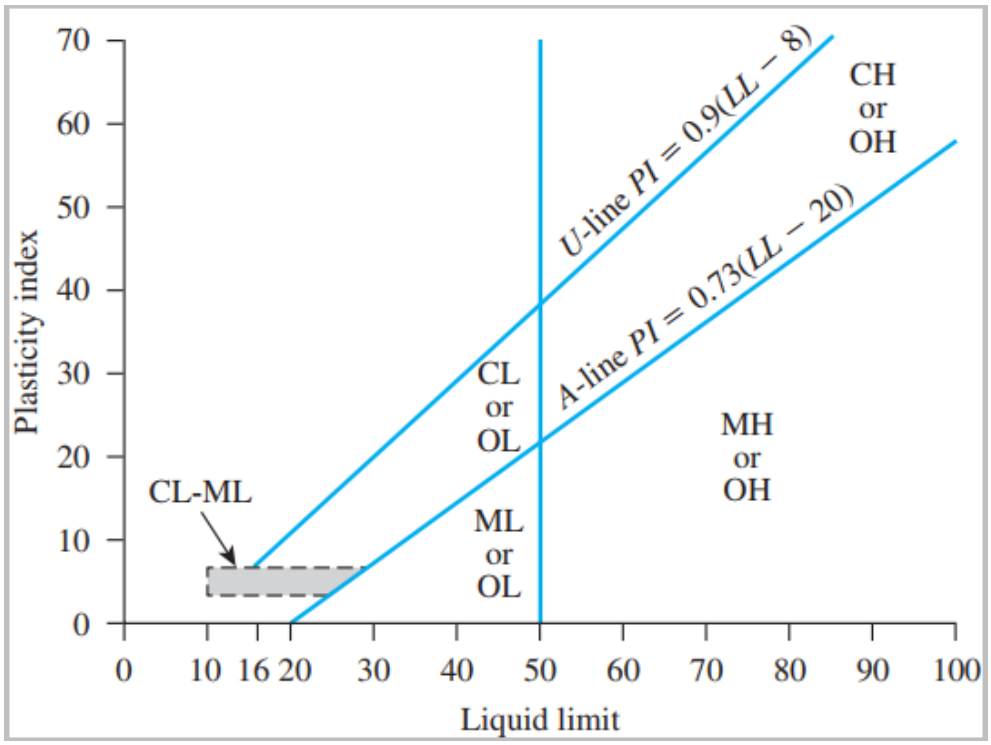

Figure 16 : Plasticity chart

Table 9: Atterberg limit test results

Label	Liquid Limit (LL)	Plastic limit (PL)	Plasticity index (LL-PL)	Description
Test Pit 1	95.847	44.69	51.157	Very high plasticity
Test Pit 2	87.5	36.8	51	Very high plasticity
Test Pit 3	111.9	40.9	70.29	Very high plasticity
Test Pit 4	50.21	22.94	27.27	High plasticity
Test Pit 5	90.5	47.6	42.9	High plasticity

4.3.3 In Situ Density and Natural Moisture Content

Field tests showed that the natural moisture content varied between 26% and 52%, and dry density values ranged from 0.83 to 1.53 g/cm³. These values highlight the variation in compaction and water retention properties across the sampling sites.

Table 10: In situ density and Natural moisture content test results

Label	Natural moisture content	Bulk density	Dry density
Test Pit 1	39.82	1.667	1.194
Test Pit 2	43.56	1.26	0.87
Test Pit 3	46.97	1.98	1.34
Test Pit 4	26.14	1.93	1.53
Test Pit 5	51.47	1.26	0.83

4.3.4 Specific Gravity

The specific gravity of the soil samples ranged from 2.74 to 2.83, which falls within the expected range for mineral soils with significant clay content..

$$\mathbf{G_S} = \frac{unit\ weight\ of\ soil\ solids}{unit\ weight\ of\ water} \qquad \text{Equation 4.1}$$

Table 11: Specific gravity test results

Label	Test Pit 1	Test Pit 2	Test Pit 3	Test Pit 4	Test Pit 5
Specific gravity	2.82	2.76	2.82	2.74	2.83

4.3.5 Soil Classification

Using the Unified Soil Classification System (USCS), the soils were identified as high-plasticity clays (CH), sands (SC), and clayey gravels (GC) as shown in Table 12. The classifications were confirmed through plotting on the plasticity chart.

Table 12: Soil classification results

Label	Gravel	Sand	Silt and Clay	USCS soil classification symbols	On the plasticity chart
Test Pit 1	11.11%	4.9%	83.99%	Clay (CH)	Above A line
Test Pit 2	46.84%	22.22%	30.94%	Clayey gravel (GC) with high plasticity fines	Above A line
Test Pit 3	0.47%	8.44%	91.09%	Clay (CH)	Above A line
Test Pit 4	17.1%	43.4%	39.5%	Sand(SC)	Below A line
Test Pit 5	0%	1.57%	98.43%	Clay(MH)	Below A line

4.3.6 Consolidation

One-dimensional consolidation tests were conducted to determine preconsolidation pressure and compute the over-consolidation ratio (OCR). The OCR values varied significantly between test pits, indicating differences in stress history and compaction levels.

Table 13**:** Over consolidation ratio values

	Test pit 1			Test pit 4		
σ'_p (Kpa)	100	200	400	100	200	400
σ'_c(Kpa)	80	80	80	305	305	305
OCR($\frac{\sigma'c}{\sigma'p}$)	0.8	0.4	0.2	2.05	1.025	0.5125

4.3.7 Cyclic Simple Shear Test

Cyclic simple shear tests were performed on undisturbed samples to evaluate shear modulus and damping ratio under varying axial stresses (100, 200, and 400 kPa) and shear strain amplitudes (0.01% to 5%). The lateral force and displacement data were used to derive stress-strain curves and calculate dynamic parameters. The applied shear strain and axial load values are listed in the Table 14

Table 14: Axial stress and shear strain values (Note CH-High plasticity and SC- Clayey sand)

Soil type	Axial stress (kPa)	Shear strain (%)				
CH(Test pit 1)	100	0.01	0.1	1	2.5	5
	200	0.01	0.1	1	2.5	5
	400	0.01	0.1	1	2.5	5
SC(Test pit 4)	100	0.01	0.1	1	2.5	5
	200	0.01	0.1	1	2.5	5
	400	0.01	0.1	1	2.5	5

From the output of the cyclic simple shear test, the shear stress and shear strain of the specimen were calculated from the lateral LVDT (specimen displacements) and lateral force values. The specimen height after consolidation was less than 20 mm, and its diameter was 70 mm. The shear stress and shear strain were then calculated using the following equations.

$$\text{Shear Stress } (\tau) = \frac{Force}{Area} = \frac{Shear\ force}{\pi * r\text{^}2} * 10^3 (\text{MPa}) \qquad \text{Equation 4.3}$$

$$\text{Shear Strain } (\sigma) = \frac{\Delta L}{L} = \frac{displacement}{height\ after\ consolidation} * 10^3 (\text{MPa}) \qquad \text{Equation 4.4}$$

The values of cyclic shear test determined at 5^{th} cycle were likely to provide reasonable values for all practical purposes based on this references [2], [4].

Table 15: Shear strain and shear stress values (TP1, 5 % strain and 200 kPa)

Cycle	Time	Lateral lvdt	Lateral force	Shear stress(kPa)	Shear strain (%)	G tan
5	0	-1.30674	-0.07703	-0.02001559	-0.0695296	0.000905
	0.019	-1.28551	-0.05178	-0.01345459	-0.0684	0.001285
	0.038	-1.24743	-0.01509	-0.00392101	-0.0663738	0.001695
	0.057	-1.18085	0.0354	0.00919839	-0.0628312	0.001274
	0.076	-1.00896	0.07747	0.02012992	-0.0536852	0.001849
	0.095	-0.7824	0.15213	0.03952969	-0.0416303	0.000843
	0.114	-0.66335	0.19432	0.0504924	-0.0352958	0.000572
	0.133	-0.56568	0.22799	0.05924126	-0.030099	0.000542
	0.152	-0.44005	0.26695	0.06936469	-0.0234144	0.000235
	0.171	-0.24704	0.29174	0.07580616	-0.0131446	-1.5E-05
	0.19	-0.01996	0.28778	0.07477719	-0.001062	1.39E-05
	0.209	0.14531	0.27976	0.07269326	0.00773172	2.9E-05
	0.228	0.26026	0.27459	0.07134988	0.01384804	3.18E-05
	0.247	0.34272	0.27077	0.07035728	0.01823561	3.17E-05
	0.266	0.40389	0.2677	0.06955957	0.02149037	3.36E-05
	0.285	0.44789	0.26485	0.06881902	0.02383154	3.31E-05
	0.304	0.48125	0.26227	0.06814863	0.02560658	3.7E-05
	0.323	0.50574	0.25956	0.06744446	0.02690965	4.38E-05
	0.342	0.52285	0.25648	0.06664415	0.02782005	5.06E-05
	0.361	0.53506	0.25302	0.0657451	0.02846972	5.55E-05
	0.38	0.54396	0.2493	0.06477849	0.02894328	5.93E-05
	0.399	0.54971	0.24538	0.06375991	0.02924923	6.04E-05
	0.418	0.5532	0.24142	0.06273093	0.02943493	6.28E-05
	0.437	0.55429	0.23732	0.06166558	0.02949292	6.35E-05
	0.456	0.55455	0.23318	0.06058984	0.02950676	5.88E-05
	0.475	0.55386	0.22934	0.05959205	0.02947004	0.000181
	0.494	0.54768	0.21745	0.05650253	0.02914122	0.000539
	0.513	0.52056	0.18097	0.04702352	0.0276982	0.000942
	0.532	0.43793	0.10992	0.02856178	0.02330159	0.000738
	0.551	0.14101	0.01767	0.0045914	0.00750293	5.41E-05
	0.57	-0.08345	-0.05027	-0.01306223	-0.0044402	-9.8E-05
	0.589	-0.15807	-0.07951	-0.02066	-0.0084107	-0.00031
	0.608	-0.30332	-0.12817	-0.03330388	-0.0161392	-0.00038
	0.627	-0.52345	-0.16151	-0.041967	-0.027852	0.000242
	0.646	-0.7957	-0.14823	-0.03851631	-0.042338	0.000318
	0.665	-0.96387	-0.13516	-0.03512018	-0.051286	0.00017
	0.684	-1.06295	-0.12911	-0.03354814	-0.0565579	8.06E-05
	0.703	-1.12795	-0.12645	-0.03285696	-0.0600165	2.52E-05
	0.722	-1.17808	-0.12566	-0.03265168	-0.0626838	-4E-06

	0.741	-1.21951	-0.12578	-0.03268286	-0.0648883	0
	0.76	-1.25547	-0.12578	-0.03268286	-0.0668016	4.7E-05
	0.779	-1.28233	-0.12444	-0.03233468	-0.0682308	7.46E-05
	0.798	-1.30056	-0.12235	-0.03179161	-0.0692008	9.93E-05
	0.817	-1.3118	-0.1196	-0.03107704	-0.0697989	8.29E-05
	0.836	-1.31784	-0.11732	-0.0304846	-0.0701203	9.2E-05
	0.855	-1.32144	-0.1148	-0.0298298	-0.0703118	8.55E-05
	0.874	-1.32256	-0.11246	-0.02922177	-0.0703714	7.97E-05
	0.893	-1.32279	-0.11028	-0.02865532	-0.0703836	6.8E-05
	0.912	-1.32285	-0.10842	-0.02817202	-0.0703868	5.05E-05
	0.931	-1.32265	-0.10704	-0.02781343	-0.0703762	0.001091

Table 15 presents the calculated shear stress and shear strain values derived from measured lateral force and lateral displacement during the 5th cycle of testing at Test Pit 1, conducted under a 5% target shear strain and an axial load of 200 kPa. The data illustrates the material's response to cyclic shear loading, where an initial increase in shear stress with shear strain suggests elastic behavior, followed by potential nonlinearity indicating the onset of plastic deformation or cyclic softening. The lateral force versus lateral displacement values reflects the stiffness of the soil-structure system and any changes due to repeated loading. By the 5th cycle, the behavior typically begins to stabilize, offering insights into the residual strength and deformation characteristics under sustained loading conditions. This dataset is essential for understanding the shear resistance and long-term performance of the material subjected to cyclic stress.

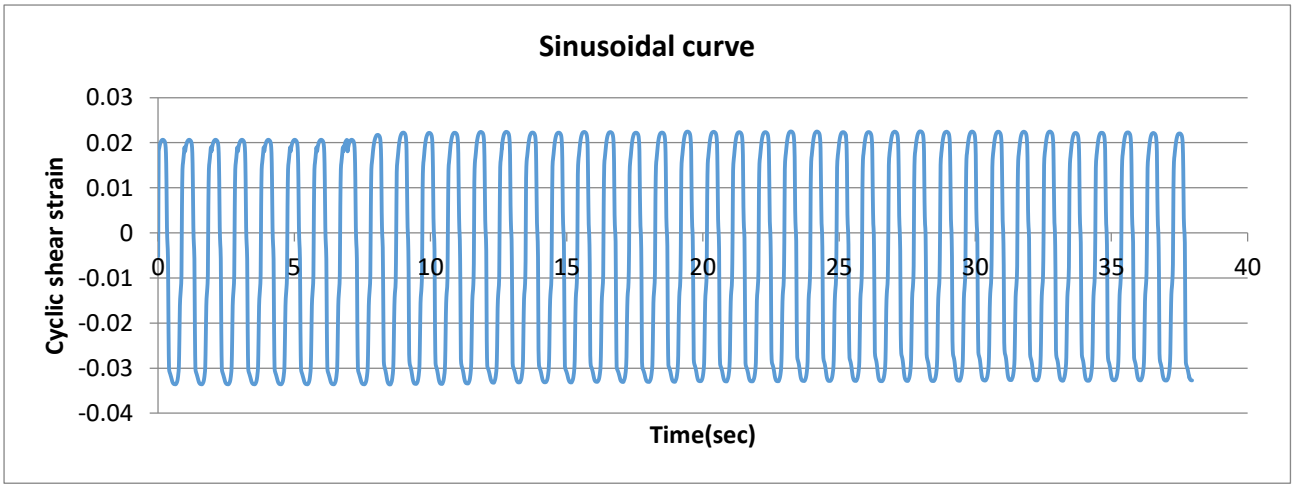

Figure 17 : Sinusoidal wave shape plot of cyclic shear strain versus time in second

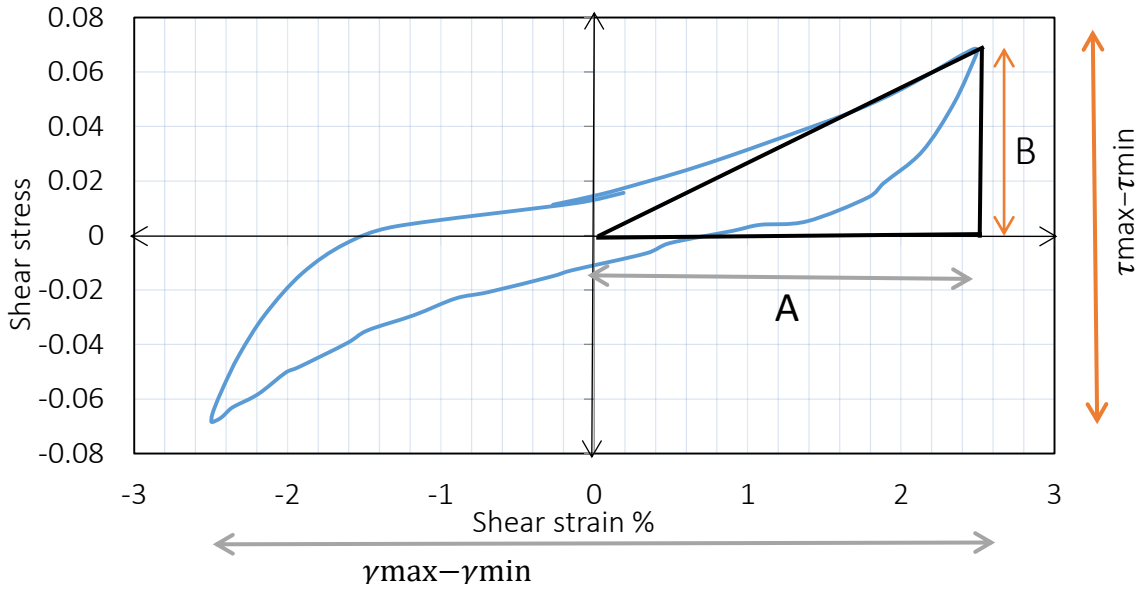

Figure 18 : Hysteresis loop and triangle using stress strain values at 5th cycle

Table 16: Typical calculation for shear modulus and damping ratio for test pit 3,

(5th cycle,400 kPa and 5% strain)

Calculation of shear modulus		Calculation of damping ratio	
τ_{max}	0.09901	Area of hysteresis loop =0.5*(τ_i-τ_{i+1}) * γ_i+γ_{i+1}	0.010272
τ_{min}	-0.05272	Area of triangle =0.5*A*B	0.00198
τ_{max} - τ_{min} =2B	0.151727		
γ_{max}	0.070216	$D=\frac{Aloop}{4\pi*A\Delta}$ *100%	41.30119
γ_{min}	-0.03419		
γ_{max}- γ_{min}=2A	0.104404		
$G=\frac{\tau max-\tau min}{\gamma max-\gamma min}$ in MPa	1.453268		

The values of shear modulus and damping ratio for the rest of the cycles are calculated in a similar manner.

4.4 DISCUSSION

The primary objective of this study was to determine the shear modulus and damping ratio of soil samples extracted from bole sub city subjected to cyclic loading. Unlike previous researches conducted in different locations, this study focuses on the unique geotechnical characteristics of Bole, an urbanized area with distinct soil composition, groundwater conditions, and construction impacts. The results obtained from cyclic simple shear tests provide insights into the stiffness and energy dissipation characteristics of Bole's soils.

4.4.1 Effect of Shear Strain Level on Shear Modulus and Damping Ratio Values

As it can be seen from Figure 19 to Figure 20, The results showed that shear modulus decreased with increasing shear strain, consistent with typical nonlinear soil behavior. Higher confining pressures yielded higher initial shear modulus values, reflecting increased stiffness under stress.

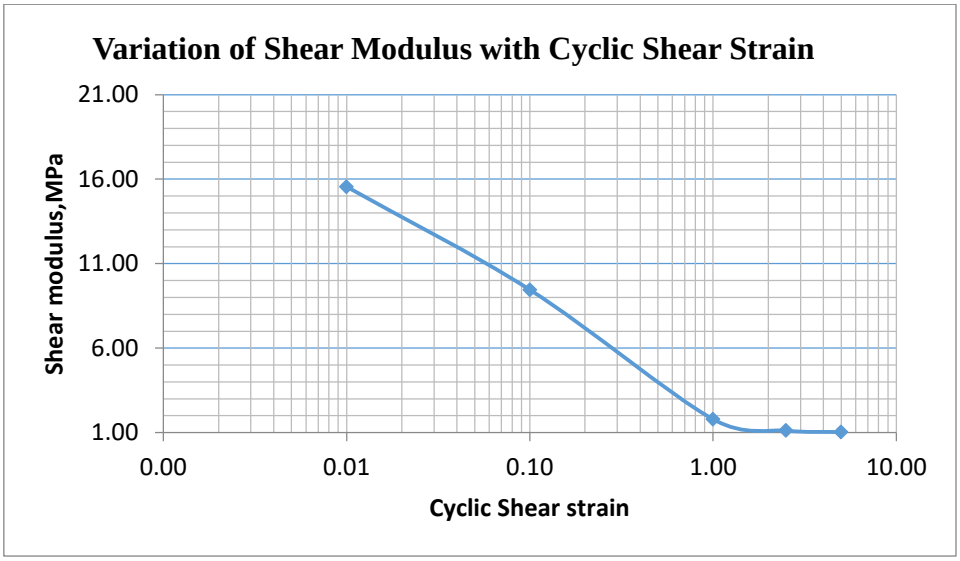

Figure 19: Effect of strain level on shear modulus for Test Pit 3 at 100 kPa

Damping ratio (D) provides insight into the soil's ability to dissipate cyclic energy. As expected, the damping ratio increased with higher strain amplitudes. This trend is indicative of greater energy dissipation in soils subjected to large deformations. Clayey soils showed lower damping at low strain but a rapid increase at higher strain levels. [7].

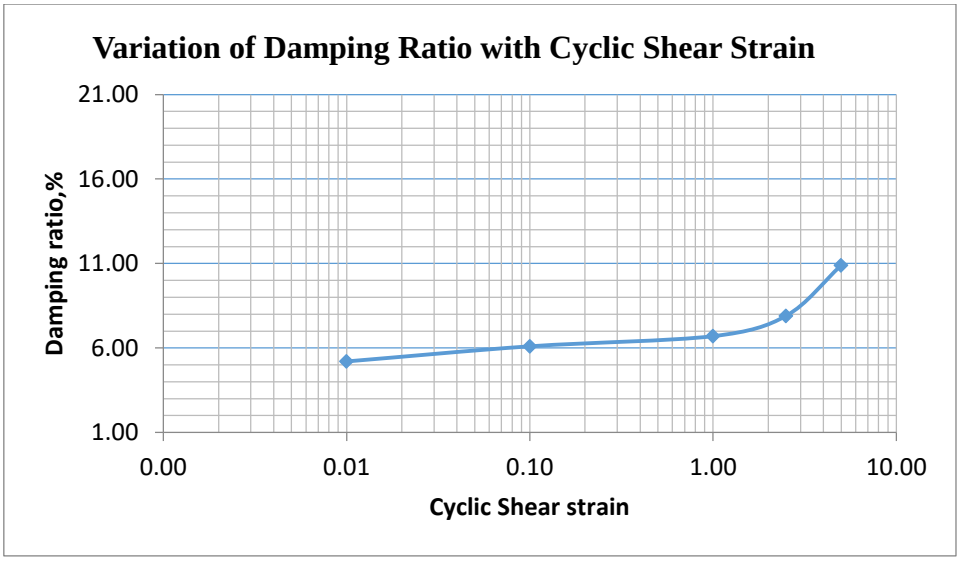

Figure 20 : Effect of strain level on damping ratio for Test Pit 3 at 100 kPa

4.4.2 Effect of Shear Strain Level on Shear Modulus and Damping Ratio Values on Selected Cycles

The variation of she ar modulus and damping ratio for test pit 3 under axial stress of 400 kPa for the selected cycles is shown in Figure 21 and Figure 22 respectively.

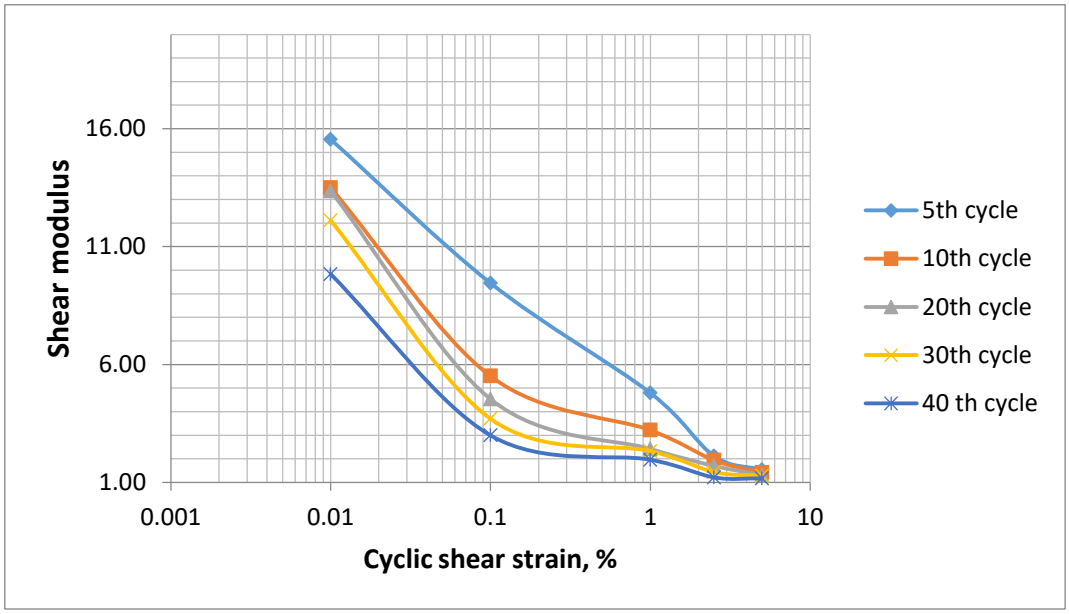

Figure 21: Variation of shear modulus with shear strain for different cycles for Test Pit 3 Under axial stress of 400 kPa

The graph correctly illustrates the reduction of shear modulus with increasing cyclic shear strain across multiple loading cycles, which is typical in soil and material behavior under cyclic loading conditions. Each curve represents a different cycle (5th to 40th), showing that the shear modulus decreases more significantly with both higher strain and repeated loading.

At higher strain amplitude values, the shear modulus values for different cycles often tend to converge to the same point due significant material degradation reducing stiffness.

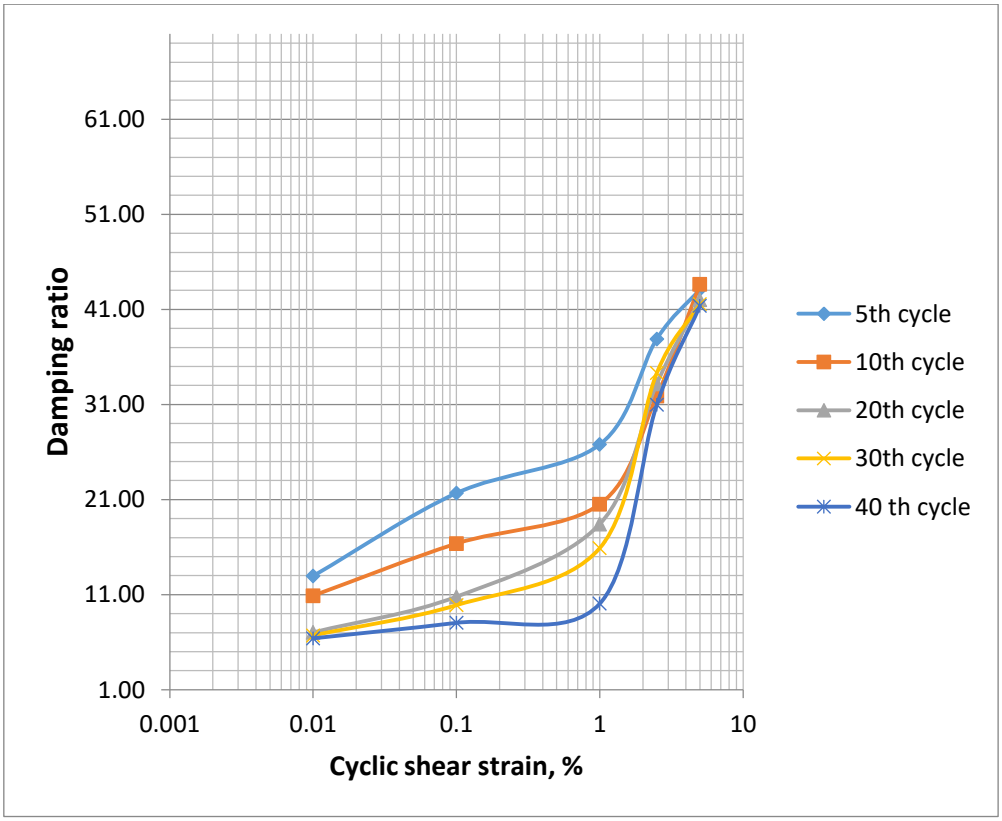

Figure 22 : Variation of damping ratio with shear strain for different cycles for Test Pit 3 Under axial stress of 400 kPa

The graph effectively illustrates the progressive increase in damping ratio with rising cyclic shear strain across multiple loading cycles, which is consistent with the typical mechanical behavior of geo materials subjected to dynamic or seismic loading. Damping ratio, which represents the energy dissipated per loading cycle, is shown to increase in a nonlinear fashion as the shear strain amplitude grows. This behavior indicates that the material becomes more dissipative as it experiences larger deformations, which is often due to microstructural changes, increased particle friction, and the development of irreversible strains within the soil or material matrix. Furthermore, the inclusion of multiple cycles (5th, 10th, 20th, 30th, and 40th) reveals that with repeated loading, the damping ratio tends to stabilize at higher values, suggesting cumulative degradation or softening of the material over time.

4.4.3 Effect of Effective Vertical Stress on Shear Modulus and Damping Ratio Values

Increased confining pressure resulted in higher shear modulus and lower damping ratios, particularly for sandy soils. In clays, the effect was less pronounced, but the trend remained consistent.

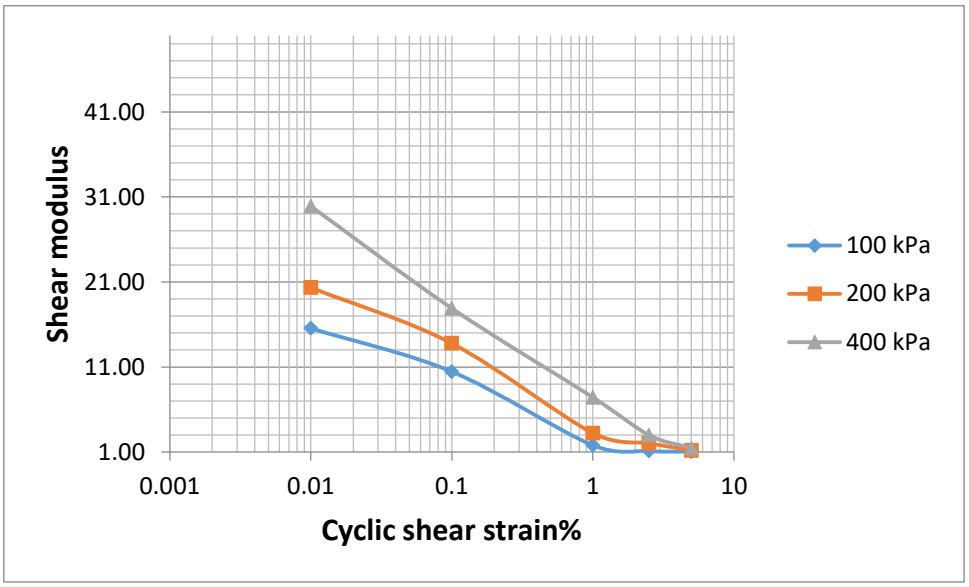

Figure 23: Effect of confining pressure on shear modulus values for Test Pit 3

The graph correctly shows the degradation of shear modulus with increasing cyclic shear strain under varying confining pressures (100, 200, and 400 kPa), which reflects expected soil behavior under dynamic loading. As cyclic strain increases, shear modulus decreases nonlinearly, and higher confining pressures result in stiffer responses with greater initial modulus values. This trend is consistent with experimental observations in cyclic tri axial or resonant column tests.

Damping ratio decreases with increasing effective vertical stress: As soil stiffness increases under higher stress, it dissipates less energy per cycle, leading to lower damping ratios. Soils with lower effective vertical stress tend to have more particle rearrangement and energy dissipation, increasing their damping ratio.These findings highlight the importance of considering effective vertical stress in seismic hazard assessment and foundation design, as soils under higher stress conditions transmit more seismic energy but deform less under cyclic loads.

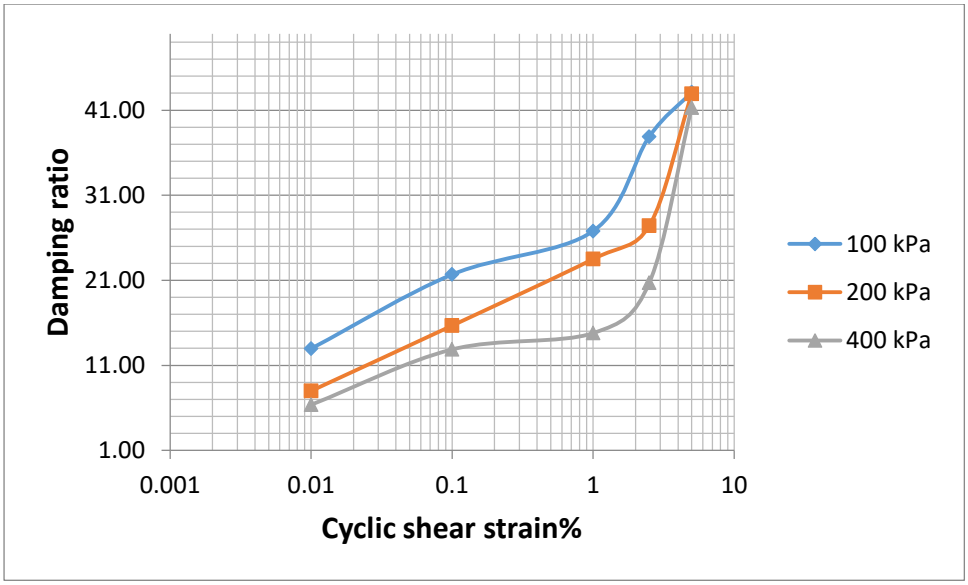

Figure 24 : Effect of confining pressure on damping ratio values for Test Pit 3

The graph effectively shows the relationship between cyclic shear strain and damping ratio under different confining pressures (100, 200, and 400 kPa), illustrating that damping increases with strain and decreases slightly with higher confinement. This reflects the physical behavior of soils, where increased strain leads to greater energy dissipation, and higher confining pressures tend to restrain deformation and reduce damping.

4.3.4 Estimation of Maximum Shear Modulus

Table 17: Estimation of maximum shear modulus

Parameter	Symbol			
Test pit 1				
Effective vertical stress	P_0	100 kPa	200 kPa	400 kPa
Void ratio	E	1.362		
Plasticity index	PI	58.92		
Parameter depending on soil plasticity	A	0.40406		
Over consolidation ratio	OCR	0.8	0.4	0.2
Maximum shear modulus	G_{max}	26.47	28.21	30.142
Test pit 3				
Effective vertical stress	P_0	100 kPa	200 kPa	400 kPa
Void ratio	E	1.104		
Plasticity index	PI	72.9		
Parameter depending on soil plasticity	A	0.45515		
Over consolidation ratio	OCR	0.8	0.4	0.2

Maximum shear modulus	G_{max}	39.43	40.68	41.988
Test pit 4				
Effective vertical stress	P_0	100 kPa	200 kPa	400 kPa
Void ratio	E	0.791		
Plasticity index	PI	24.302		
Parameter depending on soil plasticity	A	0.2058		
Over consolidation ratio	OCR	3.05	1.525	0.7625
Maximum shear modulus	G_{max}	88.06	107.83	132.2

Summary of the normalized shear modulus values (G/G_{max}) for all test pits under axial stress of 100 kPa, 200 kPa and 400 kPa is presented in Table 18.

Table 18: G/G_{max} calculation for test pit 1,test pit 3 and test pit 4

	G/G_{max}				
Shear strain	0.01	0.1	1	2.5	5
Effective vertical stress	100 kPa				
Test pit 1	0.545	0.537	0.047	0.0375	0.01456
Test pit 3	0.394	0.2397	0.0454	0.0284	0.026
Test pit 4	0.553	0.164	0.01486	0.0109	0.0056
Effective vertical stress	200 kPa				
Test pit 1	0.66	0.6543	0.0175	0.067	0.0417
Test pit 3	0.47053	0.264	0.0793	0.049	0.0219
Test pit 4	0.492	0.1366	0.01267	0.00466	0.00313
Effective vertical stress	400 kPa				
Test pit 1	0.257	0.312	0.1028	0.026	0.01285
Test pit 3	0.5125	0.28699	0.13701	0.0713	0.0346
Test pit 4	0.369	0.02475	0.01181	0.00293	0.00856

4.4.5 Effect of Plasticity on Shear Modulus and Damping Ratio Values

The Plasticity Index (PI), a key parameter reflecting the clay content and cohesion in a soil sample, plays a significant role in influencing the shear modulus (G) and damping ratio (D) of the soil. The results of this study demonstrate a notable relationship between the plasticity index and the dynamic properties of the soils under cyclic loading conditions. As PI increases, the soil structure becomes more susceptible to deformation, leading to a reduction in shear modulus.

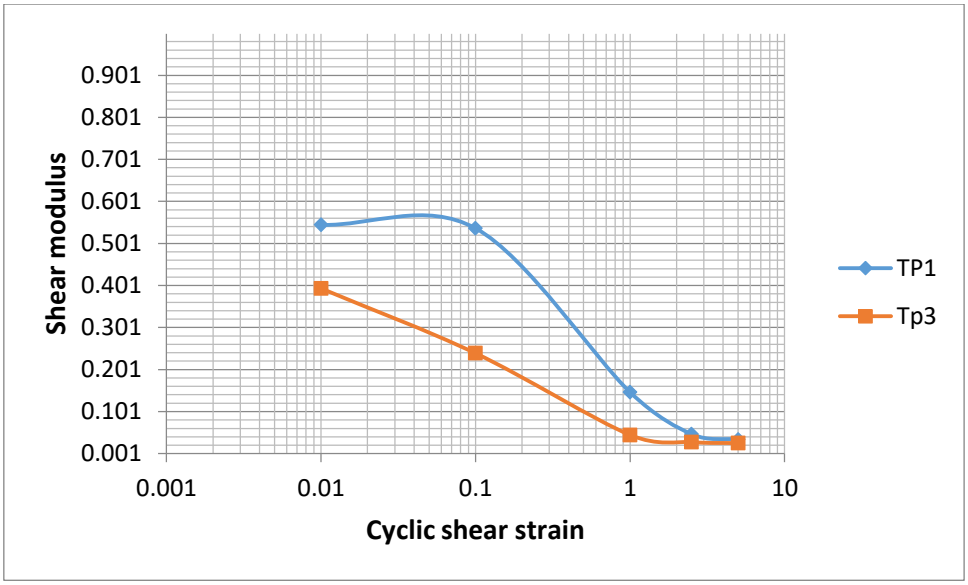

Figure 25 : Influence of plasticity on shear modulus values of TP3 and TP1under axial stress of 100 kPa

Figure 25 indicates that the soil with a lower value of plasticity index (TP1) has a higher value of modulus reduction value as compared with the soil with higher value of plasticity index (TP3) just like the study by vucetic and dobry [14]. As G/Gmax is a measure of how much the shear modulus (G) decreases relative to the maximum shear modulus (Gmax) as the soil is subjected to increasing strain. High PI soils indeed show more gradual modulus reduction in the G/Gmax curve, meaning they lose stiffness more slowly compared to low-PI soils. This is why soils with higher plasticity tend to show greater modulus reduction at large strains.

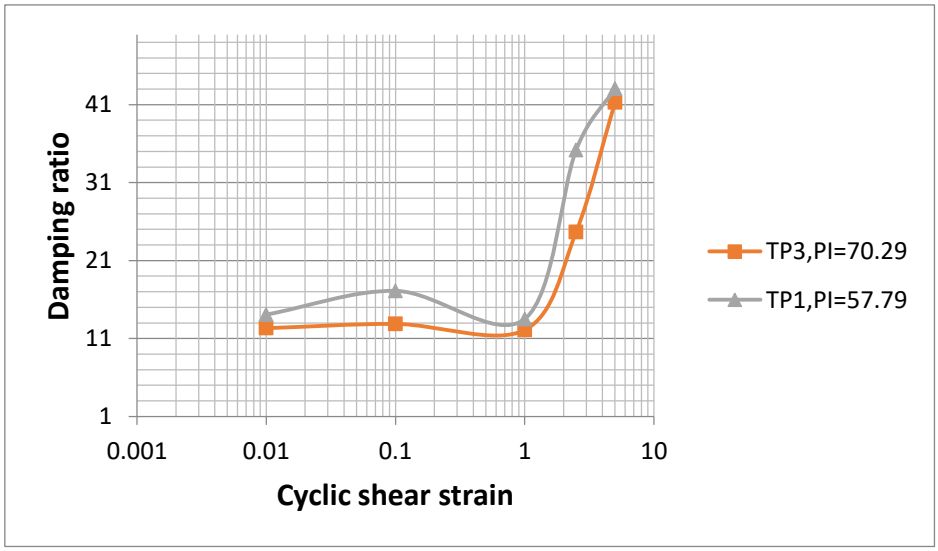

Figure 26 : Influence of plasticity on damping ratio values (TP 3 and TP 1) under axial stress of 400 kPa

Figure 26 illustrates that a soil with a low plasticity index value are more granular and tend to have a higher rate of energy dissipation under cyclic loads, resulting in higher damping. Whereas high plasticity index soils although more deformable, do not dissipate energy as effectively in a cyclic loading scenario. This is due to the reason that these soils tend to deform plastically rather than dissipate energy through frictional sliding. Instead of significant particle rearrangement, much of the strain is absorbed internally as plastic deformation, leading to less energy dissipation per cycle which leads to lower value of damping ratio.

4.4.6 Comparison of Test Results with Previous Researchers

The modulus reduction values of test pits in bole sub city is compared with the curve developed by seed and idriss.

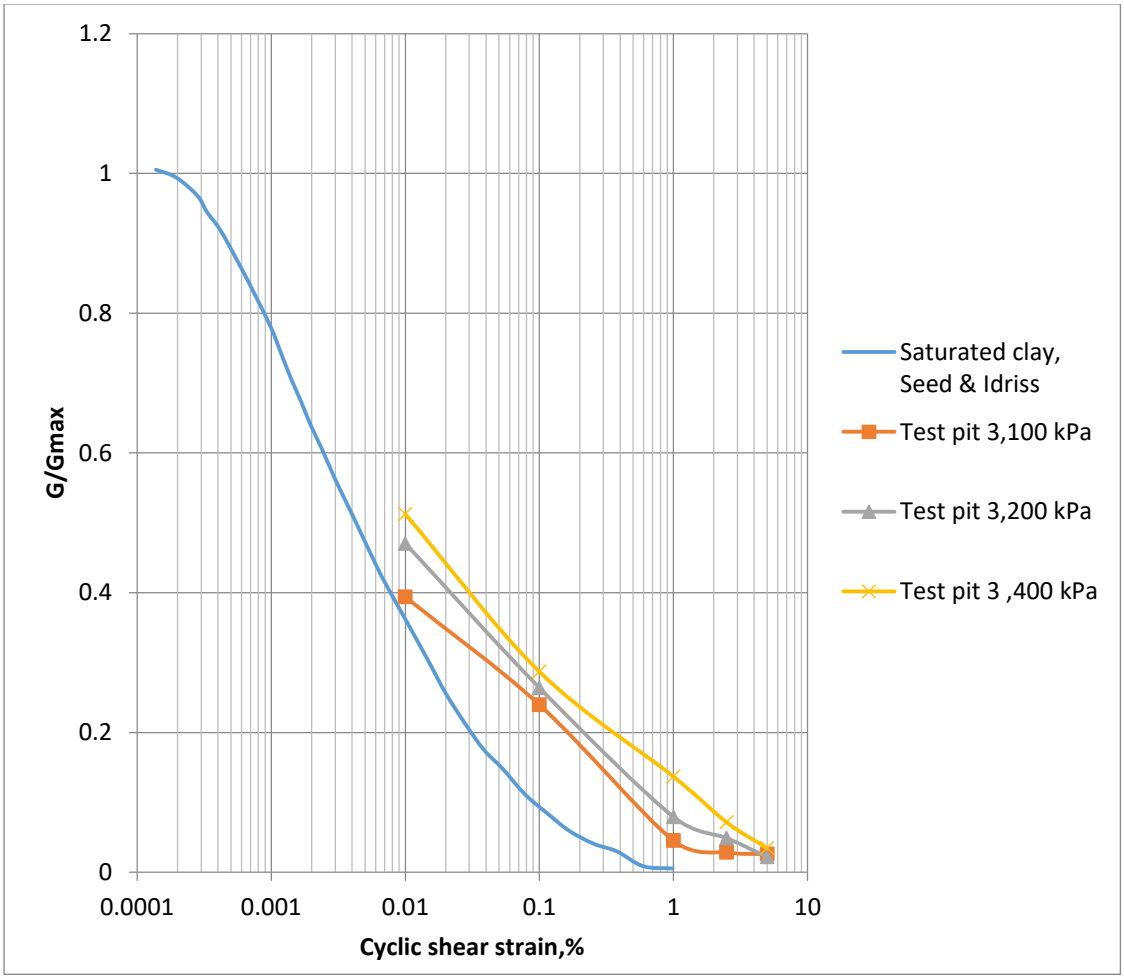

Figure 27 : Comparison of modulus reduction values of Test pit 3(PI=70.29) with curves developed By seed and idriss

The graph presents the normalized shear modulus reduction curve (G/Gmax) versus cyclic shear strain for clay under different confining pressures (100, 200, and 400 kPa). It shows that shear modulus decreases with increasing strain, following a typical nonlinear degradation pattern. Experimental data points from three confining pressures are compared against the empirical average curve developed by seed and edriss for clays. The results indicate that higher confining pressures at 400 kPa help maintain greater stiffness at equivalent strain levels. This behavior reflects the influence of confinement in limiting soil deformation and reducing modulus degradation under cyclic loading. The plotted data mostly fall near the empirical bounds, validating the consistency and reliability of the test results.

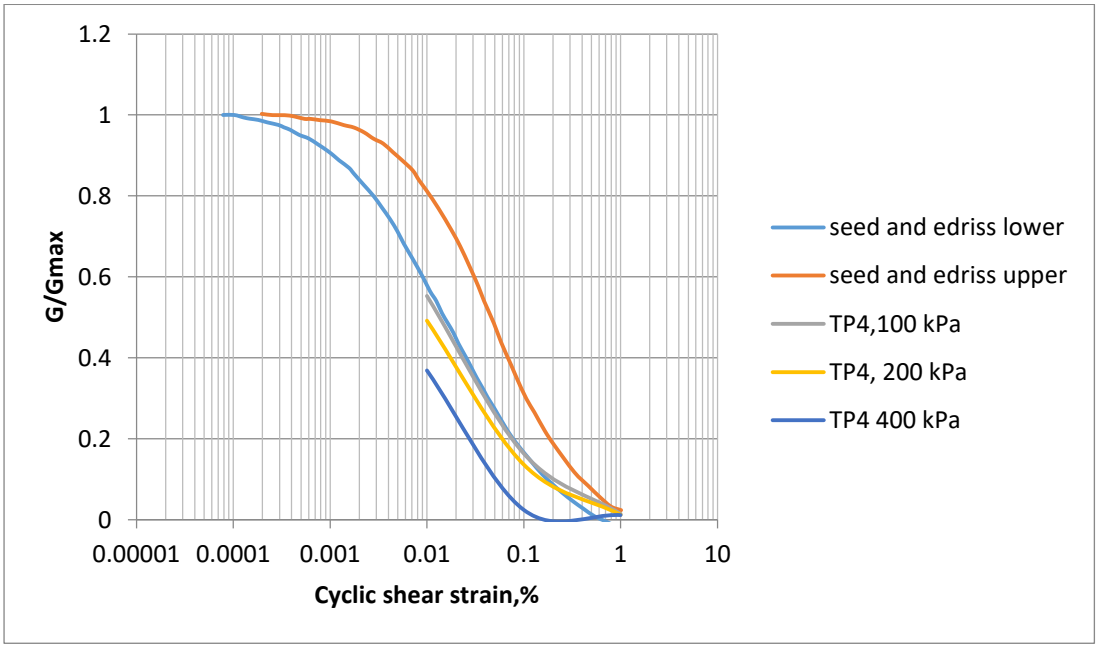

Figure 28 : Comparison of modulus reduction values of Test pit 4 with curves developed By seed and idriss for sands

The graph presents the comparison of normalized shear modulus reduction curve (G/Gmax) versus cyclic shear strain for clayey sand soil under different confining pressures (100, 200, and 400 kPa) with the curve developed by seed and idriss for sand soil. It shows that at lower strain the value of shear modulus degradation lies below the reference curve developed by seed and edriss but at higher strain the data from test pit 4 agrees with seed and edriss. The results also indicate that the curves follow the same trend. The plotted data mostly fall near the empirical bounds, validating the consistency and reliability of the test results.

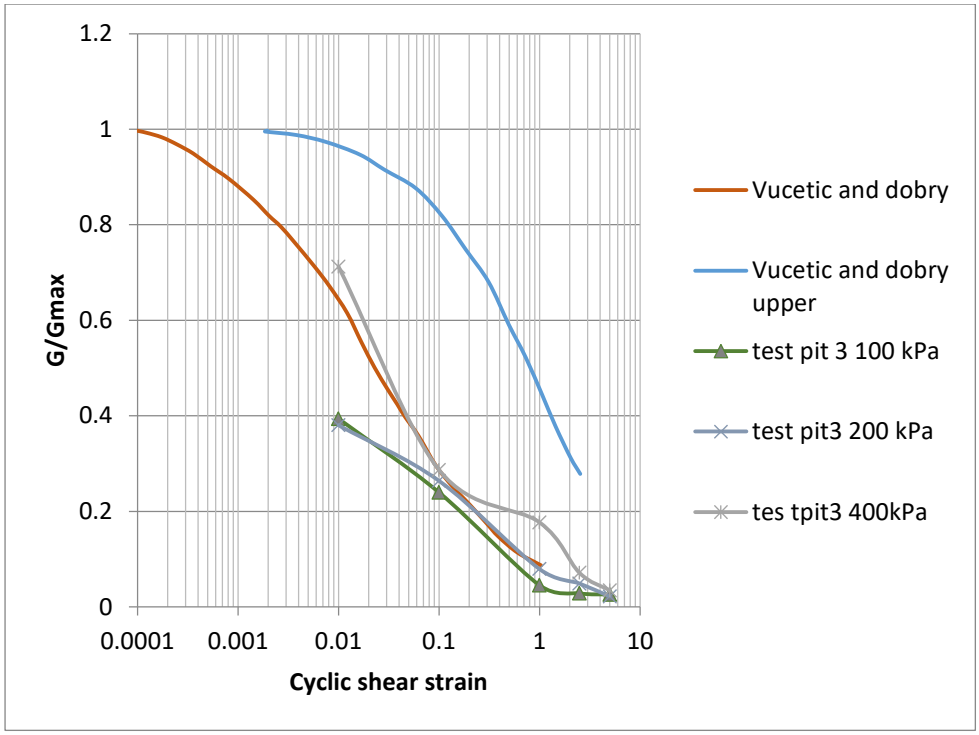

Figure 29 : Comparison of modulus reduction values of Test pit 3 with curves developed by vucetic and dobry for clay soil

Figure 29 shows the relationship between normalized shear modulus (G/G max) and cyclic shear strain for a highly plastic cohesive soil on test pit 3. The data indicates a rapid reduction in shear modulus as strain increases, with the curve falling below the reference line from the Vucetic and Dobry model. This behavior is consistent with the high plasticity of the soil, which results in significant stiffness degradation and increased damping capacity under cyclic loading. The observed trend aligns with the theoretical expectation that soils with higher PI values experience more pronounced stiffness loss compared to non-plastic or low-plasticity soils.

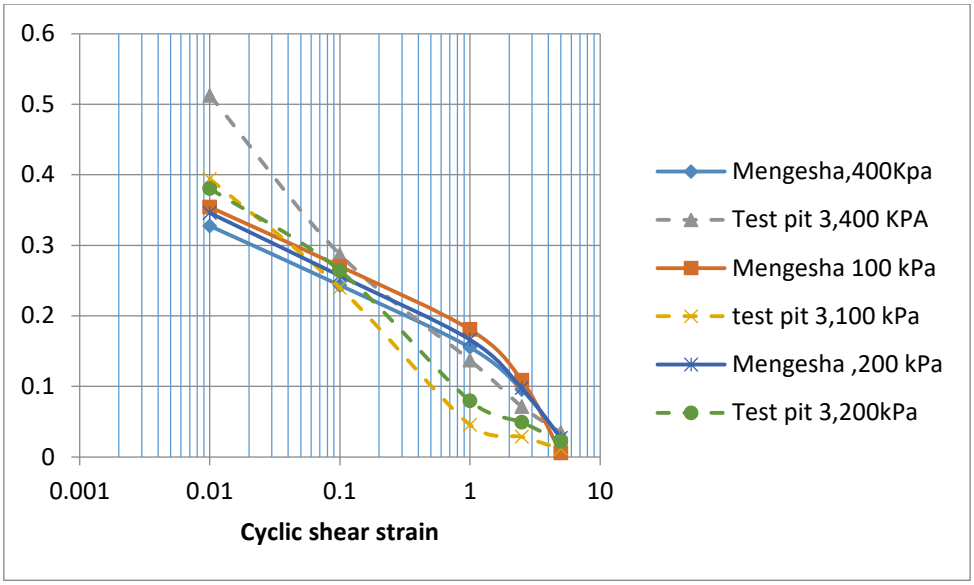

Figure 30 : Comparison of modulus reduction values of Test pit 3 with curves developed for clay soils by mengesha

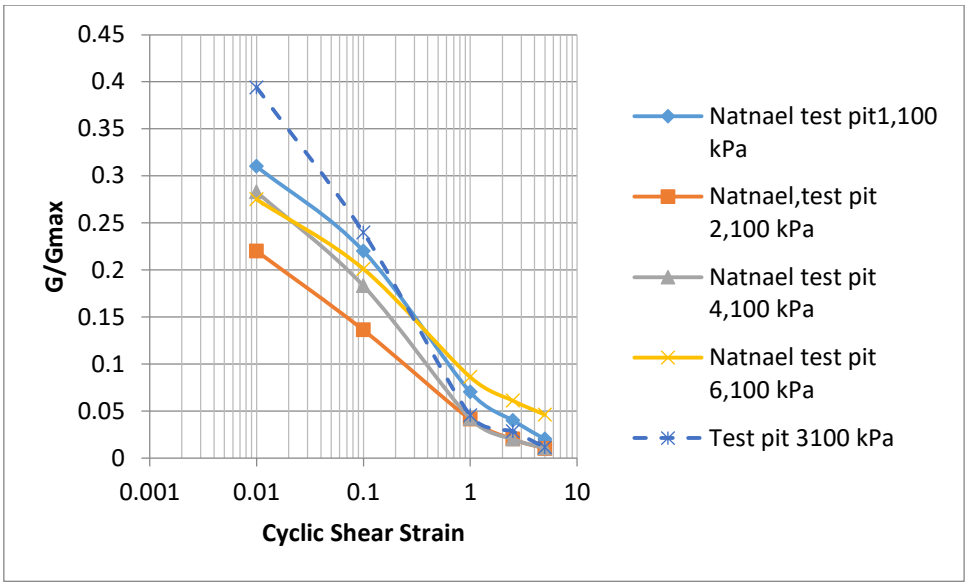

Figure 31 : Comparison of modulus reduction values of Test pit 3 with curves developed for clay soils under 100 kPa by Natnael

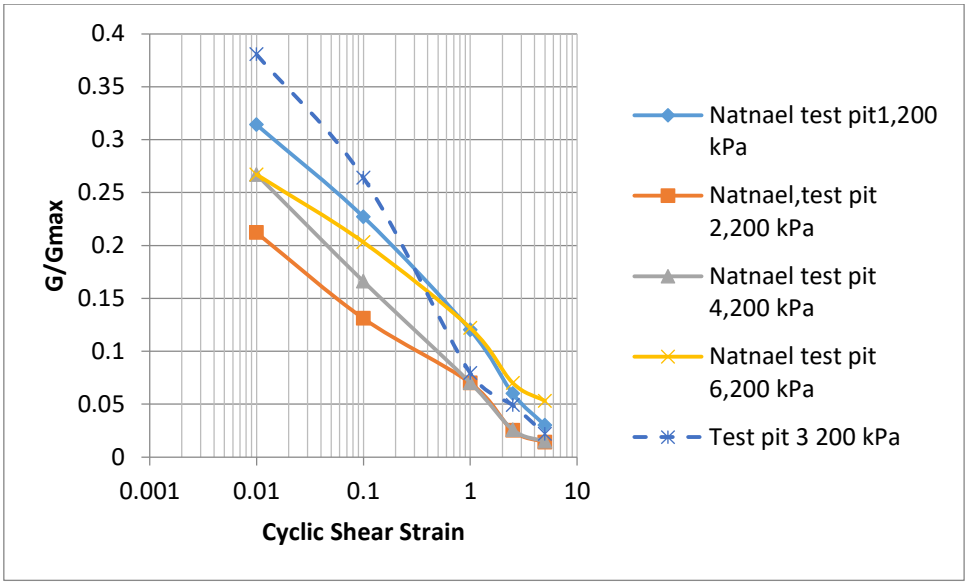

Figure 32 : Comparison of modulus reduction values of Test pit 3 with curves developed for clay soils under 200 kPa by Natnael

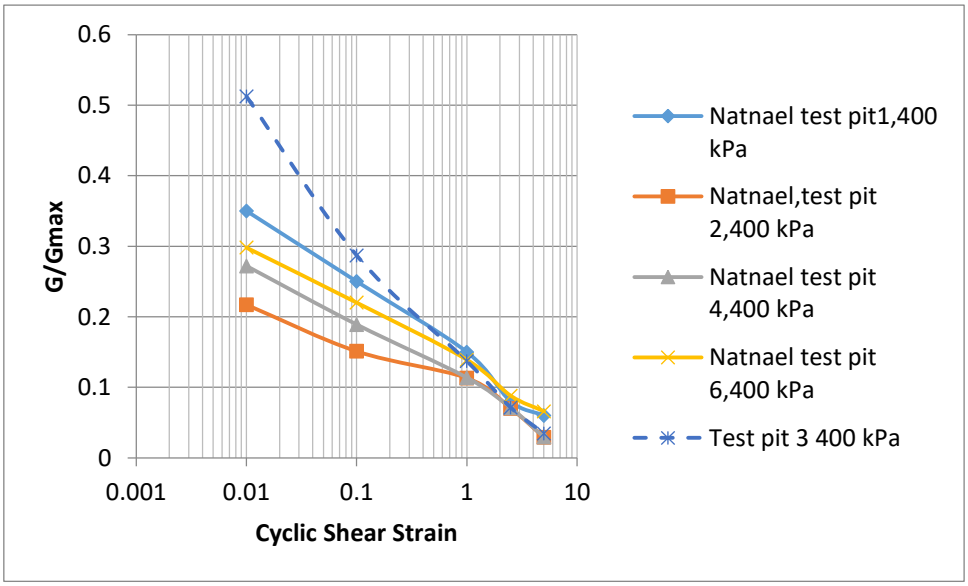

Figure 33 : Comparison of modulus reduction values of Test pit 3 with curves developed for clay soils under 400 kPa by Natnael

The comparison of Test Pit 3 data with local soils, as presented in **Figure 30** to **Figure 33**, shows that the modulus reduction values at lower strain levels are higher than those reported in previous literature, indicating that the Test Pit 3 soil exhibits greater initial stiffness. This difference may be attributed to factors such as higher density, increased compaction, or differences in soil composition, possibly involving a more cohesive or structured material.

However, at higher shear strain values, the modulus reduction curves of Test Pit 3 align well with those of local soils, suggesting that once the soil structure breaks down, the stiffness degradation pattern becomes consistent, reflecting the inherent behavior of cohesive soils under large deformations.

4.4.7 Damping ratio

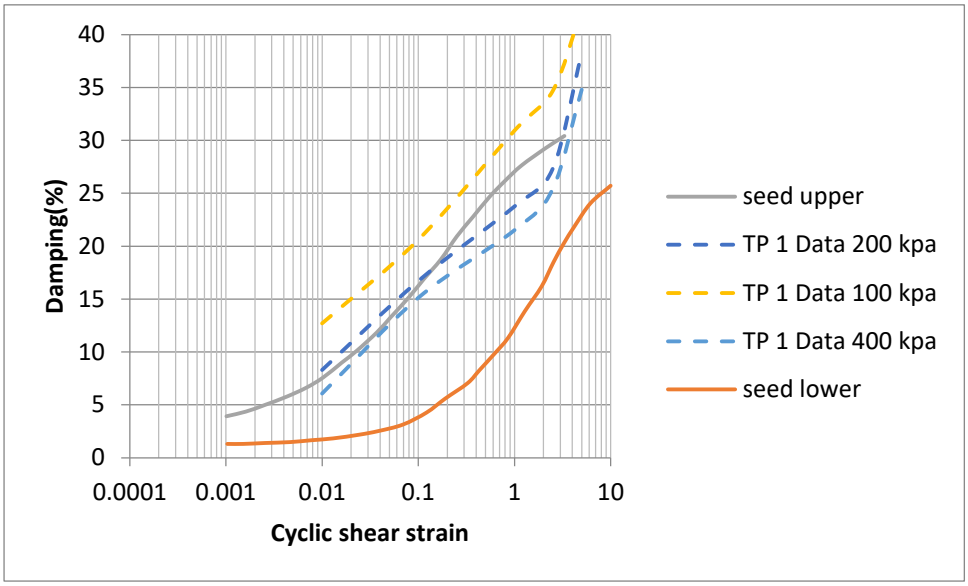

Figure 34 : Comparison of damping ratio values of test pit 1 with the curve of seed and Idriss for saturated clay

The plot of damping ratio versus cyclic shear strain for Test Pit 1 shows that under axial stresses of 200 kPa and 400 kPa, the measured damping ratio values closely follow the curve developed by Seed and Idriss (1970), indicating that the soil behavior under these conditions aligns well with established empirical data. However, at an axial stress of 100 kPa, the damping ratio values lies above the upper limit of the Seed and Idriss curve. This suggests that at lower axial stress, the cohesive soil exhibits relatively higher damping, likely due to less confinement, which allows for increased energy dissipation through greater particle movement and reorientation. In contrast, at higher axial stresses, the soil structure becomes more compacted and disturbed, reducing particle mobility and resulting in lower damping values within the expected range of the Seed and Idriss curve.

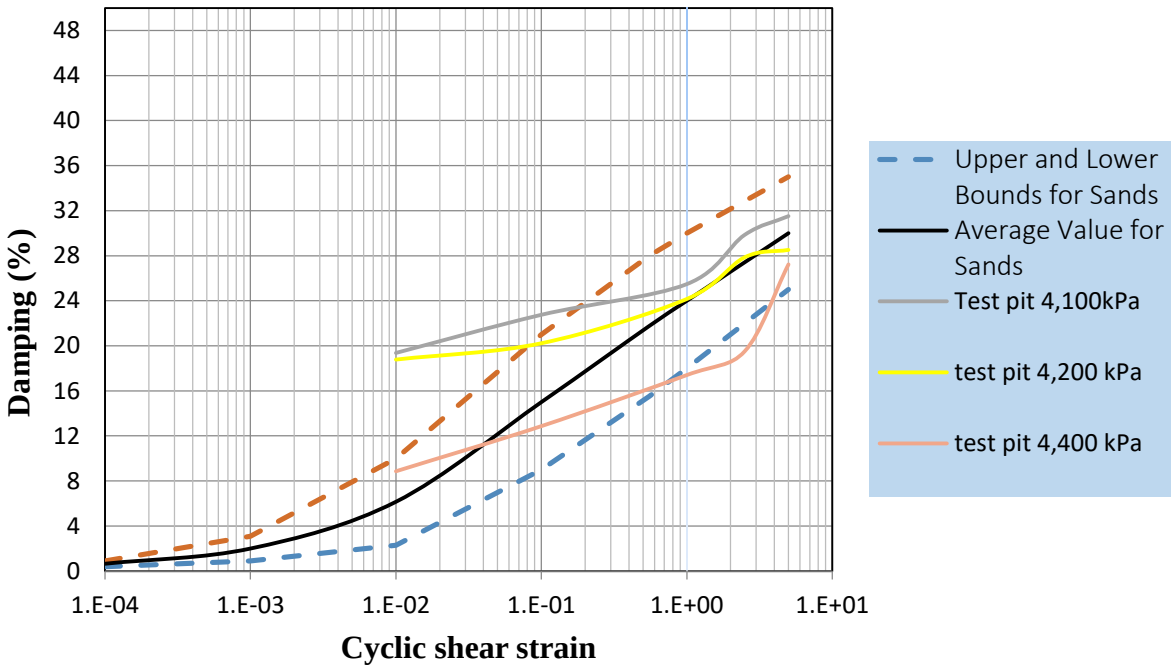

Figure 35: Comparison of damping ratio values of test pit 4 with the curve of seed and Idriss

The plot of damping ratio versus cyclic shear strain for Test Pit 4, compared with the Seed and Idriss (1970) curve, reveals that the damping ratio values under axial stresses of 100 kPa and 200 kPa generally align well with the reference curve, indicating consistency with the established empirical relationship. However, at lower strain levels, the damping ratio values lie above the Seed and Idriss curve, suggesting that the cohesive soil exhibits higher damping when subjected to small deformations under relatively lower axial stresses. This behavior could be attributed to the initial structural arrangement of the soil, which, at low strains, allows for more internal friction and energy dissipation. In contrast, at a higher axial stress of 400 kPa, the damping ratio versus shear strain curve closely matches the Seed and Idriss model throughout the strain range, indicating that the increased confining pressure stabilizes the soil structure, reducing deviations and leading to more predictable damping behavior.

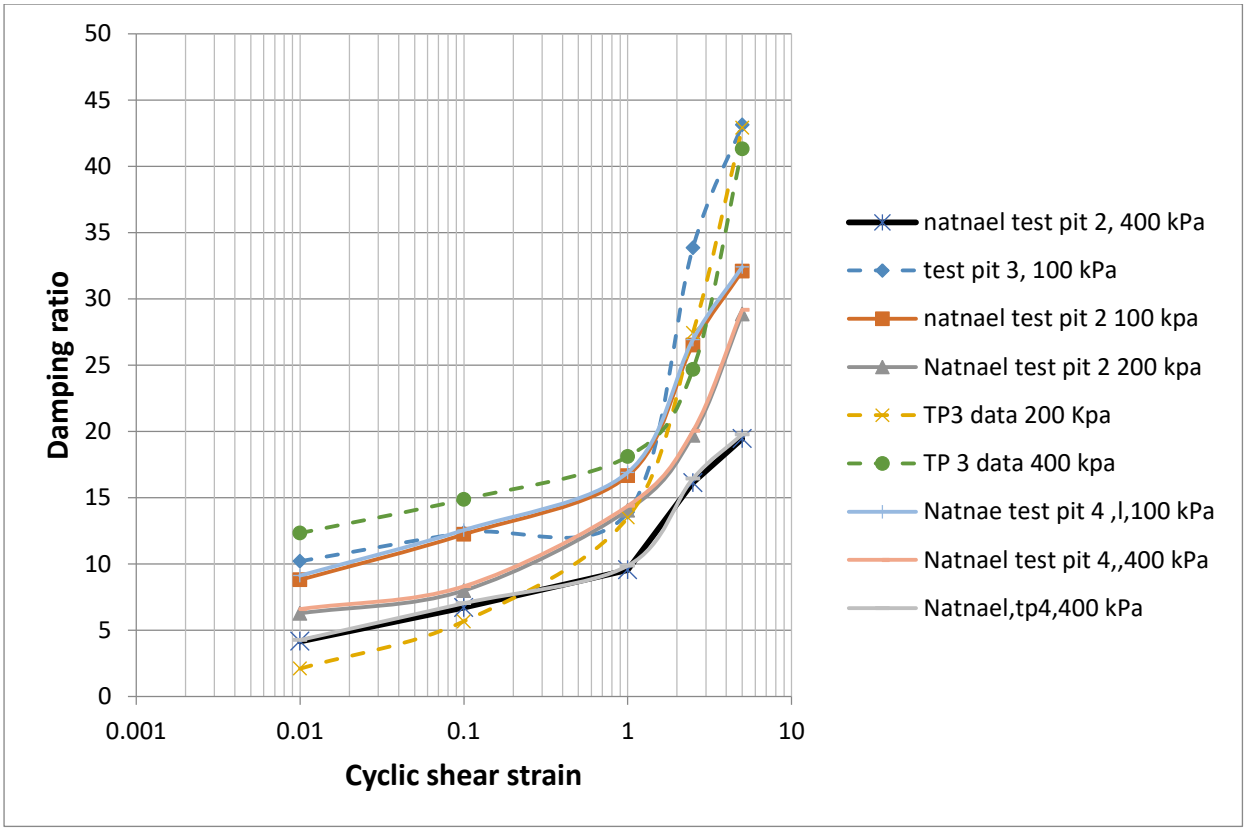

Figure 36 : Comparison of damping ratio values of test pit 4 with the curve of Natnael

The plot of damping ratio versus cyclic shear strain for Test Pit 3, compared with the reference curve developed by Natnael[2], indicates that the damping ratio values align closely throughout the strain range. This strong agreement suggests that the dynamic behavior of Test Pit 3 soil is similar to that described by Natnael[2], likely because both soils share common characteristics as local soils. Local soils often exhibit similar geotechnical properties due to comparable mineral composition, formation processes, and environmental conditions. As a result, their response to cyclic loading, including energy dissipation and deformation patterns, tends to be consistent.

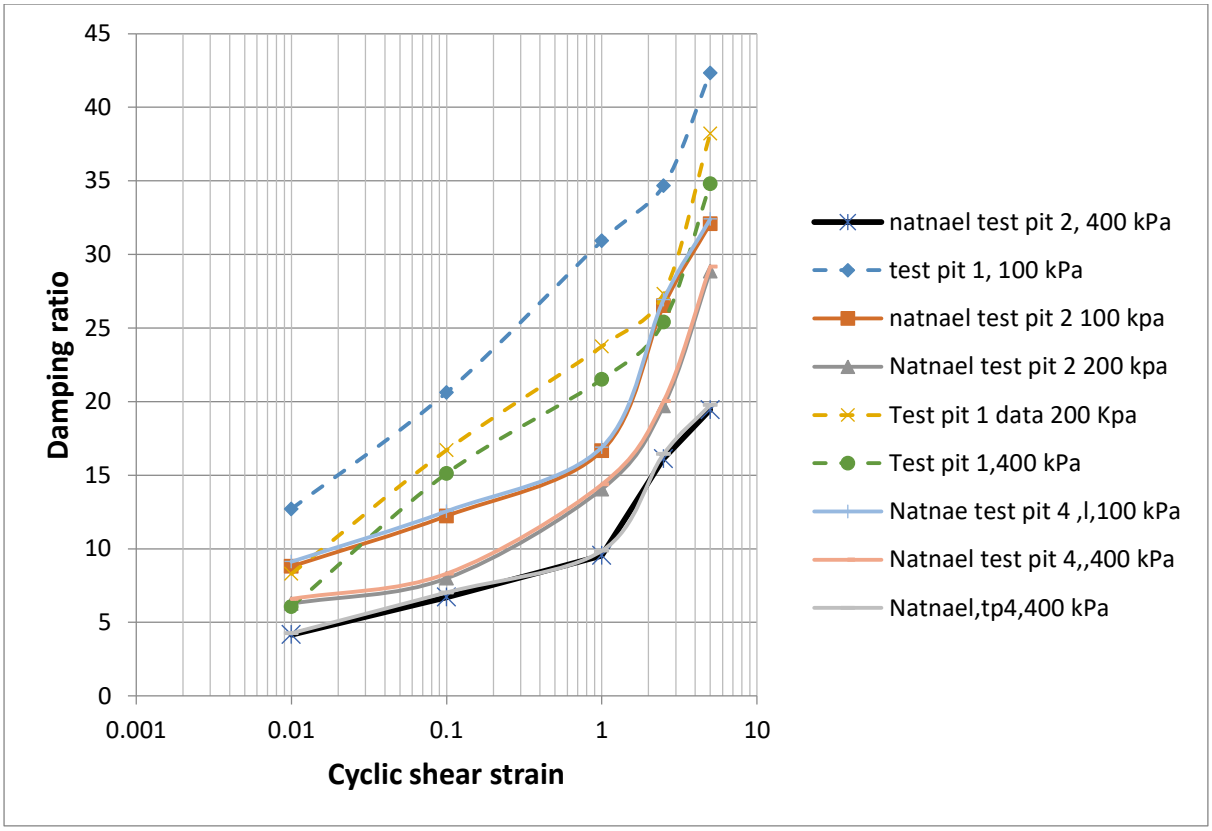

Figure 37 : Comparison of damping ratio values of test pit 1 with the curve of Natnael

The plot of damping ratio versus cyclic shear strain for Test Pit 1, compared with the reference curve developed by Natnael [2], shows that the damping ratio values for Test Pit 1 consistently lie above Natnael's curve throughout the strain range. This discrepancy indicates that the damping characteristics of Test Pit 1 soil are higher than those predicted by Natnael's model, suggesting that the inherent properties of the soil at Test Pit 1, such as plasticity, density, or moisture content, differ from those of the soil studied by Natnael. Despite this difference in magnitude, both plots follow the same trend, indicating that the fundamental relationship between damping ratio and cyclic shear strain remains consistent across the two soils. This observation highlights the importance of considering site-specific soil properties when evaluating dynamic behavior, as relying solely on empirical models from different locations may lead to inaccuracies. Therefore, local calibration of damping ratio models is crucial for accurate prediction and analysis.

CHAPTER FIVE

CONCLUSIONS AND RECOMMENDATIONS

5.1 Conclusions

This study contributes to the understanding of soil behavior under cyclic loading by providing localized data for Bole Sub-City of Addis Ababa. The variation of shear modulus and damping ratio with strain amplitude, soil type, and effective stress highlights the complexity of soil response in urbanized settings, where heterogeneity in development and construction practices influence subsurface conditions. The degradation of shear modulus with increasing strain amplitude underscores the need for careful consideration in geotechnical design, particularly for structures subjected to seismic loading in Addis Ababa. The test results have been compared with the previous findings. From the results of this study, the following can be stated:

- ✓ The shear modulus values for soil on bole sub city at sampling depth of 2.5m ranges from 0.13 MPa -31 MPa for clayey sand soil and 0.18 MPa -31 MPa for clay soil. The damping ratio values ranges from 1.79 %-31% for clayey sand soil and 0.75% - 44% for clay soil type on selected test pits.
- ✓ The results of this study demonstrate a clear strain-dependent behavior of soil stiffness and damping characteristics. Specifically, the shear modulus exhibits a decreasing trend with increasing shear strain amplitude, indicating a reduction in soil stiffness under larger deformations. Conversely, the damping ratio increases with higher strain amplitudes, reflecting enhanced energy dissipation capabilities.
- ✓ An increase in effective vertical stress leads to higher shear modulus values, indicating enhanced soil stiffness. Conversely, the damping ratio decreases with increasing effective vertical stress, reflecting reduced energy dissipation. These observations highlight the significant influence of effective stress on the dynamic properties of soil.
- ✓ The comparison of G/Gmax plots against cyclic shear strain indicates that higher confining pressures, particularly contributes to maintaining greater soil stiffness at equivalent strain levels. This outcome highlights the critical role of confinement in restricting soil deformation and minimizing modulus degradation under cyclic loading conditions.

- ✓ The comparison between the normalized shear modulus (G/Gmax) versus cyclic shear strain relationship for the highly plastic cohesive soil and the reference curve by Vucetic and Dobry reveals a rapid reduction in shear modulus with increasing strain. This behavior confirms that soils with higher plasticity index (PI) exhibit more significant stiffness degradation under cyclic loading compared to soils with low or no plasticity.
- ✓ The comparison with local soils reveals that the modulus reduction values at lower strain levels are higher than those reported in previous studies, indicating that the soil possesses greater initial stiffness. This suggests that the specific characteristics of the highly cohesive soil contribute to enhanced resistance to deformation at small strain levels.
- ✓ The study indicates that cohesive soils exhibit higher damping at lower axial stresses, likely due to reduced confinement that permits greater particle movement and energy dissipation. In contrast, higher axial stresses lead to a more compacted and stabilized soil structure, limiting particle mobility and resulting in lower, more consistent damping values aligning with the Seed and Idriss reference curve. Increased confining pressure further enhances structural stability, contributing to more predictable and uniform damping behavior under cyclic loading.

5.2. Recommendations for Future Work

The findings of this study have significant implications for foundation design, soil improvement techniques, and seismic hazard assessment in urban areas like Addis Ababa. Future research should focus on

- ✓ **Expanding the Study Scope** – Conducting similar tests in different geographic locations or under varying environmental conditions such as on other sub cities of Addis Ababa as this city is being visited by continuous shocks from nearby earth quake events it is recommended to conduct more similar researches on other sub cities to determine the dynamic property of the existing soil.
- ✓ **Advanced Testing Methods** – Utilizing more sophisticated laboratory or field testing techniques, such as cyclic tri axial apparatus, to improve accuracy and reliability.
- ✓ **Numerical Modeling and Simulations** – Developing advanced numerical models to simulate the behavior of a soil with the specified shear modulus and damping ratio property under different seismic loading conditions, which can provide deeper insights into real-world applications.
- ✓ **Practical Engineering Applications** – Applying findings of cyclic simple shear test to real-world engineering projects, such as foundation designs, to evaluate their effectiveness in practical scenarios.
- ✓ **Long-Term Performance Assessment** – the long-term behavior of cyclically loaded soils should also be studied in detail which means how the soil responds over an extended period when subjected to repeated loading and unloading cycles, such as those caused by earthquakes and so on.

REFERENCE

[1] Kramer S. L., *Geotechnical Eartquake Engineering*. 1996.

[2] Natnael, "A Study of Dynamic Properties of Soils Found in Yeka subcity Area of Addis Ababa," no. January, pp. 1–147, 2020.

[3] R. Luna and H. Jadi, "Determination of dynamic soil properties using geophysical methods," *First Int. Conf. Appl. Geophys. NDT Methodol. to Transp. Facil. Infrastruct.*, no. December, pp. 1–15, 2000.

[4] A. G. Feyissa, "Shear Modulus and Damping Ratio values of Soils found in Adama," pp. 1–104, 2011.

[5] G. Yimer, "shear modulus and damping ratio of dry koka sand using cyclic simple shear test,", 2010.

[6] T. B. KEBEDE, "Cyclic Behaviour and Dynamic Properties of Soils : a Case of Jimma Town Teshome Birhanu Kebede Master of Science Addis Ababa Science and Technology, 2019.

[7] A. Gashaw, "Addis Ababa University School of Graduate Studies Shear Modulus and Damping Ratio Values of Soils Commonly Found in Hawassa," no. January, 2012.

[8] B. Mengesha Dimer, "Investigation of Dynamic property of soil found in Arba Minch Town Addis Ababa institute of technology, school of graduate studies," 2013.

[9] B. O. Hardin, "Shear Modulus and Damping in Soils : Design Equations and Curves," no. June, 2016.

[10] H. B. Seed and I. M. Idriss, "Soil Moduli and Damping Factors for Dynamic Response Analyses [Report No. EERC 70-10]," *Earthq. Eng. reserach Cent.*, no. December, p. 48, 1970.

[11] D. Braja M and So. Khaled, *Principles of Geotechnical engineering, Eight Edition*, vol. 5, no. 1. 2014. [Online]. Available: https://ejournal.poltektegal.ac.id/index.php/siklus/article/view/298%0Ahttp://repositorio.unan.edu.ni/2986/1/5624.pdf%0Ahttp://dx.doi.org/10.1016/j.jana.2015.10.005%0Ahttp://www.biomedcentral.com/1471-2458/12/58%0Ahttp://ovidsp.ovid.com/ovidweb.cgi?T=JS&P

[12] K. Ishihara, *zyxw*.

[13] Yohannes, "Investigation to Dynamic Properties of Modjo Town Soils Using

Cyclic Simple Shear Machine," *Int. J. Sci. Eng. Res.*, vol. 8, no. 7, pp. 1–13, 2015.

[14] M. Vucetic, "Soil Properties and seismic response," 1992.

[15] Abreham, "Addis Ababa January, 2015," 2015.

[16] T. Mammo, "Site-specific ground motion simulation and seismic response analysis at the proposed bridge sites within the city of Addis Ababa, Ethiopia," *Eng. Geol.*, vol. 79, no. 3–4, pp. 127–150, 2005, doi: 10.1016/j.enggeo.2005.01.005.

[17] M. Bonini *et al.*, "Evolution of the Main Ethiopian Rift in the frame of Afar and Kenya rifts propagation," *Tectonics*, vol. 24, no. 1, pp. 1–21, 2005, doi: 10.1029/2004TC001680.

[18] "ES EN 8.pdf."

[19] "Mechanics › Soil testing systems".

APPENDICES

Appendix A Field Density and Moisture Content

Table A-1: Field density and moisture content for test pit 1

Weight of ring(gm)	762	
Weight of ring + soil(gm)	2979	
Weight of soil(gm)	2217	
Diameter of the ring(cm)	11	
Height of the ring(cm)	14	
Can Label	C1	C2
Weight of empty can (gm)	21.9	16
Weight of empty can + Moist Soil Sample (gm)	116.3	58
Weight of Can + Dry Sample (gm)	89.5	46
Weight of Water (gm)	26.8	12
Weight of Dry Soil (gm)	67.6	30
Natural Moisture Content (%)	**39.6**	**40.0**
Average moisture content (%)	**39.82**	
Bulk density	**1.667**	
Dry density	**1.194**	

Table A-2: Field density and moisture content for test pit 2

Weight of ring	**762**	
Weight of ring + soil	**2582**	
Weight of soil	**1818**	
Diameter of the ring	11	
Height of the ring	**15.2**	
Can Label	C1	C2
Weight of empty can (gm)	14	15
Weight of empty can + Moist Soil Sample (gm)	48	47
Weight of Can + Dry Sample (gm)	38	37
Weight of Water (gm)	10	10
Weight of Dry Soil (gm)	24	22
Natural Moisture Content (%)	**41.7**	**45.5**
Average moisture content (%)	**43.56**	
Bulk density	**1.26**	
Dry density	**0.87**	

Table A-3: Field density and moisture content for test pit 3

Weight of ring	**793**	
Weight of ring + soil	**3035**	
Weight of soil	**2242**	
Diameter of the ring	**9.8**	
Height of the ring	**15**	
Can Label	C1	C2
Weight of empty can (gm)	16	15
Weight of empty can + Moist Soil Sample (gm)	63	40
Weight of Can + Dry Sample (gm)	48	32
Weight of Water (gm)	15	8
Weight of Dry Soil (gm)	32	17
Natural Moisture Content (%)	**46.875**	**47.059**
Average moisture content (%)	**46.97**	
Bulk density	**1.98**	
Dry density	**1.34**	

Table A-4: Field density and moisture content for test pit 4

Weight of ring	**1762**	
Weight of ring + soil	**3687**	
Weight of soil	**1925**	
Diameter of the ring	**9.2**	
Height of the ring	**15.2**	
Can Label	C1	C2
Weight of empty can (gm)	**14**	**15**
Weight of empty can + Moist Soil Sample (gm)	**28**	**35**
Weight of Can + Dry Sample (gm)	**25**	**31**
Weight of Water (gm)	**3**	**4**
Weight of Dry Soil (gm)	**11**	**16**
Natural Moisture Content (%)	**27.273**	**25**
Average moisture content (%)	**26.14**	
Bulk density	**1.93**	
Dry density	**1.53**	

Table A-5: Field density and moisture content for test pit 5

Weight of ring	**762**	
Weight of ring + soil	**2494**	
Weight of soil	**1732**	
Diameter of the ring	**11**	
Height of the ring	**14.5**	
Can Label	C1	C2
Weight of empty can (gm)	15	16
Weight of empty can + Moist Soil Sample (gm)	42	42
Weight of Can + Dry Sample (gm)	33	33
Weight of Water (gm)	9	9
Weight of Dry Soil (gm)	18	17
Natural Moisture Content (%)	**50**	**52.94**
Average moisture content (%)	**51.47**	
Bulk density	**1.26**	
Dry density	**0.83**	

Appendix B Atterberg limit test

Table B-1: Liquid limit and Plastic limit results for TP 1

	Liquid limit			Plastic limit	
Trial no	T1	T2	T3	P1	P2
Weight of Can (gm)	16.0163	16.73	15.46	14.58	16.73
Weight of can+ wet soil(gm)	31.8	37.89	33.2	20.256	19.6
Weight of Can+ Dry soil(gm)	24.137	27.56	24.45	18.49	18.72
Weight of water	7.663	10.33	8.75	1.766	0.88
Weight of dry soil	8.1207	10.83	8.99	3.91	1.99
Moisture content	94.36	95.38	97.33	45.17	44.22
Number of blows	30	27	20	-	-
Average	**95.847%**			**44.69%**	

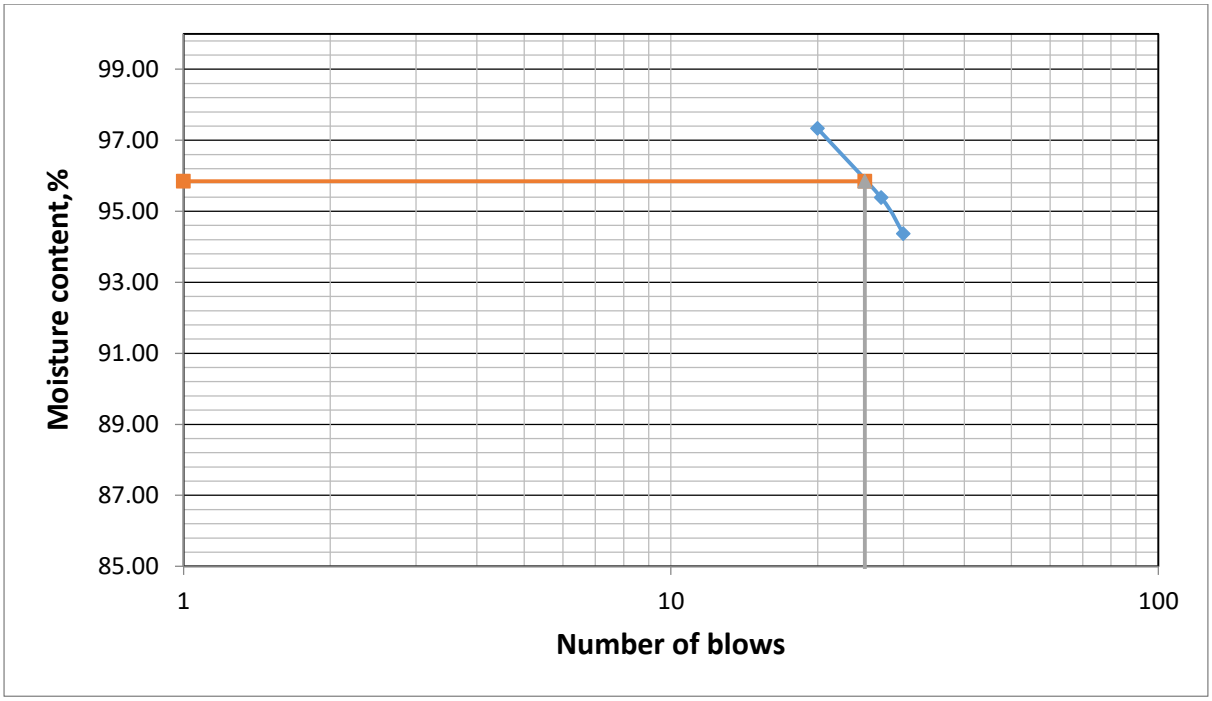

Figure B-1: Flow curve for TP1

Liquid limit (%) =95.847 Plastic limit(%)=44.69 Plasticity index(%)=51.157

Table B-2: Liquid limit and Plastic limit results for TP 2

	Liquid limit			Plastic limit	
Trial no	T1	T2	T3	P1	P2
Weight of Can (gm)	21.992	21.837	21.848	14.2	14.399
Weight of can+ wet soil(gm)	41.028	41.261	41.485	16.366	16.374
Weight of Can+ Dry soil(gm)	32.256	32.238	32.273	15.788	15.838
Weight of water	8.77	9.02	9.21	0.58	0.54
Weight of dry soil	10.26	10.40	10.43	1.59	1.44
Moisture content	85.46	86.75	88.36	36.4	37.25
Number of blows	33	28	22	-	-
Average	**LL=87.5%**			**PL=36.8%**	

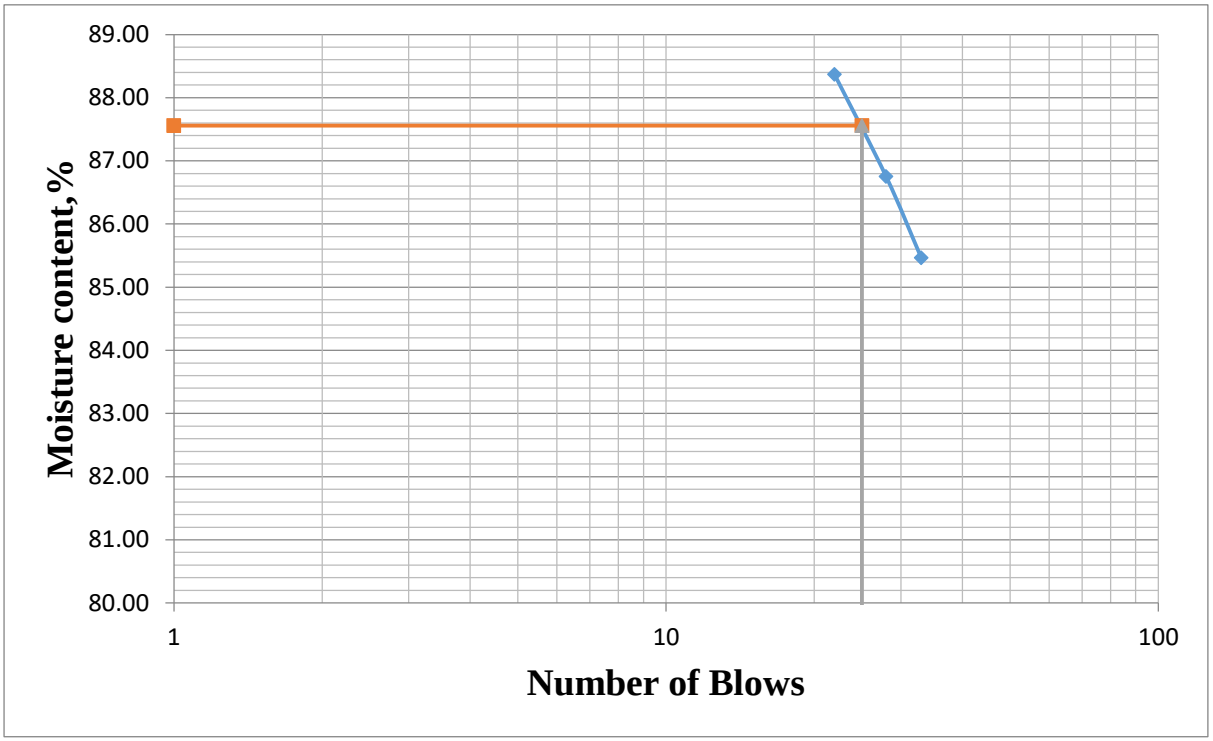

Figure B-2 Flow curve for TP2

Liquid limit(%)= 87.5% Plastic limit (%)=36.8% Plasticity index(%)=51%

Table B-3: Liquid limit and Plastic limit results for TP 3

	Liquid limit			Plastic limit	
Trial no	T1	T2	T3	P1	P2
Weight of Can (gm)	20.5506	15.3546	15.7546	15.8513	16.0163
Weight of can+ wet soil(gm)	54.1755	50.2164	49.2204	18.0134	23.0357
Weight of Can+ Dry soil(gm)	36.5695	31.8802	31.5486	17.39	20.9843
Weight of water	17.606	18.3362	17.6718	0.6234	2.0514
Weight of dry soil	16.0189	16.5256	15.794	1.5387	4.968
Moisture content	109.91	110.96	111.89	40.51	41.29
Number of blows	35	28	16	-	-
Average	111.19%			40.9%	

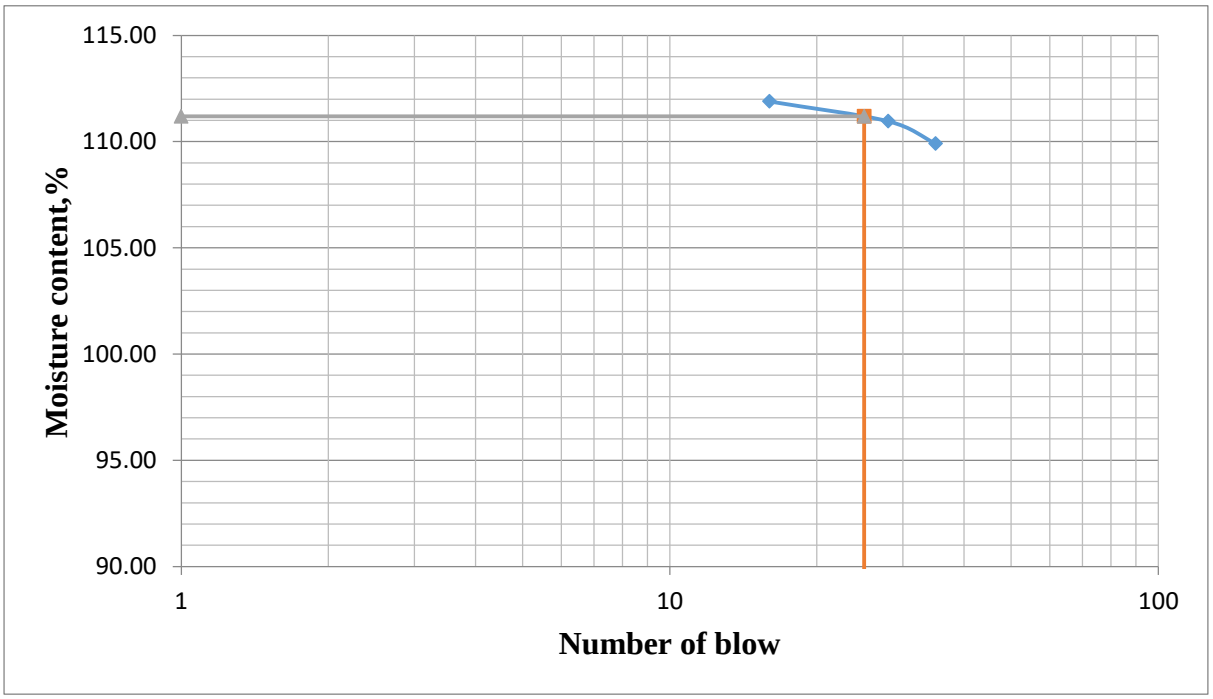

Figure B-3 Flow curve for TP3

Liquid limit(%)= 111.19 Plastic limit (%)=40.9 Plasticity index(%)=70.29

Table B-4: Liquid limit and Plastic limit results for TP 4

	Liquid limit			Plastic limit	
Trial no	T1	T2	T3	P1	P2
Weight of Can (gm)	T1	T2	T3	15.8523	15.7546
Weight of can+ wet soil(gm)	15.9727	15.5813	15.93	21.2435	22.4689
Weight of Can+ Dry soil(gm)	61.1662	65.3892	57.345	20.2043	21.2578
Weight of water	46.756	48.9908	42.9921	1.0392	1.2111
Weight of dry soil	14.4102	16.3984	14.3529	4.352	5.5032
Moisture content	30.7833	33.4095	27.0621	23.88	22.01
Number of blows	46.81	49.08	53.04	-	-
Average	**LL=50.21%**			**PL=22.94%**	

Figure B-4: Flow curve for TP4

Liquid limit (%) = 50.21 Plastic limit (%) =22.94 Plasticity index (%) =27.27

Table B-5: Liquid limit and Plastic limit results for TP 5

	Liquid limit			Plastic limit	
Can Label	T1	T2	T3	P1	P2
Weight of empty Can (gm)	21.816	21.529	21.806	14.173	14.104
Weight of Can + Sample (gm)	40.207	40.239	40.672	16.388	16.318
Weight of Can + Dry Sample (gm)	31.632	31.510	31.678	15.667	15.611
Weight of Water (gm)	8.58	8.93	8.99	0.27	0.71
Weight of Dry Soil (gm)	9.82	9.98	9.88	1.49	1.51
Moisture content (%)	87.36	89.46	91.08	48.26	46.91
Number of Blows	32	27	23	-	-
Average liquid limit	90.5			47.6	

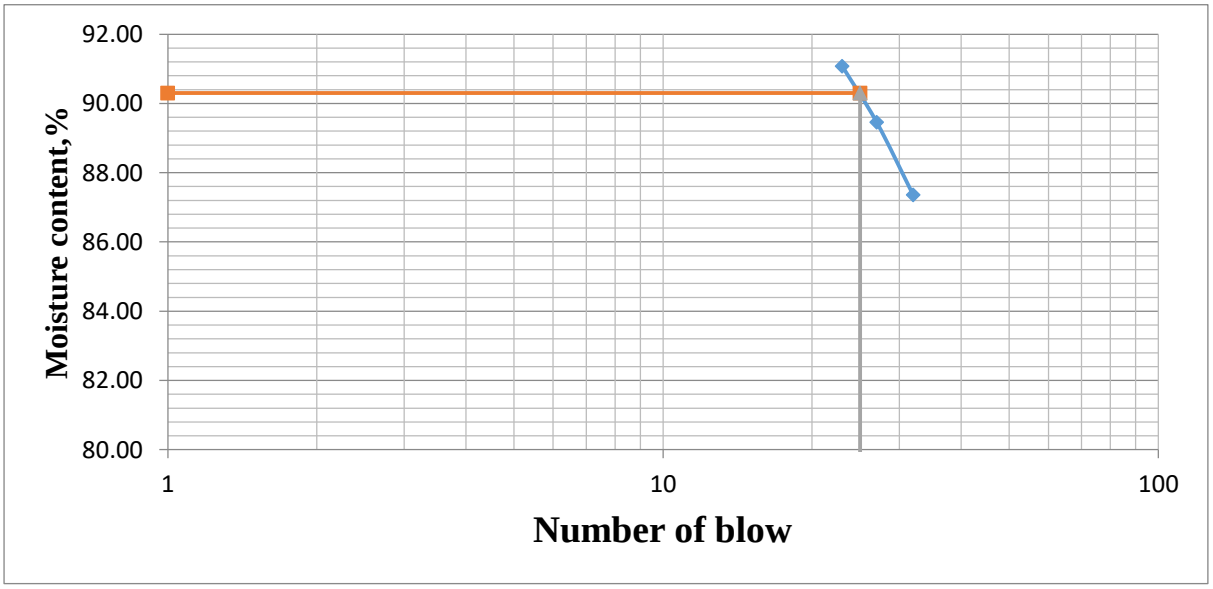

Figure B-5: Flow curve for TP4

Liquid limit (%) = 90.5 Plastic limit (%) =47.6 Plasticity index (%) =42.9

Appendix C: Particle Size Distribution Test Results

Test Pit 1	
Sieve Openings(mm)	Percentage Passing (%)
50	100.00
37.5	100.00
25	100.00
20	93.35
19	93.13
12.5	92.72
9.5	90.25
6.3	89.41
4.75	88.89
2.36	88.00
2	87.82
1.18	87.18
0.6	86.46
0.425	86.11
0.3	85.79
0.15	85.01
0.075	83.99
0.0263	65.64
0.01685	64.015
0.0099	60.77
0.0071	59.19
0.00505	57.60
0.002483	53.22
0.0010724	50.87

Test pit 2	
Sieve Openings (mm)	Percentage Passing (%)
50	100.00
37.5	100.00
25	100.00
20	100.00
19	100.00
9.5	100.00
4.75	77.82
2.36	61.08
2	53.16
1.18	48.04
0.6	46.73
0.425	43.38
0.3	40.37
0.15	39.12
0.075	37.74
0.0263	34.31
0.01685	30.94
0.0099	25.980318
0.0071	21.05612418
0.00505	18.06732018
0.002483	16.87179858
0.0010724	15.67627698

Test pit 3	
Sieve Openings (mm)	Percentage Passing (%)
50	100.00
37.5	100.00
25	100.00
20	100.00
19	100.00
12.5	100.00
9.5	100.00
6.3	100.00
4.75	99.53
98.86	98.86
98.72	98.72
98.29	98.29
97.36	97.36
96.74	96.74
95.99	95.99
93.65	93.65
91.09	91.09
77.025704	77.025704
63.83887797	63.83887797
62.07901917	62.07901917
58.55930157	58.55930157
56.79944277	56.79944277
0.002482646	55.47954867
0.001072387	49.36403934

Test Pit 4	
Sieve Openings (mm)	**Percentage Passing (%)**
75	100.00
63.5	100.00
50	100.00
37.5	100.00
25	100.00
20	100.00
19	100.00
12.5	87.20
9.5	86.00
4.75	82.90
2.36	76.50
2	73.80
1.18	65.10
0.6	54.70
0.425	50.80
0.3	46.90
0.15	42.30
0.075	39.50
0.026784191	27.85935
0.017161254	18.367895
0.010096797	12.948495
0.007227118	10.64525
0.005141037	7.58716
0.002592458	3.17422
0.00109226	0.23226

Test pit 5	
Sieve Openings (mm)	**Percentage Passing (%)**
75	100.00
63.5	100.00
50	100.00
37.5	100.00
25	100.00
20	100.00
19	100.00
12.5	100.00
9.5	100.00
4.75	100.00
2.36	100.00
2	100.00
1.18	99.90
0.6	99.70
0.425	99.60
0.3	99.30
0.15	98.90
0.075	98.43
0.026784191	76.53247476
0.017161254	55.5617664
0.010096797	53.6325384
0.007227118	51.7515411
0.005141037	49.8705438
0.002592458	48.8094684
0.00109226	40.0797117

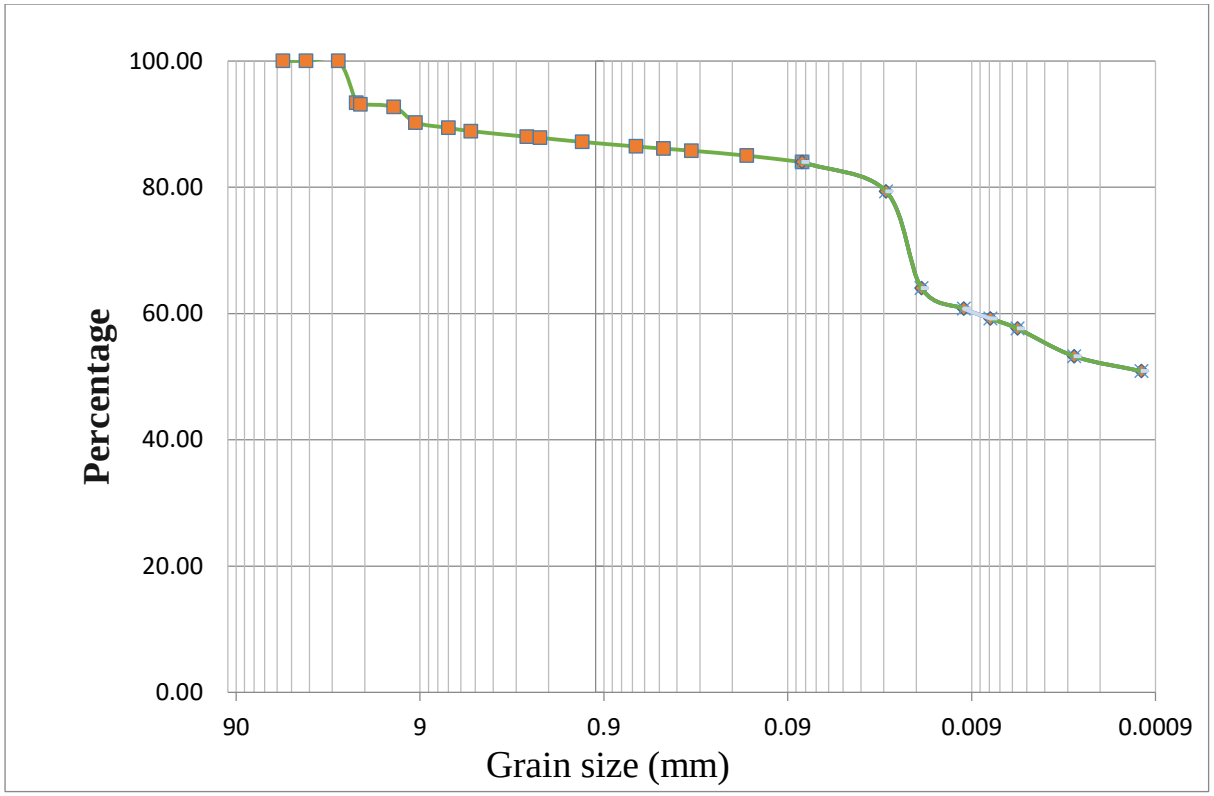

Figure C1: Particle size distribution for test pit 1

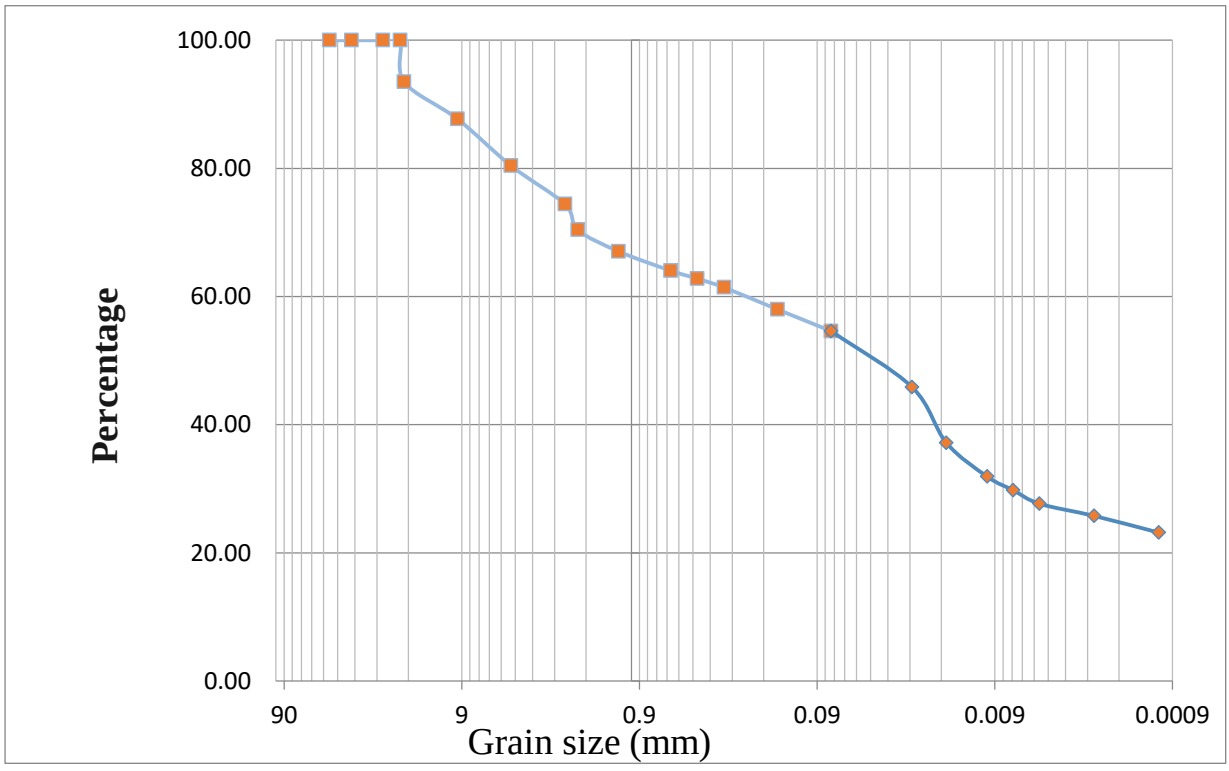

Figure C2: Particle size distribution for test pit 2

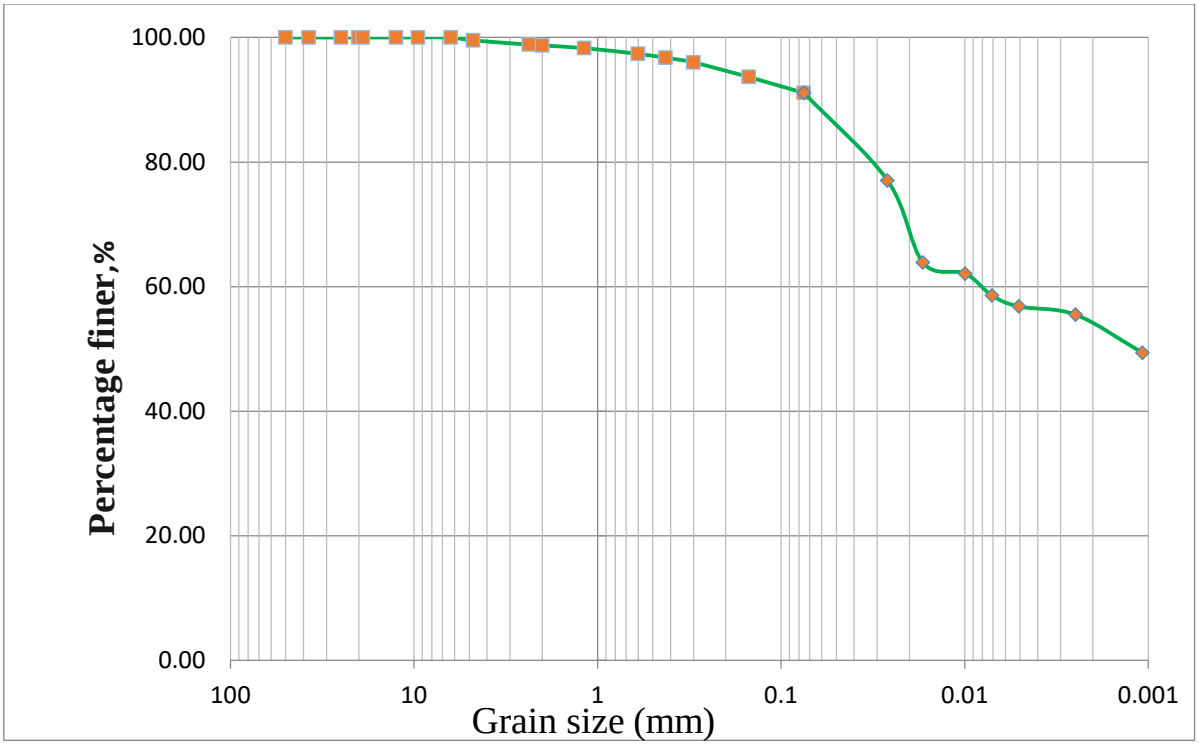

Figure C3: Particle size distribution for test pit 3

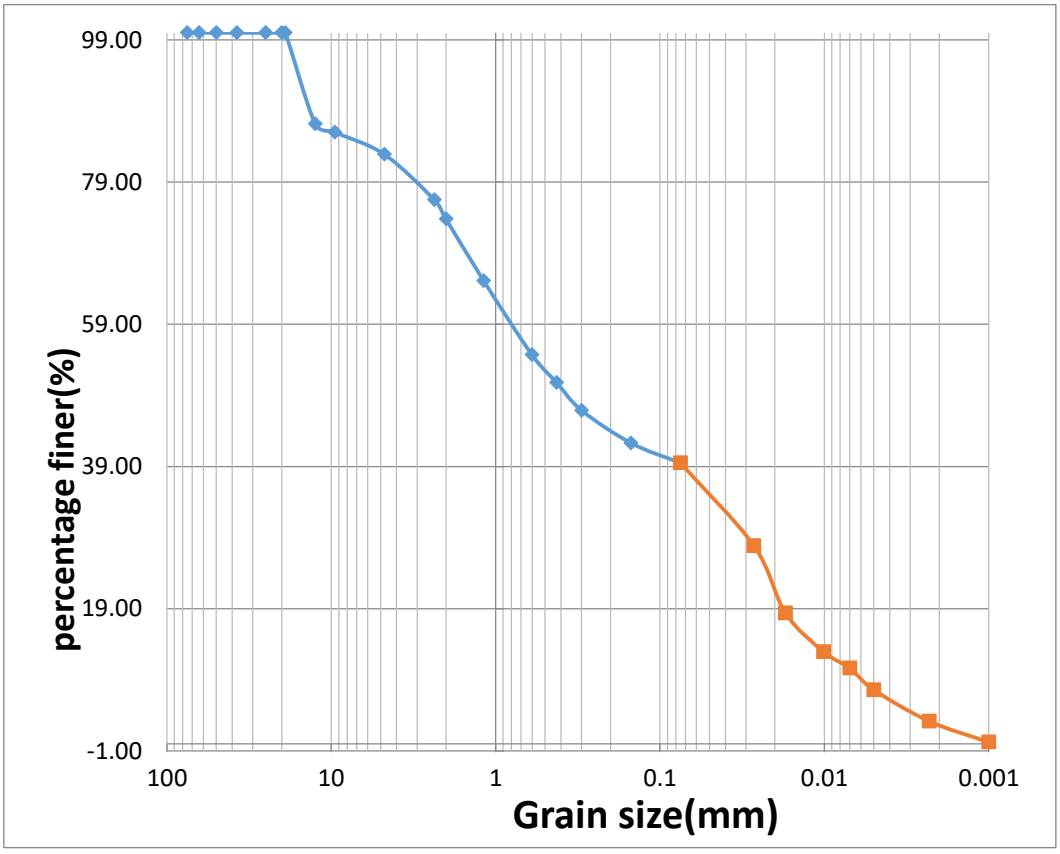

Figure C4: Particle size distribution curve for test pit 4

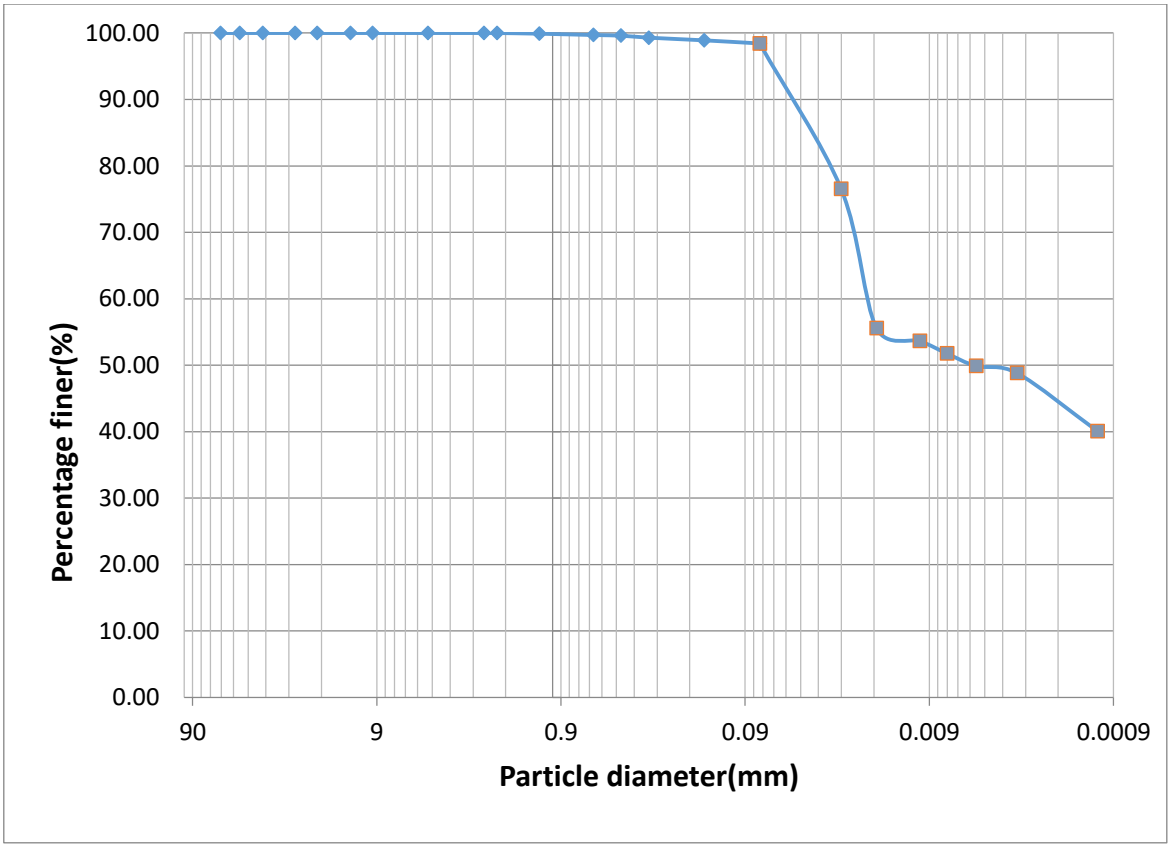

Figure C5: Particle size distribution curve for test pit 5

Appendix D Specific Gravity Test Results

Table D-1: Specific Gravity result for TP 1

Specimen Number	1	2
WP = Mass of Empty, Clean Pycnometer (gm)	145	151
WPS = Mass of Empty Pycnometer + Dry Soil (gm)	245	251
WB = Mass of Pycnometer + Dry Soil + Water (gm)	707	713
WA = Mass of Pycnometer + Water (gm)	642	649
Temprature (Degree Celsius)	17.5	18.5
Specific Gravity (GS)	2.853	2.8
Average Specific Gravity	2.82	

Table D-2: Specific Gravity result for TP 2

Specimen Number	1	2
WP = Mass of Empty, Clean Pycnometer (gm)	144	152
WPS = Mass of Empty Pycnometer + Dry Soil (gm)	244	252
WB = Mass of Pycnometer + Dry Soil + Water (gm)	706	711
WA = Mass of Pycnometer + Water (gm)	642	648
Temprature (Degree Celsius)	16.3	16.3
k = Conversion factor from table	1.007	1.007
Ws=mass of oven dried sample	100	100
Specific Gravity (GS)	2.79722	2.721622
Average Specific Gravity	2.76	

Table D-3: Specific Gravity result for TP 3

Specimen Number	1	2
WP = Mass of Empty, Clean Pycnometer (gm)	145	148
WPS = Mass of Empty Pycnometer + Dry Soil (gm)	245	248
WB = Mass of Pycnometer + Dry Soil + Water (gm)	707	709
WA = Mass of Pycnometer + Water (gm)	642	645
Temprature (Degree Celsius)	17.5	18.4
k = Conversion factor from table	1.001	1.0003
Ws=mass of oven dried sample	100	100
Specific Gravity (GS)	2.85857	2.778611
Average Specific Gravity	2.82	

Table D-4: Specific Gravity result for TP 4

Specimen Number	1	2
WP = Mass of Empty, Clean Pycnometer (gm)	179	176
WPS = Mass of Empty Pycnometer + Dry Soil (gm)	279	276
WB = Mass of Pycnometer + Dry Soil + Water (gm)	740	737
WA = Mass of Pycnometer + Water (gm)	676	674
Temprature (Degree Celsius)	15.8	16.4
k = Conversion factor from table	1.001	1.0007
Ws=mass of oven dried sample	100	100
Specific Gravity (GS)	2.77972	2.704595
Average Specific Gravity	2.74	

Table D-5: Specific Gravity result for TP 5

Specimen Number	1	2
WP = Mass of Empty, Clean Pycnometer (gm)	179	177
WPS = Mass of Empty Pycnometer + Dry Soil (gm)	280	277
WB = Mass of Pycnometer + Dry Soil + Water (gm)	742	739
WA = Mass of Pycnometer + Water (gm)	677	674
Temprature (Degree Celsius)	15.8	15.4
k = Conversion factor from table	1.001	1.0007
Ws=mass of oven dried sample	100	100
Specific Gravity (GS)	2.80752	2.859143
Average Specific Gravity	2.83	

Appendix E Free Swell Test Results

Table E-1: Free Swell test result for TP1

Trial no	1	2	3
Weight of soil(g)	10	10	10
Initial volume	10	10	10
Final volume	22	24	23
Free swell (%)	120	140	130
Average Free Swell (%)	130		

Table E-2: Free Swell test result for TP 2

Trial no	1	2	3
Weight of soil(g)	10	10	10
Initial volume	10	10	10
Final volume	19	19	18
Free swell (%)	90	90	80
Average Free Swell (%)	85		

Table E-3: Free Swell test result for TP 3

Trial no	1	2	3
Weight of soil(g)	10	10	10
Initial volume	10	10	10
Final volume	21	20	20
Free swell (%)	110	100	100
Average Free Swell (%)	105		

Table E-4: Free Swell test result for TP 4

Trial no	1	2	3
Weight of soil(g)	10	10	10
Initial volume	10	10	10
Final volume	13	14	13.5
Free swell (%)	30	40	35
Average Free Swell (%)	35		

Table E-5: Free Swell test result for TP 5

Trial no	1	2	3
Weight of soil(g)	10	10	10
Initial volume	10	10	10
Final volume	24	22	22
Free swell (%)	140	120	120
Average Free Swell (%)	130		

Appendix F: Consolidation test results

F-1 Test pit 1 consolidation test result

A, At the beginning of the test	
Sample type	Undisturbed
Ring Area, cm2:	30.19
Height of sample, mm	20
Seating Load, kPa	12.5
Initial Void Ratio, eo:	0.88
Initial moisture content, %	39.64
Specific Gravity:	2.50
Wet density, g/cm3	2.04
B, At the end of the test	
Final moisture content,%	31.96
Dry specimen wt(m_s),gm	80.1
Dry density,g/cm^3	1.33
Height of solids(H_s),mm	10.61
Final Void Ratio,e_f	0.72

Calculation table

Applied Pressure P (kPa)	Final Dial Reading (mm)	Change In specimen Height (mm)	Final specimen Height (mm)	Void Height,H_v (mm)	Void Ratio,e
Loading					
0	5.220	-0.20	19.80	9.19	0.87
12.5	5.420	0.05	20.05	9.44	0.89
25	5.370	0.00	20.00	9.39	0.88

50	5.220	-0.15	19.85	9.24	0.87
100	4.900	-0.47	19.53	8.92	0.84
200	4.530	-0.84	19.16	8.55	0.81
400	4.000	-1.37	18.63	8.02	0.76
800	3.640	-1.73	18.27	7.66	0.72
Unloading					
800	0.000	-1.73	18.27	7.66	0.72
25	4.000	-1.37	18.63	8.02	0.76
Pre consolidation pressure =80 kPa					

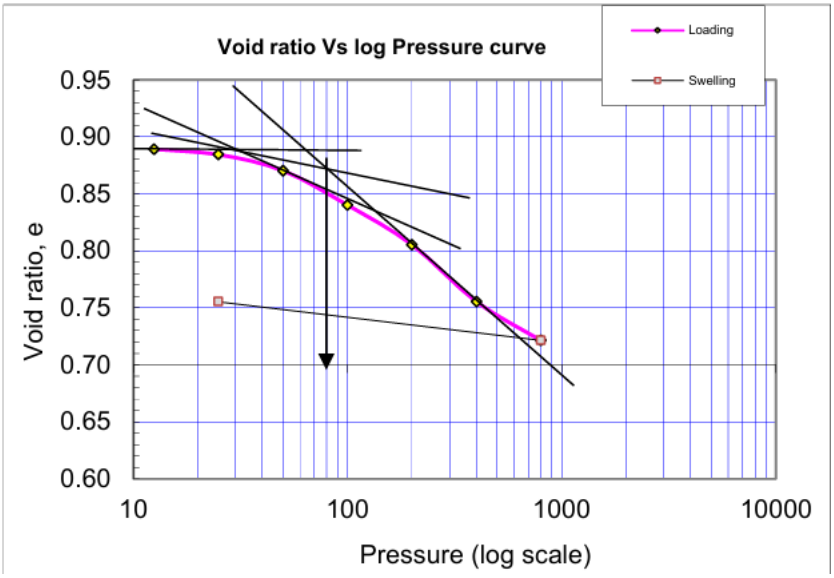

Figure-F-1: Consolidation pressure versus the void ratio of Test pits 1 soil.

F-2 Test pit 4 consolidation test result

A, At the beginning of the test	
Sample type	Undisturbed
Ring Area, cm2:	78.5
Height of sample, mm	18
Seating Load, kPa	5
Initial Void Ratio, eo:	5.83
Initial moisture content, %	31.34
Specific Gravity:	2.50
Wet density, g/cm3	0.50
B, At the end of the test	
Final moisture content,%	29.42
Dry specimen wt(m_s),gm	51.319
Dry density,g/cm^3	0.36
Height of solids(H_s),mm	2.61
Final Void Ratio,e_f	4.74

Calculation table

Applied Pressure P (kPa)	Final Dial Reading (mm)	Change In specimen Height (mm)	Final specimen Height (mm)	Void Height,H_v (mm)	Void Ratio,e
Loading					
0	5.220	-0.20	17.80	15.19	5.81
50	5.420	0.05	17.85	15.24	5.83
100	5.370	0.00	17.85	15.24	5.83
200	5.220	-0.15	17.70	15.09	5.77

400	4.900	-0.47	17.23	14.62	5.59
800	4.530	-0.84	16.39	13.78	5.27
1600	4.000	-1.37	15.02	12.41	4.74
Unloading					
1600	3.580	-1.37	13.65	11.04	4.22
800	3.526	-0.84	12.81	10.20	3.90
400	3.474	-0.47	12.34	9.73	3.72
Pre consolidation pressure =305 kPa					

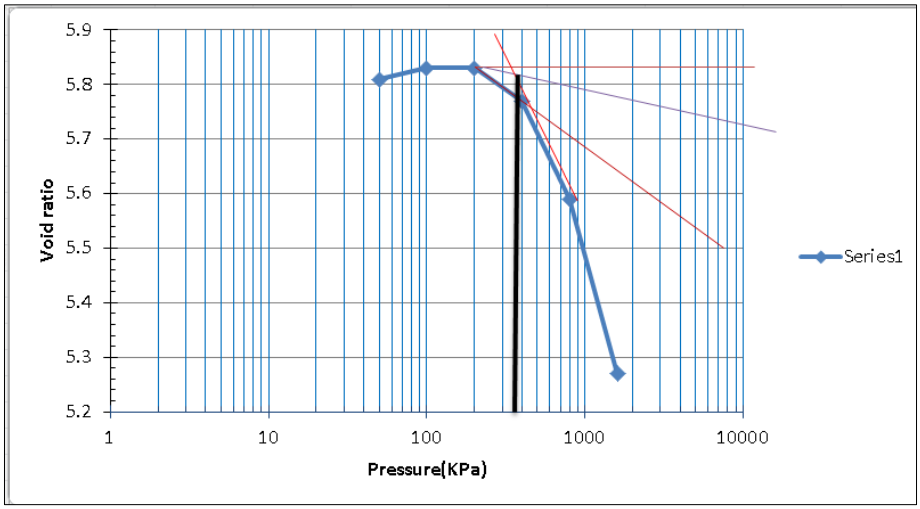

Figure-F-2: Consolidation pressure versus the void ratio of Test pits 4 soil.

Appendix G: Cyclic simple shear test result

G-1: Typical Tabulation of Shear Stress and Shear Strain Values of Selected Strain of TP1,5% strain and 200 kPa at 5^{th} cycle

Cycle	Time	Lateral lvdt	Lateral force	Shear stress(kPa)	Shear strain (%)	G tan
5	0	-1.30674	-0.07703	-0.02001559	-0.0695296	0.000905
	0.019	-1.28551	-0.05178	-0.01345459	-0.0684	0.001285
	0.038	-1.24743	-0.01509	-0.00392101	-0.0663738	0.001695
	0.057	-1.18085	0.0354	0.00919839	-0.0628312	0.001274
	0.076	-1.00896	0.07747	0.02012992	-0.0536852	0.001849
	0.095	-0.7824	0.15213	0.03952969	-0.0416303	0.000843
	0.114	-0.66335	0.19432	0.0504924	-0.0352958	0.000572
	0.133	-0.56568	0.22799	0.05924126	-0.030099	0.000542
	0.152	-0.44005	0.26695	0.06936469	-0.0234144	0.000235
	0.171	-0.24704	0.29174	0.07580616	-0.0131446	-1.5E-05
	0.19	-0.01996	0.28778	0.07477719	-0.001062	1.39E-05
	0.209	0.14531	0.27976	0.07269326	0.00773172	2.9E-05
	0.228	0.26026	0.27459	0.07134988	0.01384804	3.18E-05
	0.247	0.34272	0.27077	0.07035728	0.01823561	3.17E-05
	0.266	0.40389	0.2677	0.06955957	0.02149037	3.36E-05
	0.285	0.44789	0.26485	0.06881902	0.02383154	3.31E-05
	0.304	0.48125	0.26227	0.06814863	0.02560658	3.7E-05
	0.323	0.50574	0.25956	0.06744446	0.02690965	4.38E-05
	0.342	0.52285	0.25648	0.06664415	0.02782005	5.06E-05
	0.361	0.53506	0.25302	0.0657451	0.02846972	5.55E-05
	0.38	0.54396	0.2493	0.06477849	0.02894328	5.93E-05
	0.399	0.54971	0.24538	0.06375991	0.02924923	6.04E-05
	0.418	0.5532	0.24142	0.06273093	0.02943493	6.28E-05
	0.437	0.55429	0.23732	0.06166558	0.02949292	6.35E-05
	0.456	0.55455	0.23318	0.06058984	0.02950676	5.88E-05
	0.475	0.55386	0.22934	0.05959205	0.02947004	0.000181
	0.494	0.54768	0.21745	0.05650253	0.02914122	0.000539
	0.513	0.52056	0.18097	0.04702352	0.0276982	0.000942
	0.532	0.43793	0.10992	0.02856178	0.02330159	0.000738
	0.551	0.14101	0.01767	0.0045914	0.00750293	5.41E-05
	0.57	-0.08345	-0.05027	-0.01306223	-0.0044402	-9.8E-05
	0.589	-0.15807	-0.07951	-0.02066	-0.0084107	-0.00031
	0.608	-0.30332	-0.12817	-0.03330388	-0.0161392	-0.00038
	0.627	-0.52345	-0.16151	-0.041967	-0.027852	0.000242
	0.646	-0.7957	-0.14823	-0.03851631	-0.042338	0.000318
	0.665	-0.96387	-0.13516	-0.03512018	-0.051286	0.00017
	0.684	-1.06295	-0.12911	-0.03354814	-0.0565579	8.06E-05
	0.703	-1.12795	-0.12645	-0.03285696	-0.0600165	2.52E-05
	0.722	-1.17808	-0.12566	-0.03265168	-0.0626838	-4E-06

	0.741	-1.21951	-0.12578	-0.03268286	-0.0648883	0
	0.76	-1.25547	-0.12578	-0.03268286	-0.0668016	4.7E-05
	0.779	-1.28233	-0.12444	-0.03233468	-0.0682308	7.46E-05
	0.798	-1.30056	-0.12235	-0.03179161	-0.0692008	9.93E-05
	0.817	-1.3118	-0.1196	-0.03107704	-0.0697989	8.29E-05
	0.836	-1.31784	-0.11732	-0.0304846	-0.0701203	9.2E-05
	0.855	-1.32144	-0.1148	-0.0298298	-0.0703118	8.55E-05
	0.874	-1.32256	-0.11246	-0.02922177	-0.0703714	7.97E-05
	0.893	-1.32279	-0.11028	-0.02865532	-0.0703836	6.8E-05
	0.912	-1.32285	-0.10842	-0.02817202	-0.0703868	5.05E-05
	0.931	-1.32265	-0.10704	-0.02781343	-0.0703762	0.001091

Table-G-2: Shear stress and shear strain values of TP1, 5% strain and 200kPa at 10th cycle

Cycle	Time	Lateral lvdt	Lateral force	Shear stress(kPa)	Shear strain (%)	G tan
10	0	-1.29544	-0.05505	-0.028972327	-0.071213153	0.001352858
	0.019	-1.25275	-0.01665	-0.014304274	-0.068928381	0.001796993
	0.038	-1.17622	0.03686	-0.004326361	-0.066656912	0.001292496
	0.057	-0.97681	0.08028	0.009577758	-0.062584868	0.001739472
	0.076	-0.74478	0.15336	0.020860075	-0.051974566	0.000732892
	0.095	-0.62038	0.19219	0.039849292	-0.039628605	0.000549502
	0.114	-0.51486	0.2272	0.049938937	-0.033009471	0.000501287
	0.133	-0.36177	0.26856	0.059035988	-0.027394913	0.000130776
	0.152	-0.15146	0.28699	0.069783032	-0.019249228	-4.72637E-06
	0.171	0.06726	0.28293	0.074571911	-0.008058955	2.81E-05
	0.19	0.23883	0.27629	0.073516955	0.003578802	4.44454E-05
	0.209	0.36317	0.27095	0.071791607	0.012707779	1.69408E-05
	0.228	0.44829	0.26944	0.070404054	0.01932372	1.52753E-05
	0.247	0.50416	0.26828	0.070011693	0.023852825	1.30228E-06
	0.266	0.54242	0.26819	0.069710277	0.026825583	8.4712E-06
	0.285	0.5716	0.26764	0.069686891	0.028861339	1.57822E-05
	0.304	0.5932	0.26666	0.069543978	0.030413962	2.70932E-05
	0.323	0.60902	0.26503	0.069289334	0.031563265	3.17554E-05
	0.342	0.61923	0.26316	0.068865792	0.032405023	3.6833E-05
	0.361	0.62567	0.26102	0.068379888	0.032948281	4.11181E-05
	0.38	0.62919	0.25865	0.067823827	0.033290944	4.63219E-05
	0.399	0.63036	0.25599	0.067208003	0.033478238	5.07583E-05
	0.418	0.63125	0.25308	0.066516825	0.033540492	4.25758E-05
	0.437	0.63082	0.25064	0.065760686	0.033587847	6.51769E-05
	0.456	0.62965	0.2469	0.065126673	0.033564968	0.000184536
	0.475	0.62479	0.23626	0.064154866	0.033502714	0.000536702
	0.494	0.60327	0.20465	0.061390152	0.03324412	0.001005868
	0.513	0.53921	0.14097	0.053176562	0.032099074	0.001205085

	0.532	0.32421	0.04002	0.036629856	0.02869054	0.000330298
	0.551	-0.03707	-0.04318	0.010398857	0.017250718	-5.08557E-05
	0.57	-0.10528	-0.06902	-0.011219956	-0.001972438	-0.000212759
	0.589	-0.23182	-0.11467	-0.01793426	-0.005601788	-0.000395995
	0.608	-0.42737	-0.15812	-0.029796024	-0.012334788	-0.000112294
	0.627	-0.68372	-0.16543	-0.041086137	-0.022739704	0.000260722
	0.646	-0.87864	-0.15336	-0.042985579	-0.036379696	0.000185046
	0.665	-1.01177	-0.14628	-0.039849292	-0.046751091	0.000141154
	0.684	-1.10638	-0.14146	-0.038009614	-0.053834734	9.86623E-05
	0.703	-1.17353	-0.13833	-0.036757178	-0.058868788	6.92969E-05
	0.722	-1.22463	-0.13624	-0.035943874	-0.062441737	6.40406E-05
	0.741	-1.26568	-0.13438	-0.035400806	-0.06516069	8.64048E-05
	0.76	-1.29561	-0.13194	-0.0349175	-0.067344897	0.000102223
	0.779	-1.31698	-0.12911	-0.034283487	-0.068937427	0.000130619
	0.798	-1.32937	-0.12554	-0.033548136	-0.070074492	0.00010984
	0.817	-1.33661	-0.12256	-0.032620501	-0.070733745	0.000102872
	0.836	-1.33987	-0.11978	-0.031846174	-0.071118974	8.52557E-05
	0.855	-1.34119	-0.11748	-0.031123814	-0.071292434	8.0836E-05
	0.874	-1.34081	-0.1153	-0.030526179	-0.071362669	5.56138E-05
	0.893	-1.34084	-0.1138	-0.029959725	-0.07134245	4.18921E-05
	0.912	-1.34058	-0.11267	-0.029569962	-0.071344046	0.000115974
	0.931	-1.33938	-0.10954	-0.029276341	-0.071330212	0.001984984

G-2: Shear modulus and damping ratio of selected cycles

Shear modulus and damping ratio values for TP 1, TP3 and TP4 under axial stress of 100,200 and 400 Kpa.

TP1- Axial stress,100 kPa										
Strain (%)	0.01	0.1	1	2.5	5	0.01	0.1	1	2.5	5
Cycle no	G (MPa)					D (%)				
1	4.25371	4.19635	1.26015	0.47419	0.44598	12.5113	17.96676	25.8682	29.1065	36.063
5	14.3783	14.1844	1.2508	1.14569	0.84478	12.7008	20.60613	30.9164	34.6663	42.315
10	31.4454	31.0213	2.50128	1.43366	0.8674	9.6828	17.1619	20.9783	28.8203	40.1153
20	14.4258	14.2313	2.07086	1.37281	0.88826	12.0129	20.2348	23.9409	28.7679	35.1769
40	22.6014	22.2966	1.99381	1.33001	0.68598	11.3166	23.0277	24.0573	28.6949	37.23
TP1- Axial stress ,200 kPa										
Strain (%)	0.01	0.1	1	2.5	5	0.01	0.1	1	2.5	5
Cycle no	G (MPa)					D (%)				
1	7.03892	6.46502	3.68468	0.73898	0.68488	8.67656	10.56505	16.1142	37.3469	39.6259
5	18.4102	17.4397	3.03063	1.90294	1.17899	8.29559	16.7053	23.7504	27.3185	38.2155
10	10.2431	4.9208	2.79447	1.25773	1.12012	10.5434	12.30461	14.3609	33.4487	38.1243
20	15.4108	10.9464	3.71944	1.33077	1.01786	7.65368	10.12381	17.3509	31.6648	37.9818
40	17.336	7.51911	3.72782	1.38244	0.9531	18.0806	23.7128	26.3609	28.4963	37.4652

TP1- Axial stress,400 kPa										
Strain (%)	0.01	0.1	1	2.5	5	0.01	0.1	1	2.5	5
Cycle no	G (MPa)					D (%)				
1	8.19357	1.01451	0.77769	0.51185	0.46577	6.2588	6.41097	13.7028	31.7102	36.2357
5	7.34416	8.7441	3.22552	2.03145	0.89094	6.0669	15.1169	21.5086	25.412	34.7896
10	10.3535	6.434	3.4745	2.25563	0.45912	4.54564	15.832	24.8084	35.625	43.2963
20	9.95661	6.68078	3.31731	2.04179	0.32236	11.6684	16.3608	20.273	33.8864	43.9668
40	9.57444	8.39414	3.43501	0.26959	0.18484	0.21777	4.57685	10.992	34.9491	44.1151

TP3 Axial stress ,100 kPa										
Strain (%)	0.01	0.1	1	2.5	5	0.01	0.1	1	2.5	5
Cycle no	G (MPa)					D (%)				
1	1.98	0.79	1.08209	0.45784	0.91847	12.4832	16.1666	20.2887	37.7331	31.3858
5	15.55	9.45182	4.79221	2.11955	1.5319	12.96	21.6796	26.7896	37.8954	43.1123
10	13.50	5.50569	3.21286	1.93752	1.41281	10.89	16.37	20.5132	31.8969	43.6356
20	13.3643	4.53335	2.41967	1.6987	1.3078	7.026	10.786	18.4263	33.1792	42.026
40	9.8356	2.99475	1,9608	1.2110	1.1695	6.40313	8,04	10.053	30.9686	41.3701

TP3- Axial stress,200 kPa										
Strain (%)	0.01	0.1	1	2.5	5	0.01	0.1	1	2.5	5
Cycle no	G (MPa)					D (%)				
1	8.19357	1.01451	0.77769	0.51185	0.46577	2.09964	5.605	13.4981	27.4201	42.3103
5	7.34416	5.7441	3.22552	2.03145	0.89094	7.9864	15.6695	23.4563	27.4201	42.9103
10	10.3535	6.434	3.4745	2.25563	0.45912	7.37786	8.56884	11.8834	28.3116	31.0137
20	9.95661	6.68078	3.31731	2.04179	0.32236	7.8583	15.6681	19.4769	30.6111	35.8204
40	9.57444	8.39414	3.43501	0.26959	0.18484	7.23375	17.9616	20.49675	31.0815	39.9784
TP3 Axial stress ,400 kPa										
Strain (%)	0.01	0.1	1	2.5	5	0.01	0.1	1	2.5	5
Cycle no	G (MPa)					D (%)				
1	4.180801	4.119132	3.688056	1.473871	1.312277	14.0505	18.86956	24.38758	30.0376	32.48673
5	29.91499	12.05026	7.432404	2.993994	1.453268	6.3645	12.86961	14.09655	20.66602	41.30119
10	25.02189	22.74992	3.977382	2.689062	1.266476	0.753905	1.613528	10.80387	27.28966	39.72909
20	23.04025	10.42204	4.000441	2.595423	1.244201	7.791385	9.175839	19.146872	26.55779	39.06019
40	10.08385	9.19038	4.044081	2.469404	1.326098	1.973257	8.156971	10.269844	26.06341	39.92134

TP4- Axial stress,100 kPa										
Strain (%)	0.01	0.1	1	2.5	5	0.01	0.1	1	2.5	5
Cycle no	G (MPa)					D (%)				
1	2.31	1.97	0.620836	0.56813	0.445358	14.03	17.56	22.59	26.79	28.85268
5	28.67	5.65	1.308609	0.962628	0.495002	19.37	22.95	25.48	27.59	31.51946
10	23.14	9.94061	1.614263	0.701733	0.345694	21.82	25.96	26.72	28.03	30.57822
20	29.79	5.538507	1.676134	0.516255	0.245772	9.93	11.49	16.60	24.34	27.3521
40	23.20	1.957707	1.628174	0.138949	0.200557	12.61	16.39	19.74	23.71	28.95

TP4 Axial stress ,200 kPa										
Strain (%)	0.01	0.1	1	2.5	5	0.01	0.1	1	2.5	5
Cycle no	G (MPa)					D (%)				
1	3.53	2.56	1.457302	0.946508	0.688103	14.43	17.14	23.91	27.52	29.85268
5	22.27	3.95	2.013099	1.581428	1.165934	18.78	20.23	24.16	27.86	28.51946
10	27.11	27.82	2.179733	1.355377	1.903319	19.02	22.43	24.99	28.77	30.57822
20	27.35	14.64	2.379608	1.225884	2.673766	16.78	19.12	22.31	24.05	27.3521
40	25.80	2.844357	2.378715	1.143646	3.147079	18.30	19.74	22.40	27.09	29.95

TP4: Axial stress ,400 kPa

Strain (%)	0.01	0.1	1	2.5	5	0.01	0.1	1	2.5	5
Cycle no	G (MPa)					D (%)				
1	4.16	3.23	2.930225	1.806075	1.364773	12.79	15.31	19.67	25.54	27.80654
5	27.46	8.56	7.675615	3.82485	1.131621	8.86	12.87	17.41	19.51	27.22814
10	28.75	10.21	3.729803	2.219111	2.096052	14.77	17.74	21.75	25.29	28.76939
20	21.02	18.59	4.222861	5.702911	2.724716	1.79	5.68	8.85	11.91	18.78444
40	31.44	14.0026	4.273971	6.483332	3.088324	4.16	10.39	17.98	20.55	26.44

Appendix G: Sampling and Testing Procedures in Photos

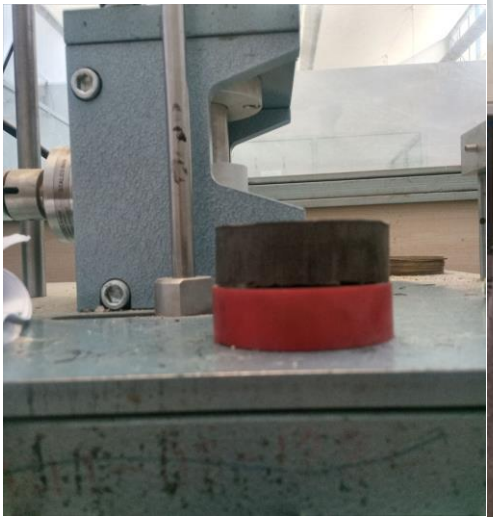


MULTISPEED